Differential Response and Susceptibility to Oxidative Stress in Mouse Lung Fibroblasts Heterozygous for Phospholipid Hydroperoxide Glutathione Peroxidase (GPx4)

Michael R. Garry

A dissertation
submitted in partial fulfillment of the
requirements for the degree of

Doctor of Philosophy

University of Washington

2006

Program Authorized to Offer Degree:
Department of Public Health and Community Medicine –
Environmental and Occupational Health Sciences

INFORMATION TO USERS

The quality of this reproduction is dependent upon the quality of the copy submitted. Broken or indistinct print, colored or poor quality illustrations and photographs, print bleed-through, substandard margins, and improper alignment can adversely affect reproduction.

In the unlikely event that the author did not send a complete manuscript and there are missing pages, these will be noted. Also, if unauthorized copyright material had to be removed, a note will indicate the deletion.

ProQuest Information and Learning Company
300 North Zeeb Road
P.O. Box 1346
Ann Arbor, MI 48106-1346

University of Washington
Graduate School

This is to certify that I have examined this copy of a doctoral dissertation by

Michael R. Garry

and have found that it is complete and satisfactory in all respects,
and that any and all revisions required by the final
examining committee have been made.

Chair of the Supervisory Committee:

Elaine M. Faustman

Reading Committee:

Elaine M. Faustman

Elaine M. Faustman

Terrance J. Kavanagh

Evan P. Gallagher

Date: 8/9/06

In presenting this dissertation in partial fulfillment of the requirements for the doctoral degree at the University of Washington, I agree that the Library shall make its copies freely available for inspection. I further agree that extensive copying of the dissertation is allowable only for scholarly purposes, consistent with "fair use" as prescribed in the U.S. Copyright Law. Requests for copying or reproduction of this dissertation may be referred to ProQuest Information and Learning, 300 North Zeeb Road, Ann Arbor, MI 48106-1346, 1-800-521-0600, to whom the author has granted "the right to reproduce and sell (a) copies of the manuscript in microform and/or (b) printed copies of the manuscript made from microform."

Signature: 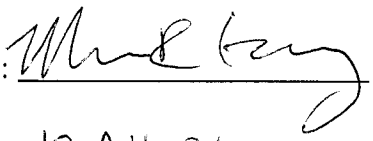

Date: 10 AUG 06

University of Washington

Abstract

Differential Response and Susceptibility to Oxidative Stress in
Mouse Lung Fibroblasts Heterozygous for
Phospholipid Hydroperoxide Glutathione Peroxidase (GPx4)

Michael Robert Garry

Chair of Supervisory Committee:
Professor Elaine M. Faustman
Department of Environmental and Occupational Health Sciences

Phospholipid hydroperoxide glutathione peroxidase (GPx4) is a member of the family of selenium dependent enzymes that catalyze the reduction of cell membrane-bound phospholipid hydroperoxides *in situ* and thus, protects against membrane damage. The research described in this dissertation focused on 1) characterization of GPx4 activity levels in *GPx4*$^{-/-}$ mice and cells from those mice, 2) development of a cell culture model that provides a physiologically relevant basis for evaluating the roles of GPx4 and the mechanisms of its actions, and 3) investigation of the relative susceptibility to toxicant-induced oxidative stress using this model. It was demonstrated that a *GPx4*$^{-/-}$ genotype is embryonic lethal, but that *GPx4*$^{+/-}$ mice survive and appear phenotypically normal. GPx4 activity is significantly lower in testis and liver tissue from *GPx4*$^{+/-}$ mice than *GPx4*$^{+/+}$ mice. Cultured lung fibroblasts (LFs) from adult *GPx4*$^{+/-}$ mice had approximately 50% GPx4 activity of *GPx4*$^{+/+}$ LFs, and were significantly more susceptible to H_2O_2, cadmium, and cumene hydroperoxide-induced cytotoxicity. *GPx4*$^{+/-}$ LFs had lower mitochondrial membrane potential, greater cardiolipin oxidation, and lower amounts of reduced thiols relative to *GPx4*$^{+/+}$ LFs, but were more resistant to further decrements in these endpoints following phospholipid hydroperoxide treatment. After treatment with $CdCl_2$, *GPx4*$^{+/-}$ LFs had a

decreased survival response compared to *GPx4*$^{+/+}$ LFs. Specifically, a *GPx4*$^{+/-}$ genotype was associated with increased morphological evidence of stress, decreased Akt activation, and increased caspase 3 activation. *GPx4*$^{+/-}$ cells exhibited decreased p38 and JNK activation, but the overall survival response, as measured by the ratio of survival pathway activation (Akt) to stress pathway activation (p38 and JNK), was attenuated in *GPx4*$^{+/-}$ LFs. *GPx4*$^{+/-}$ cells also exhibited diminished accumulation of high molecular weight poly-ubiquitinated proteins than *GPx4*$^{+/+}$ cells in response to $CdCl_2$ treatment. The *GPx4*$^{+/-}$ mouse appears to provide a useful model for studying susceptibility to chemically induced oxidative stress, particularly where lipid peroxidation is a primary mediator of cellular injury. Furthermore, *GPx4*$^{+/-}$ LFs provide a useful model for understanding the mechanisms by which GPx4 protects against oxidative injury and mediates cellular functions in the face of chemical insult.

Table of Contents

List of Figures

Acknowledgments

The research described in this dissertation was supported by NIH Grants P30-ES07033, T32-ES07032, R01-ES09601 and R01-ES10613-01, and EPA Grant R826886. The generation and characterization of the targeted mice was supported by the Nathan Shock Center for Excellence in Basic Biology of Aging (5P30AG013280-09) and a grant from the University of Washington Royalty Research Fund to Samir S. Deeb. Appreciation to the Transgenic Resource Program, University of Washington for assistance in generating the targeted ES cells and mice, and to Lakshmi Goripathy for genotyping the mice. A large number of people provided assistance to me throughout my tenure at the University, but special thanks to the following people who provided extraordinary support above and beyond the call of duty: Melinda Vredevoogd for her extraordinary work on the outline and draft introductory section of the manuscript that became Chapter 3 of this dissertation; Euvin Kim and Sungwoo Hong for their help on Westerns; Jaspreet Sidhu for his direction and guidance in my signaling studies; Collin White for guidance with analytical cytometry and all things mechanical; Diane Botta who early on taught me all I know about cell culture; Elaine Faustman and Terry Kavanagh for their guidance, patience, and friendship through this process; and of course, Lynn Bekris for, ultimately, making the whole thing worthwhile.

Chapter 1 – Introduction

Glutathione Peroxidases

Glutathione peroxidases are the primary mammalian antioxidant enzymes that scavenge and reduce hydrogen peroxide and lipid peroxides, thereby protecting cells from oxidative damage (Takebe *et al.* 2002). Glutathione peroxidases catalyze the reduction of hydroperoxides as a component of the glutathione redox cycle, using glutathione or other thiols (e.g., cysteine, thioredoxin) as reducing substrates in conjunction with glutathione reductase and NADPH. There are both selenium-dependent and selenium-independent enzymes with glutathione peroxidase activity. The selenium-dependent glutathione peroxidases are characterized by the presence of a highly homologous region with a so-called catalytic triad of selenocysteine, glutamine, and tryptophan at the active site.

Four selenium-dependent glutathione peroxidases have been identified: GPx1, GPx2, GPx3, and GPx4. The first three are tetramers comprised of four identical subunits. They primarily reduce small hydroperoxide substrates such as hydrogen peroxide (H_2O_2) and nonesterified lipid peroxides. Classical, or cytosolic glutathione peroxidase (cGPx or GPx1), is ubiquitous throughout the body and is typically present at the highest levels among the glutathione peroxidases, with the notable exception being the testis, where GPx4 predominates (Dreher *et al.* 1997). Gastrointestinal glutathione peroxidase (GI-GPx or GPx2), also cytosolic, was first identified in cells of the rat gastrointestinal epithelium (Chu and Esworthy 1995), but has also been identified in human liver and gall bladder, as well as gastrointestinal cells (Komatsu *et al.* 2001). Plasma glutathione peroxidase (pGPx or GPx3), an extracellular form, has been identified in pigs, rats, mice, and humans. In humans, it is most highly expressed in the kidney proximal tubular cells (Avissar *et al.* 1994), but has also been identified in lung epithelial cells (Avissar *et al.* 1996).

Unlike the other members of the family, phospholipid hydroperoxide glutathione peroxidase (PHGPx or GPx4) is a 20 to 23kDa monomeric protein (Takebe *et al.* 2002; Ursini *et al.* 1985). Although GPx4 is less than 40% homologous with GPx1, like all members of the selenium-dependent glutathione peroxidases it is highly homologous at the active site (Lei *et al.* 1995). GPx4 is unique among the glutathione peroxidases in that it has a high specific affinity for larger, membrane bound substrates such as phospholipid and cholesterol hydroperoxides and can directly reduce membrane bound hydroperoxides *in situ*. Sequence comparisons with the tetrameric forms of glutathione peroxidase show a lack of conservation in regions corresponding to the arginine residues presumed to bind glutathione, and in contact sites between the individual subunits of the tetramers. These differences may, in large part, explain the monomeric nature and unique substrate specificity of GPx4 (Brigelius-Flohe *et al.* 1994). The lack of strongly hydrophilic arginine residues may impact GPx4 in two ways. First, the greater hydrophobicity that would accompany the lack of arginine residues, along with the associated alteration in tertiary structure, could improve substrate specificity for larger, hydrophobic organic molecules such as phospholipid and cholesterol hydroperoxides. Second, the increased hydrophobicity could also improve the molecule's ability to insinuate itself within biological membranes where *in situ* reduction of membrane bound hydroperoxides is possible.

Other enzymes have been shown to also have glutathione peroxidase activity, including several glutathione S-transferases (human GSTs A1-1, T1-1, M1-1, A2-2, and A4-4) (Hurst *et al.* 1998), selenoprotein P, catalase, and the peroxiredoxins, but with lower specific activity than members of the GPx family. In addition, a selenium-independent, extracellular glutathione peroxidase is localized to the epididymis, and is bound to sperm predominantly in the acrosomal region (Vernet *et al.* 1999).

Phospholipid Hydroperoxide Glutathione Peroxidase

GPx4 has been identified and cloned in several animal species, including humans (Esworthy *et al.* 1994), rats (Imai *et al.* 1995; Pushpa-Rekha *et al.* 1995), mice (Borchert *et al.* 1999; Knopp *et al.* 1999; Nam *et al.* 1997), pigs (Brigelius-Flohe *et al.* 1994; Sunde *et al.* 1993), and chickens (Kong *et al.* 2003). In addition, homologues have been identified in several plant species, including spinach (Sugimoto *et al.* 1997), and the orange *Citrus sinensis* (Holland *et al.* 1993), although the plant version is selenium-independent. In mammals, GPx4 is present in all tissues, but is most highly expressed in testis, and in sperm (Roveri *et al.* 1994) where it converts into a structural protein in the mitochondrial capsule during spermatogenesis (Ursini *et al.* 1999). It is expressed in an age-dependent manner in testis and in a stage-specific manner in developing spermatocytes (Maiorino *et al.* 1998; Nam *et al.* 1998). Testis GPx4 is indirectly induced by testosterone and appears to play an important role in spermatogenesis (Maiorino *et al.* 1998). Decreased GPx4 levels of both the enzymatically active form (Imai *et al.* 2001) and the inactive structural form (Flohe *et al.* 2002) in humans spermatocytes have been correlated with lower sperm quality and fertility.

Its unique substrate specificity and membrane localization highlights the role of GPx4 in protecting cellular membranes against the ongoing potential for lipid peroxidation. Lipid peroxidation is initiated when reactive oxygen species (ROS), such as the hydroxyl radical react with unsaturated lipids. There are many sources of these ROS within the cell, including normal cellular processes such as oxidative phosphorylation and NAD(P)H oxidases, and following xenobiotic exposure and metabolism by cytochrome P450 oxidases. The consequences of lipid peroxidation include further reaction with other cellular macromolecules, disruption of membrane integrity, suppression of mitochondrial respiration, and eventually cell death.

Phospholipase A2 has the ability to terminate lipid peroxidation by excising oxidized fatty acids from membrane phospholipids, so they can be released from the membranes and reduced by GPx1 or other glutathione peroxidases (Maiorino *et al.* 1991; Thomas *et al.* 1990). However, this process is not as efficient or effective as the protection afforded by GPx4, which directly reduces phospholipid hydroperoxides *in situ* without the need to remove the damaged fatty acids. Although GPx1 levels are approximately 500-fold higher than GPx4 levels in the rat liver, the rate-limiting step for GPx1 reduction of the lipid peroxides is the activity of phospholipase A2 (Antunes *et al.* 1995). A kinetic model predicts that nearly 100% of phospholipid hydroperoxide reduction is accomplished via GPx4 in rat liver (Antunes *et al.* 1995).

Three forms of GPx4 have been described: a 20 kDa cytosolic form, a 23 kDa mitochondrially targeted form (Arai *et al.* 1999), and a sperm nucleus-specific form (Borchert *et al.* 2003; Pfeifer *et al.* 2001). Except for the mitochondrial targeting leader sequence required for translocation of the long form into the mitochondrion, the two forms are identical. After translocation, mitochondrial GPx4 sheds its leader sequence to yield a 20 kDa protein identical to cytosolic GPx4 (Arai *et al.* 1996). *In situ* and fractionation studies have shown that mitochondrial GPx4 is localized to the contact space between the inner and outer mitochondrial membrane (Imai and Nakagawa 2003). In this location it can directly reduce membrane-bound hydroperoxides and terminate lipid peroxidation.

The protective role of GPx4 against xenobiotic and ROS-induced injury has been demonstrated in numerous overexpression studies in several cell types (Imai and Nakagawa 2003). Overexpression of GPx4 in guinea pig cell line 104C1 protected against phospholipid hydroperoxide induced dissipation of mitochondrial membrane potential (Yagi *et al.* 1998). Rat basophilic leukemia cells (RBL cells) transfected with the long form, but not the short form of GPx4, were protected

against KCN-induced dissipation of mitochondrial membrane potential and cell death. (Arai *et al.* 1999). Overexpression of GPx4 also protects RBL cells against apoptosis induced by hypoglycemia (Arai *et al.* 1999), staurosporine, etoposide, cycloheximide, actinomycin D, 2-deoxyglucose, and UV irradiation (Nomura *et al.* 1999). GPx4 overexpression afforded protection from arsenite-induced ROS production and apoptosis in human epidermoid carcinoma A431 cells (Huang *et al.* 2002).

GPx4 Heterozygous Knockout as a Model for Understanding GPx4 Function and Role in Protection from Oxidative Stress

Overexpression studies provide a useful tool in understanding the mechanisms by which antioxidant enzymes function and in elucidating their role in cellular defenses. However, overexpression of an enzyme to non-physiological levels may produce responses that are not easily interpretable or relevant to phenotypes that might not occur naturally. The more relevant model, especially for an enzyme typically associated with a protective role, is one in which expression is diminished or absent. This is particularly the case when genetic polymorphisms exist that are also associated with reduced expression. This premise is the basis for the research described in this dissertation.

In order to study the role of GPx4 under physiologically relevant conditions, the initial intent was to develop both a transgenic mouse model with a *GPx4* null allele ($GPx4^{-/-}$), and a mouse model with a heterozygous genotype ($GPx4^{+/-}$). However, as reported in Chapter 2 of this dissertation, as well as by other groups (Imai *et al.* 2003; Yant *et al.* 2003), the $GPx4^{-/-}$ genotype is embryonic lethal. The observations of Yant et al. (Yant *et al.* 2003) suggest that *GPx4* null embryos exhibit morphological abnormalities between 6.5 and 7.5 days post coitum (dpc) and are resorbed by 8.0 to 8.5 dpc. The mechanism of embryonic lethality is uncertain. Yant and colleagues (Yant *et al.* 2003) found no evidence of differences

in either cellular proliferation or the number of apoptotic cells in *GPx4* null embryos at 7.5 dpc relative to wild-type embryos. In addition to its antioxidant role, the authors suggest a critical role in cell signaling could play a part. Overexpression of GPx4 in rat basophile leukemia cells inhibits 2-deoxyglucose induced cytochrome c release and cardiolipin oxidation (Nomura *et al.* 2000). Imai et al. (Imai *et al.* 2003) reported that the *GPx4* null genotype in their mice resulted in embryonic death during early gastrulation, between 7.5 and 8.5 dpc. Immunohistochemical analysis showed that GPx4 was first detected in the embryonic ectoderm and the yolk sac membrane at 7.5 dpc in $GPx4^{+/+}$ and $GPx4^{+/-}$ embryos, but was absent in the $GPx4^{-/-}$ embryos. Thus, timing of expression of GPx4 coincided with the timing of embryonic death in $GPx4^{-/-}$ embryos.

Partial GPx4 expression, as with the $GPx4^{+/-}$ genotype, appears to be adequate for normal development, while complete lack of GPx4 is embryonic lethal. Oxidative stress is recognized as an important mechanism in teratogenesis (Vismara *et al.* 2001; Wells *et al.* 1997). Apoptotic cell death represents an early event in the teratogenic process of many teratogens (Mirkes *et al.* 2000). Glutathione and GPx1 are protective against chemically-induced teratogenesis. In rodents, glutathione depletion adversely affects fetal growth and increases the number of dead and malformed embryos (Hales and Brown 1991) and increases susceptibility to chemically induced teratogenesis (Harris *et al.* 1987; Saillenfait *et al.* 1993). GPx1 depletion induced by selenium deficiency increases susceptibility to phenytoin-induced teratogenesis in mice (Ozolins *et al.* 1996). Furthermore, knockout of the glutamate cysteine ligase catalytic subunit , resulting in a complete lack of glutathione synthesis, is embryonic lethal (Dalton *et al.* 2000). Glutathione supplementation, on the other hand, is protective (Faustman-Watts *et al.* 1986; Slott and Hales 1987). Thus, it is possible that increased oxidative stress during a critical stage of development could explain the embryonic lethality of the $GPx4^{-/-}$ genotype.

Mice with a heterozygous genotype (*GPx4*$^{+/-}$) develop normally. Thus, the focus of the research described in this dissertation was to 1) characterize the GPx4 activity levels of *GPx4*$^{-/-}$ mice and cells from those mice, 2) develop a cell culture model that provides a physiologically relevant basis for evaluating the roles of GPx4 and the mechanisms of its actions, and 3) investigate the relative susceptibility to toxicant-induced oxidative stress using this model.

As described in Chapter 2 of this dissertation, lung fibroblasts isolated from adult mice were cultured and propagated as a model for evaluating susceptibility to chemically-induced cytotoxicity, oxidative stress, and the underlying mechanisms that mediate differential susceptibility conferred by GPx4 genotype. Lung fibroblasts from *GPx4*$^{+/-}$ mice have approximately 50% of the GPx4 activity of lung fibroblasts from *GPx4*$^{+/+}$ mice, and exhibit genotype associated differential responses to cadmium, H_2O_2, and cumene hydroperoxide, and phospholipid hydroperoxide exposure. Because of the differential responses of wild type and GPx4 heterozygous lung fibroblasts, along with the physiologically relevant differences in GPx4 activity, adult lung fibroblast cells were considered an appropriate model for evaluating the underlying mechanisms potentially mediating the differential susceptibility conferred by GPx4 genotype.

Cadmium as a Model Compound for Characterizing GPx4 Genotype-Associated Differential Susceptibility to Oxidative Stress

Cadmium is a naturally occurring ubiquitous metal constituting 10 to 100 μg/kg of the earth's crust (ATSDR 1999). The average soil cadmium concentration in the United States is about 250 μg/kg, but varies greatly geographically. Cadmium is not usually present in the environment as a pure metal, but as complex oxides, sulfides, and carbonates. Cadmium concentrations in most drinking water supplies in the United States are less than 1 μg/L, well below the drinking water standard of

50 μg/L. Levels in drinking water, however, may vary greatly depending on local conditions.

Cadmium exposure has been associated with mutagenic, carcinogenic, teratogenic and neurotoxic endpoints (Chang 1996) (Filipic *et al.* 2006) (Goering *et al.* 1994). Outside of occupational settings, the most significant sources of human exposure to cadmium are the diet and cigarette smoke (Satarug *et al.* 2003; Satarug and Moore 2004). Inhalation exposure to cadmium has been associated with airway inflammation (Kirschvink *et al.* 2006), pulmonary edema (Beton *et al.* 1966), emphysema (Davison *et al.* 1988; Leduc *et al.* 1993), and cancer (Stayner *et al.* 1992; Takenaka *et al.* 1983; Thun *et al.* 1985). Lung cancer has been observed in workers exposed to high concentrations of cadmium oxide dust and fumes together with other exposures in the smelter setting (Thun *et al.* 1985). Urinary cadmium data available for a subset of this population suggested high cadmium exposure. However, other risk factors in the study population limit determination of a causal relationship with cadmium (i.e., smoking and prior inhalation exposure to arsenic during prior operation of the facility as an arsenic smelter). There was also a significant and dose-related increase in lung cancer in inhalation investigations with Wistar rats exposed to cadmium chloride aerosol (Takenaka *et al.* 1983). Cadmium and cadmium compounds were listed as "known to be human carcinogens" in the 11th Report on Carcinogens by the National Toxicology Program (NTP 2005).

Oxidative stress and lipid peroxidation play a significant role in cadmium induced toxic responses (Lopez *et al.* 2006) (Huang *et al.* 2006) (Elbekai and El-Kadi 2005) (Watjen and Beyersmann 2004) (Alvarez *et al.* 2004). Cadmium exposure has been shown to generate reactive oxygen species through the depletion of glutathione and protein-bound sulfhydryl groups leading to lipid peroxidation and apoptosis (Stohs *et al.* 2001). Cadmium induces superoxide anion and hydrogen

peroxide production in both a human tumor cell line and bovine aorta endothelial cells (Szuster-Ciesielska *et al.* 2000). Although this could be a result of cadmium-induced glutathione depletion, cadmium exposure also results in decreased synthesis of the antioxidant enzymes superoxide dismutase, peroxidase, and catalase (Waisberg *et al.* 2003). A combination of depleted glutathione levels and reduced levels of these antioxidant enzymes, is generally regarded as the primary mechanism by which cadmium induces lipid peroxidation (Waisberg *et al.* 2003).

Another mechanism by which cadmium may indirectly increase cellular levels of ROS is through depletion of metallothionein. Metallothionein is a cysteine rich protein that protects cells from the toxic effects of metals with thiol binding capacity by binding and sequestering these metals (Simpkins 2000). Although cadmium itself is not redox active, cadmium may displace redox active metals such as iron and copper from metallothionein or other cellular proteins (Ercal *et al.* 2001; Filipic *et al.* 2006). These redox active metals can then participate in Fenton reactions to produce hydroxyl radicals.

GPx4 appears to play some role in mediating cadmium-induced toxicity. Mussels (*Perna perna*) exposed to 200μg/L cadmium in water for 12 hours exhibit significantly increased malonaldehyde levels, indicating lipid peroxidation, and this effect was associated with GPx4 depletion (de Almeida *et al.* 2004). *Saccharomyces cerevisiae* overexpressing a yeast GPx4 homologue is resistant to lipid peroxidation and cadmium-induced cell death (Avery *et al.* 2004). And finally, as described in Chapter 2 of this dissertation, a $GPx4^{+/-}$ genotype confers increased susceptibility to cadmium-induced cell death in mouse lung fibroblasts.

Thus, cadmium is a relevant and interesting model compound to evaluate GPx4 function because 1) cadmium is abundant in the environment and an important public health concern, 2) cadmium toxicity involves lipid peroxidation, which is modulated by GPx4 activity, and 3) there is evidence to suggest GPx4 plays a role

in protection against cadmium-induced toxicity. As such, cadmium was the model compound used in the research described in Chapter 3 of this dissertation involving mechanistic aspects of the differential susceptibility conferred by *GPx4*$^{+/-}$ genotype, specifically cell signaling and post-translational modification.

Mechanistic Aspects of GPx4 Function: MAPK Stress Signaling, Apoptotic, and Survival Pathways

Cadmium-induced cytoxicity is associated with oxidative stress and apoptotic cell death in a number of cell types (Bagchi *et al.* 2000; Hansen *et al.* 2006; Jimi *et al.* 2004; Stohs *et al.* 2001). Further, the apoptosis observed following cadmium exposure is mediated, at least in part, by activation of p38 and c-Jun NH_2-terminal kinase (JNK) mitogen-activated protein kinases (MAPK) stress signaling pathways (Chuang *et al.* 2000; Kim *et al.* 2005; Lag *et al.* 2005). There are three main MAPK signaling pathways, each involving a series of three serine/threonine kinases that are activated by phosphorylation and successively activate their downstream target by phosphorylating it. Thus, each MAPK molecule is phosphorylated and activated by its specific MAPK kinase (MAPKK), and each MAPKK is phosphoylated and activated by its specific MAPKK kinase (MAPKKK) (Takeda *et al.* 2003). MAPKKK can be activated by a variety of stress or survival signals, including UV radiation, growth factors, cytokines, osmotic stress, ROS, and chemical exposures. The p38 and JNK pathways are typically associated with cell stress, inflammation, and apoptosis. A third pathway, the extracellular signal-regulated kinases (ERK), is typically associated with cell survival and proliferation and is primarily activated by growth factors (Lag *et al.* 2005).

Akt, also known as protein kinase B, is another serine/threonine kinase activated by extracellular stimuli, such as growth factors, cytokines, ROS and chemical exposures. The Akt signaling pathway, typically associated with a survival

response and cell proliferation, is activated through a phosphoinositide 3-kinase pathway initiated by receptor tyrosine kinase and G-protein signaling (Cantley 2002; Misra *et al.* 2003). Akt activation can be either induced or attenuated in response to cadmium exposure, depending on dose and duration of exposure (Konishi *et al.* 1997; Murata *et al.* 2003; Yu *et al.* 2005). More specifically, Akt activation can be transiently increased following cadmium exposure, followed by dephosphorylation and diminished signaling with prolonged exposure.

Various studies have demonstrated evidence to support a critical role of MAPKs in Cd-induced cell cycle arrest (Chao and Yang 2001), cytotoxicity (Rockwell *et al.* 2004) and apoptosis (Kefaloyianni *et al.* 2005; Lag *et al.* 2005) (Kim *et al.* 2005) (Jonak *et al.* 2004). The roles of p38 and JNK in cadmium-induced apoptosis have predominately been reported to involve caspase-3 dependent mechanisms (Kefaloyianni *et al.* 2005; Kim and Sharma 2004, 2006; Lee *et al.* 2005; Papadakis *et al.* 2006), although a caspase-3 independent pathway has also been reported for mouse neuronal cells following cadmium exposure (Rockwell *et al.* 2004).

GPx4 overexpression protects against apoptosis induced by a number of chemical agents that cause oxidative stress. One mechanism by which GPx4 affords this protection may involve its ability to suppress specific apoptotic signals. For example, overexpression of GPx4 suppresses the release of cytochrome c, caspase 3 cleavage, adenine nucleotide translocase (ANT) inactivation and apoptosis induced by 2-deoxyglucose in RBL2H3 cells (Imai and Nakagawa 2003; Nomura *et al.* 1999). Akt inhibits apoptosis, at least in part, by preventing cytochrome c release (Kennedy *et al.* 1999) and directly inhibiting caspase 9 activation (Cardone *et al.* 1998). Both the JNK (Papadakis *et al.* 2006; Tournier *et al.* 2000) and p38 (Yoshino *et al.* 2001) pathways also modulate the mitochondrial death pathway through regulation of cytochrome c release and caspase 3 activation. Thus, as described in Chapter 3 of this dissertation, the response of these stress

signaling and survival pathways in response to cadmium exposure was evaluated in relation to GPx4 genotype. The relationship of these stress signaling pathways to cadmium toxicity and GPx4 function is depicted in Figure 1.1.

Mechanistic Aspects of GPx4 Function: Ubiquitin Proteosomal System

Degradation and turnover of cellular proteins is a highly regulated process, the correct function of which is important for regulation of normal cellular function. The ubiquitin proteasomal system (UPS) is the primary mechanism by which cells package and remove damaged proteins and regulate protein turnover. Dysfunction in the system is associated with pathological states, including cancers and neurodegenerative diseases (Ciechanover and Brundin 2003; Ciechanover and Schwartz 2002). Degradation of proteins by the UPS involves two general steps. First, multiple ubiquitin molecules conjugate to protein substrates. Second, the "tagged" ubiquitin-conjugated proteins are degraded by the 26S proteasome complex and the ubiquitin molecules are released for reuse. Damaged proteins may be recognized by the system for ubiquitination by misfolding or other conformational changes such as might occur with oxidative damage. UPS is also involved in normal cell cycle progression, with ubiquitin ligases identified that regulate turnover of important cell cycle proteins such as p27Kip1, p21Cip1, p57Kip2, and cyclin E (Lim and Elenitoba-Johnson 2004). The Cullen-containing SCF E3 ubiquitin ligase family regulates cell proliferation through degradation of critical regulators such as cyclins, CDK inhibitors and transcription factors (Willems *et al.* 2004).

A dysfunctional UPS can lead to the accumulation of damaged proteins and lead to cytotoxicity. UPS perturbation may play a role in cadmium-induced oxidative stress and cytotoxicity. Gene expression studies from our laboratory of cadmium-treated mouse embronic fibroblast cells using microarray analysis indicate that

cadmium disrupted the UPS, especially Ubiquitin ligases such as the multi-function ligase/hydrolase UCH-L1 (unpublished data). Cadmium-mediated oxidative stress has been linked to the accumulation of high molecular weight polyubiquitinated protein conjugates (HMW-Ub) (Figueiredo-Pereira *et al.* 1997). Mouse HT4 neuroblastoma cells expressing a dominant negative ubiquitin are sensitive to cadmium-induced oxidative injury and cell death (Tsirigotis *et al.* 2001). Subcytotoxic doses of cadmium (25μM and below) were associated with increased levels of ubiquitinated proteins in HT4 cells, while cytotoxic doses (50μM and above) led to an attenuated UPS response (Figueiredo-Pereira *et al.* 1998). Thus, diminished function of the UPS system accompanies increased levels of oxidative stress induced cytotoxicity.

Cadmium is known to oxidize and bind protein thiols (Stohs *et al.* 2001). The UPS would normally remove these oxidized proteins. As discussed in Chapter 2 of this dissertation, protein thiols are oxidized in *GPx4*$^{+/-}$ lung fibroblasts relative to wild-type cells under baseline conditions. It is possible then, that a *GPx4*$^{+/-}$ genotype would predispose towards an attenuated UPS response following cadmium exposure, as reported for cytotoxic doses of cadmium in HT4 cells (Figueiredo-Pereira *et al.* 1998), because the already elevated levels of oxidized protein thiols places the UPS nearer to a saturated state. Thus, UPS function provides an attractive target for examining the role in GPx4 in cadmium-induced toxicity.

The remainder of this dissertation is focused on the research conducted with the overall goals of characterizing the GPx4 status of *GPx4*$^{+/+}$ and *GPx4*$^{+/-}$ mice and the lung fibroblasts from those mice, and the differential susceptibility to chemically induced stress in these cells, with an emphasis on cadmium exposure. Chapter 2 describes the knockout mouse model, GPx4 activity in various tissues, and differential susceptibility to various chemical agents. Chapter 3 describes studies related to mechanistic aspects of the GPx4 lung fibroblast model, focusing

on differential responses of p38, JNK, Akt, caspase-3, and UPS following cadmium exposure. Chapter 4 summarizes the results, provides overall conclusions and interpretation, and places the results in context of the overall field of GPx4 research.

Figure 1.1 – Stress signaling, apoptotic, and survival pathways associated with cadmium toxicity.
The apoptosis observed following cadmium exposure is mediated by activation of p38 and c-Jun NH_2-terminal kinase (JNK) mitogen-activated protein kinases (MAPK) stress signaling pathways. MAPK signaling pathways involve a series of three serine/threonine kinases that are activated by phosphorylation and successively activate their downstream target by phosphorylating it. Both the p38 and JNK pathways can be activated by reactive oxygen species (ROS) through activation of upstream kinases, including apoptosis signaling kinase-1 (ASK1). The p38 and JNK pathways are typically associated with cell stress, inflammation, and apoptosis. The roles of p38 and JNK in cadmium-induced apoptosis have predominately been reported to involve caspase-3 dependent mechanisms, and JNK can induce cytochrome c release by negatively regulating the anti-apoptotic factor Bcl-2. Akt, also known as protein kinase B, is another serine/threonine kinase activated by extracellular stimuli, such as growth factors, cytokines, ROS and chemical exposures, and is typically associated with a survival response and cell proliferation. Akt can inhibit apoptosis in at least three ways: 1) As a negative regulator of Bad, a pro-apoptotic member of the Bcl family, thus inhibiting cytochrome c release, 2) As a negative regulator of ASK1, thereby inhibiting the p38 and JNK signaling pathways, and 3) by directly inhibiting caspase-9 activation. Akt is redox sensitive; reduced glutathione and glutaredoxin levels are associated with Akt oxidation and inactivation. Cadmium can both activate and inhibit the Akt pathway, depending on conditions. GPx4 suppresses the release of cytochrome c, caspase 3 cleavage, and apoptosis.

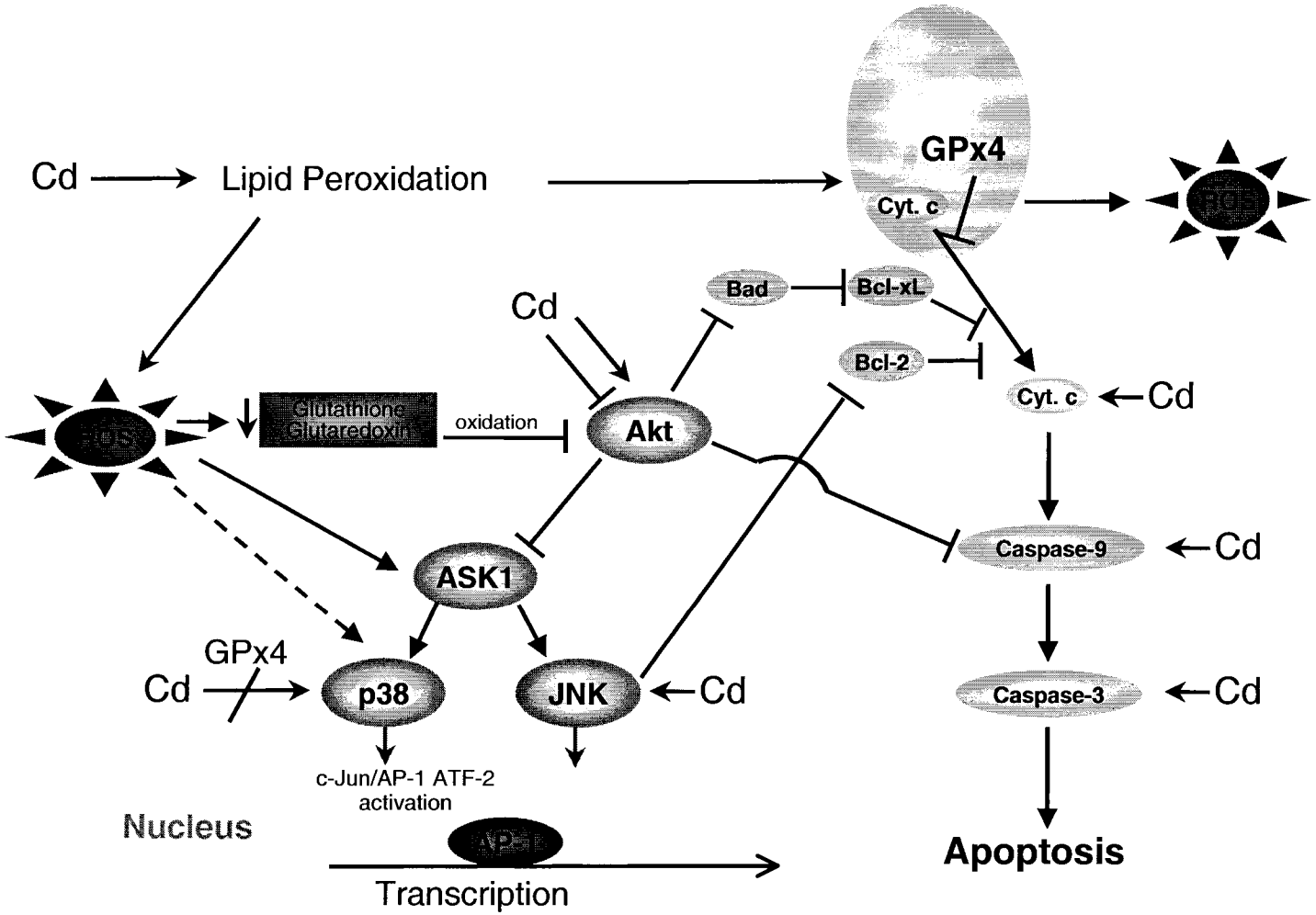
Cd
Lipid Peroxidation
GPx4
Cyt. c
ROS
Bad
Bcl-xL
Cd
Bcl-2
Cyt. c
Cd
ROS
Glutathione
Glutaredoxin
oxidation
Akt
Caspase-9
Cd
ASK1
GPx4
Cd
p38
JNK
Cd
Caspase-3
Cd
c-Jun/AP-1 ATF-2
activation
Nucleus
AP-1
Transcription
Apoptosis

Figure 1.2 – Ubiquitin proteasomal system and the effects of cadmium toxicity. Cadmium (Cd) can bind and oxidize protein thiols directly, or induce lipid peroxidation, leading to production of reactive oxygen species (ROS) and oxidation of protein thiols. Reduced levels of GPx4 are also associated with oxidation of protein thiols. Protein oxidation causes conformational changes and unfolding. Damaged proteins may be recognized by the ubiquitin proteasomal system (UPS) for ubiquitination by misfolding or other conformational changes such as might occur with oxidative damage. Degradation of proteins by the UPS involves two general steps: first, multiple ubiquitin molecules conjugate to protein substrates; second, the "tagged" ubiquitin-conjugated proteins are degraded by the 26S proteasome complex and the ubiquitin molecules are released for reuse.

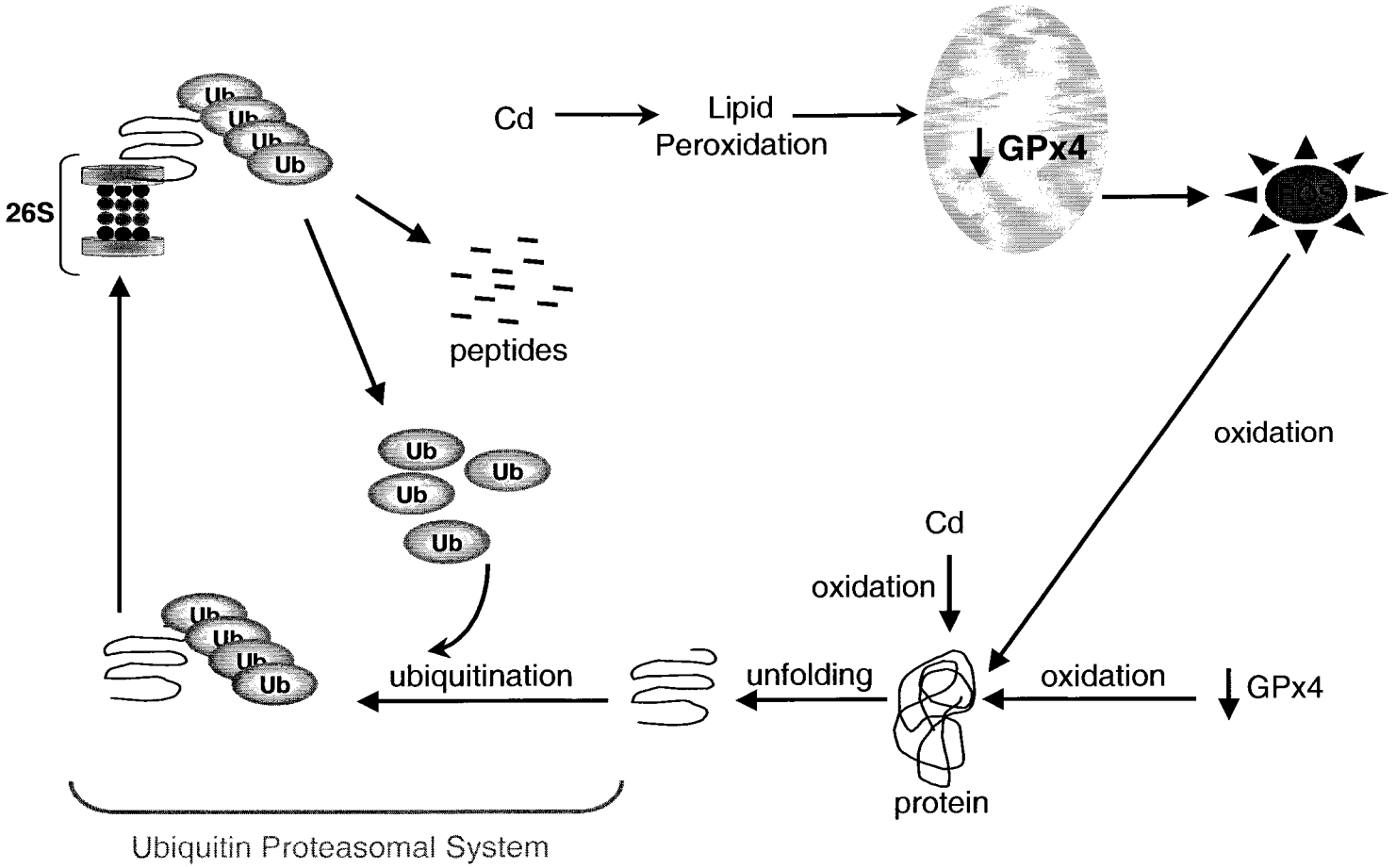
Ub
Ub
Ub
Ub
26S
peptides
Cd
Lipid
Peroxidation
GPx4
ROS
oxidation
Ub
Ub
Ub
Ub
Cd
oxidation
Ub
Ub
Ub
Ub
ubiquitination
unfolding
oxidation
GPx4
protein
Ubiquitin Proteasomal System

Chapter 2 – Sensitivity of Mouse Lung Fibroblasts Heterozygous for GPx4 to Oxidative Stress

Summary of Chapter 2

Phospholipid hydroperoxide glutathione peroxidase (GPx4) is a member of the family of selenium dependent enzymes that catalyze the reduction of cell membrane-bound phospholipid hydroperoxides *in situ* and thus, protects against membrane damage. Overexpression of GPx4 protects cultured cells from phosphatidylcholine hydroperoxide (PCOOH)-induced loss of mitochondrial membrane potential and blocks cell death induced by treatment with various apoptotic agents. We have generated mice that are heterozygous for a *GPx4* null allele ($GPx4^{+/-}$); the homozygous null genotype is embryonic lethal. We report that cultured lung fibroblasts (LFs) isolated from adult $GPx4^{+/-}$ mice had approximately 50% of the GPx4 activity of LFs from $GPx4^{+/+}$ mice, and were significantly more susceptible to H_2O_2, cadmium, and cumene hydroperoxide-induced cytotoxicity, as measured by neutral red assay. Both $GPx4^{+/+}$ and $GPx4^{+/-}$ LFs were susceptible to PCOOH-induced cytotoxicity at a high PCOOH concentration. We also found that $GPx4^{+/-}$ LFs have lower mitochondrial membrane potential, greater cardiolipin oxidation, and lower amounts of reduced thiols relative to $GPx4^{+/+}$ LFs, but are more resistant than $GPx4^{+/+}$ LFs to further decrements in these endpoints following PCOOH treatment. These results suggest that adult lung fibroblasts deficient in GPx4 may have upregulated compensatory mechanisms to deal with the highly oxidized environment in which they developed.

Introduction

Phospholipid hydroperoxide glutathione peroxidase (PHGPx or GPx4) is a member of the family of selenium-dependent enzymes that catalyze the reduction of hydroperoxides, using glutathione or other thiols (e.g., cysteine, thioredoxin) as reducing substrates (Takebe *et al.* 2002). Three of the four members of the family, classical or cellular glutathione peroxidase (cGPx or GPx1), gastrointestinal glutathione peroxidase (GI-GPx or GPx2), and plasma glutathione peroxidase (pGPx or GPx3), are tetramers and primarily reduce small hydroperoxide substrates such as H_2O_2 and nonesterified lipid peroxides. GPx4 is unique among the glutathione peroxidases in that it is monomeric, has a high specific affinity for larger, membrane bound substrates such as phospholipid and cholesterol hydroperoxides, can associate with cellular membranes, and directly reduces membrane bound hydroperoxides *in situ*. Other enzymes have been shown to also have glutathione peroxidase activity, including several glutathione S-transferases (GSTA1-1, GSTT1-1, GSTM1-1, GSTA2-2, and GSTA4-4), selenoprotein P, catalase, and the peroxiredoxins, but with lower specific activity than members of the GPx family.

GPx4 has been identified and cloned in several animal and plant species, including humans (Esworthy *et al.* 1994), rats (Imai *et al.* 1995; Pushpa-Rekha *et al.* 1995), mice (Borchert *et al.* 1999; Knopp *et al.* 1999; Nam *et al.* 1997), pigs (Brigelius-Flohe *et al.* 1994; Sunde *et al.* 1993), chickens (Kong *et al.* 2003), spinach (Sugimoto *et al.* 1997), and the orange *Citrus sinensis* (Holland *et al.* 1993), although the plant version is selenium independent. In mammals, it is present in all tissues, but is most highly expressed in testis and sperm (Roveri *et al.* 1994) where it converts into a structural protein in the mitochondrial capsule during spermatogenesis (Ursini *et al.* 1999). It is expressed in an age-dependent manner in testis and in a stage-specific manner in developing spermatocytes (Maiorino *et al.* 1998; Nam *et al.* 1998). Testis GPx4 is indirectly induced by testosterone and

appears to play an important role in spermatogenesis (Maiorino *et al.* 1998). Decreased GPx4 levels of both the enzymatically active form (Imai *et al.* 2001) and the inactive structural form (Flohe *et al.* 2002) in humans spermatocytes have been correlated with lower sperm quality.

Its unique substrate specificity and membrane localization highlights the role of GPx4 in protecting cellular membranes against the ongoing potential for lipid peroxidation. Lipid peroxidation is initiated when reactive oxygen species (ROS), such as the hydroxyl radical react with unsaturated lipids. There are many sources of these ROS within the cell, including normal cellular processes such as oxidative phosphorylation and NAD(P)H oxidases, and following xenobiotic exposure and metabolism by cytochrome p450 oxidases. The consequences of lipid peroxidation include further reaction with other cellular macromolecules, disruption of membrane integrity, suppression of mitochondrial respiration, and eventually cell death.

Three forms of GPx4 have been described: a 20 kDa cytosolic form, a 23 kDa mitochondrially targeted form (Arai *et al.* 1999), and a sperm nucleus-specific form (Pfeifer *et al.* 2001). Except for the mitochondrial targeting leader sequence required for translocation of the long form into the mitochondrion, the two forms are identical. After translocation, mitochondrial GPx4 sheds its leader sequence to yield a 20 kDa protein identical to cytosolic GPx4 (Arai *et al.* 1996). *In situ* and fractionation studies have shown that mitochondrial GPx4 is localized to the contact space between the inner and outer mitochondrial membrane (Imai and Nakagawa 2003). In this location it can directly reduce membrane-bound hydroperoxides and terminate lipid peroxidation. Overexpression of GPx4 in guinea pig cell line 104C1 protected against phospholipid hydroperoxide induced dissipation of mitochondrial membrane potential (Yagi *et al.* 1998). Furthermore, Arai et al. (Arai *et al.* 1999) demonstrated that rat basophilic leukemia cells (RBL

cells) transfected with the long form, but not the short form of GPx4, were protected against KCN-induced dissipation of mitochondrial membrane potential and cell death. Overexpression of GPx4 also protects RBLs against apoptosis induced by hypoglycemia (Arai *et al.* 1999), staurosporine, etoposide, cycloheximide, actinomycin D, 2-deoxyglucose, and UV irradiation (Nomura *et al.* 1999). Overexpression of GPx4 afforded protection from arsenite-induced ROS production and apoptosis in human epidermoid carcinoma A431 cells (Huang *et al.* 2002).

Until recently, evidence for the role of GPx4 in the protection against xenobiotic and ROS-induced injury has come from studies of cells overexpressing GPx4 (reviewed by Imai and Nakagawa (Imai and Nakagawa 2003)). Overexpression studies provide a useful tool in understanding the mechanisms by which antioxidant enzymes function and in elucidating their role in cellular defenses. However, overexpression of an enzyme to non-physiological levels may produce responses that are not easily interpretable or relevant to phenotypes that could occur naturally. In order to study the role of GPx4 under more physiologically relevant conditions we set out to develop a transgenic mouse model homozygous for a *GPx4* null allele ($GPx4^{-/-}$). We report here, as have others (Imai *et al.* 2003; Yant *et al.* 2003) that the $GPx4^{-/-}$ genotype is embryonic lethal. However, mice with a heterozygous genotype ($GPx4^{+/-}$) develop normally. We therefore isolated and cultured lung fibroblast cells from adult wild type ($GPx4^{+/+}$) and $GPx4^{+/-}$ mice and characterized their response to xenobiotic-induced oxidative stress. Specifically, response to four ROS generating chemicals (cadmium, cumene hydroperoxide, phosphatidyl choline hydroperoxide, and H_2O_2) that produce lipid peroxidation was assessed. The results from our study suggest that reduced expression of GPx4 confers increased susceptibility to toxicant exposure at expression levels that are physiologically relevant.

Materials and Methods

Reagents

Cumene hydroperoxide (CuOOH), cadmium chloride, sodium deoxycholate (DC), glutathione (GSH), glutathione reductase (GRx), NADPH, soybean lipoxidase (type IV), neutral red (NR) and 1,2-dilinoleoyl-3-phosphatidylcholine (PC) were purchased from Sigma (St. Louis, MO, USA). Mitotracker red (MTR), mitotracker green (MTG), monobromobimane (MBB), and nonylacridine orange (NAO) were purchased from Molecular Probes (Eugene, OR). Dulbecco's modified Eagle's medium (DMEM), fetal bovine serum (FBS) and penicillin-streptomycin liquid (PenStrep) were purchased from Gibco BRL (Grand Island, NY). Sep-Pak C18 columns were purchased from Waters (Milford, MA).

Construction of the targeting vector

GPx4 genomic clones were isolated from a 129/SVJ phage mouse genomic library (Stratagene, La Jolla, CA, Cat. # 946309) by screening with a mouse cDNA clone that we previously isolated and characterized (Knopp *et al.* 1999). The sequence and genomic structure was determined (Figure 2.1). The targeting vector, constructed from the genomic clone, was designed to replace part of exon 1, intron 1 and part of exon 2 with *lacZ* and Neomycin resistance genes. Upon targeted recombination, the two flanking thymidine kinase (TK) genes from the vector were eliminated. The targeting vector was constructed by cloning an *Afl* II-*Eag* I genomic fragment (1.8 kb) into the *Nhe*I site, and an *Eco R*I-*Eco R*I (5.5 kb) fragment into the *Spe* 1 site of the plasmid nNeoZTK2 (Figure 2.1A), which was kindly provided by Dr. Richard Palmiter of the University of Washington. The wild type and targeted alleles are shown in Figure 2.1A.

GPx4 targeting in mouse embryonal stem (ES) cells

The linearized targeting vector DNA was introduced into ES cells (passage 14 129/Sv) by electroporation. Homologous recombinants were selected for neomycin

resistance using G-418 200 μg/ml) for 10 days, and with ganciclovir (2 mM) during the first four days of G-418 selection. Targeted cells were detected by PCR amplification and subsequently verified by Southern blot analysis, as described below. Targeted ES cells from two independent clones were injected into C57BL/6 mouse blastocysts and two lines of chimaeric mice were generated that transmitted the targeted *GPx4* gene through the germ-line.

Animals

Since the initial germ-line chimeras, the line has been bred back to C57BL/6 for six generations. Thus, the mice are on a predominantly C57BL/6 background (>98%). Lung fibroblasts from wild-type siblings were used as controls. All work was carried out following the Institutional Animal Care and Use Committee guidelines within an Association for Assessment and Accreditation of Laboratory Animal Care approved specific pathogen-free facility.

Genotyping

DNA was extracted by digestion of cells or tissues with proteinase K followed by purification on "Qiam spin columns" (Qiagen, Valencia, CA) according to the protocol provided by the manufacturer. Rapid screening of ES cells and mouse tissues was performed by PCR amplification using the primer pairs Pr5F (promoter) and I-1R (intron 1), specific for wild-type, and Pr5F and NZTK*lac*ZR (in the *lac Z* gene) which amplified only the fragment from the targeted allele (Figure 2.1A and C). The primer sequences were: Pr5F: 5′-tccacagccctccaacgcgtc-3′; I-1R: 5′- ctaggtggaggagtctcaagg-3′; NZTK*lac*ZR: 5′-tagaggatccccgggtaccaagc-3′. The amplification conditions were: an initial denaturation at 94°C for 2 minutes, followed by 30 cycles of 10 sec at 94°C and 20 sec at 66°C, and a final step of 2 min at 72°C.

Southern blot analysis was performed on genomic DNA from mice or ES cells in order to confirm targeting. DNA was digested with *Hind* III and electrophoresed on agarose gels. A radiolabeled probe of 396 bp from the promoter region (Figure 2.1A bottom panel) was used to detect the ~14 kb Hind III fragment of wild type and the ~6 kb fragment of the targeted GPx4 gene (Figure 2.1B).

Tissue and Macrophage Isolation and Preparation

Testes, liver, and lung tissues from $GPx4^{+/+}$ and $GPx4^{+/-}$ mice were frozen in liquid nitrogen immediately after the animals were sacrificed. The tissues were subsequently frozen at –80 °C until analysis. Peritoneal macrophages were isolated from mice immediately after euthanization by injecting 10 ml of sterile PBS into the peritoneal cavity with an 18 gauge needle, gently massaging the peritoneum (with the needle still inserted), then slowly withdrawing the PBS with macrophages into the syringe. The macrophages were centrifuged at 900xG for 10 minutes at 4°C, and the PBS was aspirated away from the pelleted cells, which were then stored in sample assay buffer (0.25 M sucrose, 20 mM tris-HCl (pH 7.4), 0.1% Triton X-100 (v/v)) at –80 °C until analysis.

Lung Fibroblast Isolation and Culture

Freshly dissected lung tissue was macerated in medium (DMEM supplemented with 10% FBS (v/v), 100 μg/ml streptomycin, 100 units/ml penicillin, and 2 mM L-glutamine) on 100mm tissue culture plates using sterile razor blades. The resulting slurry was mixed with 10ml of medium, and cells and tissue fragments were allowed to adhere to 100 mm tissue culture plates. Plates were incubated for 7-10 days at 37 °C in a humidified atmosphere of 95% air/5% CO_2. Fibroblasts which migrated out of the tissue fragments were trypsinized and diluted into 10 plates for further experimentation. All experiments were conducted on cells in passage two through seven.

GPx4 Activity Assay

Tissues analyzed for GPx4 activity were homogenized in assay buffer on ice using a Polytron tissue grinder (Brinkmann, Westbury, NY) followed by three 10-second bursts of sonication, also on ice. Macrophages and fibroblasts were lysed in the same buffer using only sonication. Following homogenation/sonication, samples were centrifuged at 10,000xG for 10 minutes, and the supernatant was transferred to a clean tube for PHGPx activity analysis. Phosphatidylcholine hydroperoxides (PCOOH) were prepared by enzymatic oxidation of PC with soybean lipoxidase as described by Roveri et al. (Roveri *et al.* 1994). PC was dispersed in a concentrated DC reaction buffer (0.9 mM PC, 9 mM DC, and 0.2 M tris-HCl). An additional 0.2 M tris-HCl was added to bring the final concentrations to 0.3 mM PC, 3 mM DC, and 0.2 M tris-HCl. After initiation of peroxidation by addition of 0.7 mg lipoxidase, the reaction was allowed to continue for 30 minutes at room temperature with continual stirring. Sep Pak C-18 cartridges (Waters) were washed with one bed volume of methanol, equilibrated with two volumes of dH_2O, and loaded with the PC reaction mixture containing PCOOH. The cartridge was washed with 10 volumes of dH_2O, and the PCOOH eluted in two volumes of methanol. PCOOH was stored for no longer than one month, under argon gas, at –80C. The concentration of PCOOH was determined spectrophotometrically before each experiment using the extinction coefficient of 25,000 $M^{-1}cm^{-1}$ at 234 nm.

GPx4 activity was measured indirectly by following the oxidation of NADPH in the presence of GSH reductase, which catalyzes the reduction of oxidized GSH, as described by Maiorino et al. (Maiorino *et al.* 1998). Briefly, sample was mixed with 0.25 M tris-HCl (pH 7.4), 2.5 mM sodium azide, 0.1 mM NADPH, 12.5 mM EDTA, 2.5 mM GSH, 0.1% Triton X-100 (v/v) and 0.3 units of glutathione reductase, to a final volume of 500 µl. After pre-incubation of the reaction mixture at 37 °C for 10 minutes, the reaction was started with the addition of 25 nmoles of PCOOH. The oxidation of NADPH was recorded spectrophotometrically at 340

nm, and activity was expressed as micromoles of NADPH oxidized per minute per milligram protein in the sample. Protein was determined using a kit from BioRad (Hercules, CA) based on a modified Bradford method.

Neutral Red Cytotoxicity Assays

Lung fibroblast cells were concentrated to 500,000 cells per milliliter and plated on 30mm tissue culture plates (four islands of 25,000 cells each). After 12 hours, cells were treated with the indicated chemical for 6 hours (or 21 hours for the 24 hour treatment). At that time, treatment media was replaced with fresh media containing 0.005% NR (w/v) and cells were incubated for an additional three hours. Cells were washed in PBS, then cell-bound NR was eluted with 200 milliliters of 0.05% acetic acid in 50% ethanol. NR absorbance was recorded at 540nm on a 96-well plate reader.

Confocal Laser Cytometry

Lung fibroblast cells were plated at medium density (20,000 cells per well) on 2-well tissue culture plates with cover slip bottoms (Nunc Cat#178565, Intermountain Scientific, Kaysville, UT) and grown for 2 days with the media and conditions described above. Cells were exposed to PCOOH in media for 2 hours. During the final 20 minutes of treatment, the following vital stains were added to the treatment media, depending on the endpoint measured: 200nM MTR and 200nM MTG to measure mitochondrial membrane potential and mitochondrial mass, respectively, 2.2 mM MBB to measure reduced thiols, or 0.5 mM NAO to measure cardiolipin oxidation status. Plates were then washed in PBS, and fresh media with 20 mM HEPES and 2.2 mM probenacid. Fluorescent images were recorded on 6 randomly selected fields from each plate using confocal microscopy and image analysis (ACAS Ultima Laser Cytometer, Meridian Instruments, Okemos, MI).

Statistical analysis

All results are expressed as the mean ± standard error from three independent experiments. Enzyme activity data was analyzed for statistical differences by Student's t-test using Excel software (Microsoft Corporation, Redmond, WA). Genotype associated differences in cytotoxicity were analyzed using two-way analysis of variance (ANOVA) followed by the Bonferroni multiple comparison post-test using Prism software (Version 3.0.3, GraphPad Software Inc., San Diego, CA). All other data were analyzed using one-way ANOVA followed by either the Bonferroni (for normally distributed data) or Dunn's (for data not normally distributed) multiple comparison post-test using Prism software. A p-value of less than 0.05 was considered statistically significant.

Results

Targeted disruption of the GPx4 gene in the mouse

Two independent targeted ES clones (1-1 and 27-4) were identified as homologous recombinants by PCR amplification and verified by Southern blot analysis (Figure 2.1). The targeted ES cells were injected into mouse blastocysts and generated two lines of chimaeric mice that transmitted the targeted *GPx4* gene through the germ-line to the F1 generation. *GPx4*$^{+/-}$ males were backcrossed to wild-type C57Bl/6 females for 6 generations. The *GPx4*$^{+/-}$ mice were fertile and had no behavioral or gross morphological abnormalities. Backcrosses of line 27-4 yielded 70 males and 66 females; 67 were +/+ and 69 were +/-. Backcrosses of line 1-1 yielded 45 males and 39 females; 42 were +/+ and 42 were +/-. However, intercrosses of heterozygous males to females and *vise versa* from both lines 1-1 and 27-4 yielded 21 +/+ and 33 +/- but no -/- progeny.

We next investigated whether *GPx4*$^{-/-}$ mice died during embryonic development. We examined 16 embryos at E10.5 and 6 at E12. None of the normal embryos were homozygous null (-/-) animals. Of the 16 E10.5 embryos, two were in

advanced stages of resorption (no recognizable embryonic structures) and one was delayed (about E7). The rest appeared morphologically normal. Of the 6 at E12, two were in an advanced stage of resorption and four were morphologically normal. Therefore, expression of the mouse *GPx4* gene is essential during early embryonic development.

GPx4 activity was lower in testis, liver, and LFs from GPx4$^{+/-}$ mice relative to wild-type mice.

In order to determine if *GPx4*$^{+/-}$ mice had lower GPx4 activity relative to wild-type mice, we determined GPx4 activity in selected tissues. GPx4 has previously been shown to be most highly expressed in testicular tissue (Roveri *et al.* 1994), thus it was hypothesized that any genotype related differences would be most apparent in testis. As indicated in Figure 2.2A, GPx4 activity was indeed 37% lower in testis from heterozygous mice relative to wild-type mice (40.2$\pm$3.0 and 64.1$\pm$2.7 nmol/min/mg-protein, respectively; $p<0.001$). Genotype associated differences were less apparent in other tissues examined. Although GPx4 activity was 22% lower in liver tissue from *GPx4*$^{+/-}$ compared to wild-type mice (11.5$\pm$0.8 and 14.7$\pm$1.3; $p<0.01$), the differences for lung tissue (9.7$\pm$0.6 and 11.0$\pm$1.4) or peritoneal macrophages (5.1$\pm$0.6 and 7.3$\pm$1.5) were not statistically significant, as shown in Figure 2.2B.

After determining that some tissues from the *GPx4*$^{+/-}$ genotype could impart a detectible difference in enzymatic activity compared to wild-type, we next cultured cells from these mice in order to study the role of GPx4 in maintaining cellular redox status and mediating susceptibility to oxidative stress. We isolated lung fibroblasts (LFs) from adult mice and propagated cells representative of the two genotypes. Figure 2.3 shows enzyme activity levels from the cultured LFs. Although whole lung extract did not show genotype associated differences, GPx4 activity was significantly lower in *GPx4*$^{+/-}$ cultured LFs relative to *GPx4*$^{+/+}$ LFs (2.3$\pm$0.2 and 4.5$\pm$0.2 nmol/min/mg-protein, respectively; $p<0.001$).

$GPx4^{+/-}$ LFs are more susceptible to some forms of chemically induced cytotoxicity, but not to PCOOH.

We hypothesized that the lower GPx4 activity in the *$GPx4^{+/-}$* LFs would result in increased susceptibility to oxidative stress, particularly that induced by PCOOH, a specific substrate of GPx4. In order to test this hypothesis, we exposed cultured LFs to PCOOH for 9 hours and measured cytotoxicity using the neutral red assay. Neutral red is actively taken up into live cells in an ATP-dependent manner; dead cells do not accumulate the stain. The amount of neutral red present after a three-hour incubation followed by subsequent washing off of unincorporated stain is directly proportional to cell viability.

Surprisingly, there were no relevant genotype-related differences in susceptibility to PCOOH treatment (Figure 2.4). Viability differed between genotypes only at 1 μM PCOOH ($p \leq 0.05$), but the difference was small and viability was greater than the controls for both wild type and heterozygote cells. Viability significantly decreased compared to the same genotype control only at the highest PCOOH concentration (200 μM). PCOOH concentrations in the range of 5 to 50 μM can clearly impact cellular function, as indicated by the short-term effect on mitochondrial function (described below). However, a longer-term effect on viability at this concentration range was not apparent.

Exposure to three other chemicals that can induce oxidative stress and lipid peroxidation severely impacted cell viability. Heterozygous LFs began to exhibit significant cytotoxicity at the lowest concentration of H_2O_2 tested (25 μM), whereas wild type cells were not impacted until the 200 μM treatment (Figure 2.5A). The response was significantly different between the two genotypes at every concentration tested except the highest (400 μM). Results were similar for the other two chemicals tested. Wild type cells were more resistant to cadmium-induced cytotoxicity at concentrations between 75 and 200 μM (Figure 2.5B). The

response to cumene hydroperoxide exposure was less clear (Figure 2.5C). Although GPx4+/- cells were more susceptible to cumene hydroperoxide at 25 and 50 μM, wild type cells exhibited greater cytotoxicity at 75 μM.

Mitochondrial function and redox status are impacted in GPx4$^{+/-}$ LFs.

It has previously been demonstrated that overexpression of GPx4 protects against a PCOOH-induced reduction in mitochondrial membrane potential (Yagi *et al.* 1998). We therefore hypothesized that *GPx4*$^{+/-}$ LFs, with 50% the GPx4 activity of wild type cells, would be more susceptible to PCOOH-induced effects on the mitochondria and overall redox status. To test this, we exposed cultured LFs to 0, 5, or 50 μM PCOOH for two hours, then measured mitochondrial membrane potential with MTR and MTG, cardiolipin oxidation using NAO, and reduced thiol status using MBB, coupled with fluorescent analytical cytometry.

MTR and MTG passively diffuse through plasma membranes and are selectively retained in mitochondria. They fluoresce upon oxidation and contain a thiol-reactive chloromethyl moiety responsible for their retention in mitochondria and fixation in the fluorescent state. MTR uptake is dependent on mitochondrial membrane potential. MTG uptake is reported to be membrane potential independent (Metivier *et al.* 1998). Therefore the ratio of red (from MTR) to green (from MTG) fluorescence indicates mitochondrial membrane potential, corrected for mitochondrial number. A *GPx4*$^{+/-}$ genotype is associated with lower mitochondrial membrane potential relative to untreated wild-type LFs (Figure 2.6B and A, respectively). As expected, PCOOH induced a loss of mitochondrial membrane potential in wild-type LFs (Figure 2.6A, C, and E), as indicated by a downward shift in the red to green fluorescence ratio after a 2-hour treatment with PCOOH. *GPx4*$^{+/-}$ cells, however, were resistant to PCOOH-induced loss of membrane potential (Figure 2.6B, D, and F). In fact, mitochondrial membrane

potential was slightly increased in *GPx4*$^{+/-}$ LFs following 5μM PCOOH treatment (Figure 2.6D).

MBB passively diffuses through plasma membranes into the cytoplasm and forms blue fluorescent adducts with reduced glutathione, other low molecular weight thiols, and thiol-containing proteins. MBB is non-fluorescent until its alkylating group has reacted with a reduced thiol. Thus, the magnitude of blue fluorescence is stoichiometrically related to the number of reduced thiols present in the cell. Without treatment, *GPx4*$^{+/-}$ LFs have lower levels of reduced thiols than wild-type cells, as indicated by lower MBB blue fluorescence (Figure 2.7B and A, respectively). Although PCOOH treatment induced a shift towards lower MBB fluorescence in wild-type cells (Figure 2.7A, C, and E), indicating treatment associated thiol oxidation, less of a shift occurred in *GPx4*$^{+/-}$ cells (Figure 2.7B, D, and F), suggesting a lower sensitivity than wild-type cells to further PCOOH-induced thiol oxidation.

NAO is a cell permeant stain with high affinity for acidic phospholipids, especially cardiolipin. The two phosphate groups of a cardiolipin molecule form a dimer with the quaternary amine of NAO with 1:1 stoichiometry, increasing its affinity for cardiolipin. Upon binding a reduced cardiolipin molecule, NAO fluoresces in both red and green. NAO uptake and fluorescence is not dependent on mitochondrial membrane potential (Kirkland *et al.* 2002). *GPx4*$^{+/+}$ LFs had a higher cardiolipin content than *GPx4*$^{+/-}$ LFs without treatment (Figure 2.8A and B, respectively). Although PCOOH treatment resulted in cardiolipin oxidation in both wild-type (Figure 2.8A, C, and E) and *GPx4*$^{+/-}$ LFs (Figure 2.8B, D, and F), as indicated by a downward shift in the distribution of NAO red fluorescence, wild-type LFs were more highly impacted. After a 2-hour 50μM PCOOH treatment, cardiolipin was more oxidized in wild-type cells than heterozygous cells (Figure 2.8E and F).

Discussion

Partial GPx4 expression, as with the *GPx4*$^{+/-}$ genotype, appears to be adequate for normal development, while complete lack of GPx4 is embryonic lethal. Is this lethality due to the loss of antioxidant function of GPx4 or some other factor? Oxidative stress is recognized as an important mechanism in teratogenesis (Vismara *et al.* 2001; Wells *et al.* 1997). Apoptotic cell death represents an early event in the teratogenic process of many teratogens (Mirkes *et al.* 2000). Glutathione and GPx1 are protective against chemically-induced teratogenesis. In rodents, glutathione depletion adversely affects fetal growth and increases the number of dead and malformed embryos (Hales and Brown 1991) and increases susceptibility to chemically induced teratogenesis (Harris *et al.* 1987; Saillenfait *et al.* 1993). GPx1 depletion induced by selenium deficiency increases susceptibility to phenytoin-induced teratogenesis in mice (Ozolins *et al.* 1996). Furthermore, knockout of the glutamate cysteine ligase catalytic subunit , resulting in a complete lack of glutathione synthesis, is embryonic lethal (Dalton *et al.* 2000). Glutathione supplementation, on the other hand, is protective (Faustman-Watts *et al.* 1986; Slott and Hales 1987). Thus, it is possible that increased oxidative stress during a critical stage of development could explain the embryonic lethality of the *GPx4*$^{-/-}$ genotype. However, the importance of GPx4 beyond its role as an antioxidant has already been demonstrated for both spermatogenesis (Ursini *et al.* 1999) and inflammatory responses (Imai *et al.* 1998; Sakamoto *et al.* 2000). Similarly, there may also be an as yet unidentified function important for embryogenesis. Therefore, a function other than antioxidant protection cannot be ruled out as an explanation for the requirement of GPx4 for embryonic survival.

Mitochondrial membranes are particularly enriched in the diglycerophospholipid cardiolipin. Cardiolipin is relatively rich in unsaturated fatty acids, making it inherently susceptible to lipid peroxidation. In addition, cardiolipin associates with adenine nucleotide translocase (ANT), a component of the permeability transition

pore (PTP), and is required for its function (Hoffman *et al.* 1994) ANT regulates PTP opening and subsequent release of cytochrome *c*, a pro-apoptotic event (Halestrap *et al.* 1997; Vieira *et al.* 2000) although recent evidence suggests that ANT function is not essential for mitochondrial permeability transition (Kokoszka *et al.* 2004). The molecular weight and function of ANT can be altered under oxidative conditions and its susceptibility to oxidation depends on conformation, which is affected by the cardiolipin binding state (Hoffman *et al.* 1994). Overexpression of GPx4 suppresses the release of cytochrome C, caspase-3 cleavage, ANT inactivation and apoptosis induced by 2-deoxyglucose in RBL2H3 cells (Imai and Nakagawa 2003; Nomura *et al.* 1999). This inhibition is associated with reduced cardiolipin oxidation. Moreover, cytochrome *c* has a high affinity for cardiolipin and this affinity is lost upon cardiolipin peroxidation (Nomura *et al.* 2000; Schlame *et al.* 2000). Thus, inhibition of the pro-apoptotic signal through the mitochondrial pathway could, in part, account for the anti-apoptotic protection afforded by GPx4 overexpression.

Our results indicate that a $GPx4^{+/-}$ genotype is associated with lower mitochondrial membrane potential, lower amounts of reduced thiols, and more cardiolipin oxidation relative to wild-type. Although similar endpoints have been measured in cell lines overexpressing GPx4, this is the first report of the impact on these parameters in cells from animals underexpressing GPx4. Taken together, our results indicate that a heterozygous genotype, with lower GPx4, activity would be associated with greater susceptibility to oxidative stress. Surprisingly, we found that $GPx4^{+/-}$ LFs had lower susceptibility to PCOOH-induced oxidative stress than $GPx4^{+/+}$ LFs as indicated by a resistance to further decrements in these endpoints following a 2-hour PCOOH treatment. This resistance could not be explained by the presence of differential levels of either extracellular GPx4 activity (no GPx4 activity was detected in the culture media of either genotype, data not shown) or extracellular glutathione. As with intracellular reduced thiols, extracellular reduced

glutathione was lower in the culture media of untreated heterozygous LFs than wild type LFs (data not shown).

Although this resistance appears to contradict the protection afforded a transformed guinea pig fetal fibroblast cell line (104C1) transfected with *GPx4* reported by Yagi et al. (Yagi *et al.* 1998), in fact closer analysis shows a similarity. As we showed in our experiments, Yagi et al (Yagi *et al.* 1996) demonstrated that a high concentration of PCOOH induces cell death in wild type cells. The parental guinea pig 104C1 cells used in similar studies by this group (Sun *et al.* 1997) have GPx4 activity (4.5 mU/mg protein, where 1 U = 1 mM NADPH consumed/min) which is similar to the LFs we derived from GPx4 +/+ mice (Figure 2.3). And as with our mouse lung fibroblast cells, the wild type guinea pig 104C1 cells were susceptible to cell death at a high concentration of PCOOH (300 μM). The fact that 104C1 cells transfected with *GPx4* were resistant to cytotoxicity is not relevant to our experiments because our LFs do not have the same level of activity as the transfected 104C1 cells (Sun *et al.* 1997; Yagi *et al.* 1996). Furthermore, it is difficult to directly compare susceptibility because Yagi and colleagues used only one treatment concentration. In addition, unlike the fetal cell line used in the overexpression studies by Yagi and colleagues, the lung fibroblasts lines used in our experiments were derived from adult animals. As a result, other compensatory mechanisms may have been upregulated in the highly oxidized environment in which they differentiated. By comparison with a PCOOH treatment concentration within the range of concentrations used in our study, Kaneko et al. (Kaneko *et al.* 2000) exposed cultured human umbilical vein endothelial cells to 100 μM PCOOH with only minimal toxicity (approximately 80% survival after 14 hrs). This same group has shown that the peroxidized free fatty acid components of phosphatidylcholine are much more toxic than the parent peroxidized phospholipid (Kaneko *et al.* 1994).

Peroxiredoxins and GSTs are two examples of alternative enzyme classes with low activity towards phospholipids hydroperoxides. For example, peroxiredoxin 6 has activity towards phospholipids hydroperoxides and is found in all major mammalian organs, but is particularly highly expressed in the lung (Manevich and Fisher 2005). Purified human GSTs of alpha, mu, and theta class exhibit glutathione peroxidase activity towards phospholipids hydroperoxides, albeit with much lower specific activity than GPx4 (Hurst *et al.* 1998). Furthermore, the relatively small genotype related differences in GPx4 activity we found in liver and kidney might be explained by the high GST content in these tissues. It is possible that other antioxidant enzymes, even with low or no specific activity towards phospholipids hydroperoxides, may compensate for increased production of reactive oxygen species when GPx4 levels are reduced. Although levels of one candidate, superoxide dismutase 2 (SOD2), were the same in GPx4 heterozygous LFs than wild type LFs (data not shown). By the same token, GPx4 knockout embryos may survive to a specific stage in development through the protection afforded by another antioxidant enzyme that is downregulated during some critical stage of development coinciding with the timing of embryonic lethality of GPx4 homozygous knockouts. Alpha class GSTs have phospholipid hydroperoxide activity (Yang *et al.* 2001), and what they lack in specific activity relative to GPx4 may be compensated by the higher concentrations present. While GST alpha is expressed in most tissues during embryonic development (Raijmakers *et al.* 2001), the specific timing of expression is unknown. Another candidate, peroxiredoxin 1, is downregulated in murine interdigital cells at embryonic day 13.5, when these cells commit to apoptotic death (Shan *et al.* 2005), while peroxiredoxin 6 is present in the early stage bovine embryos but downregulated by the 16-cell stage (Leyens *et al.* 2004).

Yant et al. (Yant *et al.* 2003) have also reported that a GPx4 homozygous knockout is embryonic lethal in their transgenic mouse model. Embryonic fibroblasts (EFs)

derived from *GPx4*$^{+/-}$ mice had reduced levels of GPx4 mRNA and protein, were more susceptible to tert-butyl peroxide and H_2O_2-induced cell death, and had lower colony formation following UV radiation and paraquat treatment, relative to wild-type EFs (Ran *et al.* 2003; Yant *et al.* 2003). The relative sensitivity of *GPx4*$^{+/+}$ and *GPx4*$^{+/-}$ cells to 100 μM and 200 μM H_2O_2 was similar for the Yant et al. (Yant *et al.* 2003) EFs and our LFs (approximately 30 to 40 percent in heterozygous cells relative to wild type cells). However, at 400 μM H_2O_2 survival was very low (25 to 30 percent of controls) for both our heterozygous and wild type LFs, whereas survival in the Yant et al. heterozygous EFs was approximately one-third that of wild type cells at this concentration. In fact, survival appeared to be the same in heterozygous EFs at all concentrations of H_2O_2 tested (100 to 800 μM), whereas wild type survival decreased with increasing H_2O_2 concentrations.

The observations of Yant et al. (Yant *et al.* 2003) suggest that *GPx4* null embryos exhibit morphological abnormalities between 6.5 and 7.5 days post coitum (dpc) and are resorbed by 8.0 to 8.5 dpc. The mechanism of embryonic lethality is uncertain. Yant and colleagues (Yant *et al.* 2003) found no evidence of differences in either cellular proliferation or the number of apoptotic cells in *GPx4* null embryos at 7.5 dpc relative to wild-type embryos. In addition to its antioxidant role, the authors suggest a critical role in cell signaling could play a part. Overexpression of GPx4 in rat basophile leukemia cells inhibits 2-deoxyglucose induced cytochrome c release and cardiolipin oxidation (Nomura *et al.* 2000). Imai et al. (Imai *et al.* 2003) reported that the *GPx4* null genotype in their mice resulted in embryonic death during early gastrulation, between 7.5 and 8.5 dpc. Immunohistochemical analysis showed that GPx4 was first detected in the embryonic ectoderm and the yolk sac membrane at 7.5 dpc in *GPx4*$^{+/+}$ and *GPx4*$^{+/-}$ embryos, but was absent in the *GPx4*$^{-/-}$ embryos. Thus, timing of expression of GPx4 coincided with the timing of embryonic death in *GPx4*$^{-/-}$ embryos.

We also report differences in GPx4 activity in tissues from adult *GPx4*$^{+/+}$ and *GPx4*$^{+/-}$ mice. Most noteworthy are the 37% reduction in activity in testes tissue and 22% reduction in liver tissue. This is similar to the 36% and 24% reductions reported by Scimeca et al. (Scimeca *et al.* 2005) for testes and liver tissue, respectively. Two reports provide evidence that genotypic and/or phenotypic differences in GPx4 exist in human populations, and that these differences may be associated with disease outcomes. Imai et al. (Imai *et al.* 2001) reported that decreased levels of GPx4 in spermatozoa of infertile Japanese males were associated with oligoasthenozoospermia, a condition characterized by abnormally low sperm count and motility. GPx4 deficient spermatozoa were characterized by morphological abnormalities in their mitochondria, and reduced mitochondrial membrane potential compared to spermatozoa from fertile males. In another study, Villette and colleagues (Villette *et al.* 2002) described a T/C single nucleotide polymorphism at position 718 of the GPx4 gene in the region corresponding to the 3'UTR in a group of Scottish volunteers. Although there were no significant differences in GPx4 activity, the C/C718 variant was associated with significantly higher levels of 5-lipoxygenase metabolites, suggesting that the polymorphism may impart functional differences in the modulation of inflammatory processes. Considering the embryonic lethality of the *GPx4*$^{-/-}$ genotype, the heterozygous null model that gives reduced expression is likely to more closely mimic the condition in human populations, and provide the means to understand the potential role of GPx4 in human disease and the underlying mechanisms of action.

Figure 2.1 – Targeted disruption of *GPx4* in the mouse.
Targeted disruption of *GPx4* in the mouse. (**A**) Strategy for-homologous recombination between the wild type *GPx4* gene and the targeting vector to produce the targeted allele in which part of exon 1, introns 1 and part of exon 2 are replaced by vector sequences containing the β-galactosidase (*LacZ*) and neomycin resistance (*NeoR*) genes. Targeted recombination deleted the two herpes simplex virus thymidine kinase (HSVTK) genes that flank the *lacZ* and *NeoR* genes in the vector. The horizontal solid arrows denote primers used in genotyping mouse tissues by PCR amplification. Solid boxes represent exons and thin lines represent introns *GPx4*. The double-headed arrow represents the probe used in Southern blot analysis. X's represent sites of homologous recombination. A, *Afl* II; H, *Hind* III; E, *Eag* I, R, *EcoR* I. (**B**) Autoradiograph of Southern blot used to detect the wild-type and targeted alleles. Genomic DNA was digested with Hind III and electrophoresed on a 1% agarose gel. The probe indicated in (A) was used to detect the ~14 kb and ~6 kb fragments generated from the wild type and the targeted alleles, respectively. The *GPx4* genotypes are indicated above the lanes.
(**C**) Detection of the wild type and targeted alleles by PCR amplification. The top panel shows a photograph of an agarose gel on which DNA fragments (375 bp) amplified by primer pair Pr5F and NZTK (see A), specific for the targeted allele, were resolved. Bottom panel; DNA fragments (300 bp), amplified from the same mice as in the top panel, by primer pair Pr5F and I-1R (see A), specific for the wild type allele, are shown. The *GPx4* genotypes are indicated above the lanes. M, molecular weight marker. Note that only $GPx4^{+/+}$ and $GPx4^{+/-}$ mice were detected.

A.

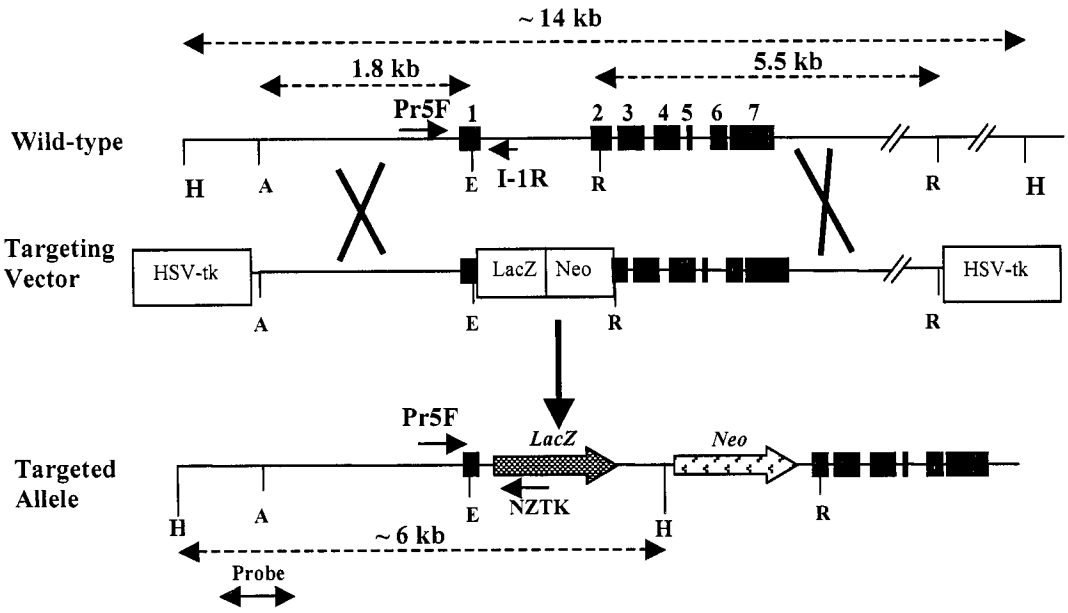
~ 14 kb
1.8 kb
5.5 kb
Pr5F
1
2 3 4 5 6 7
Wild-type
H
A
E
I-1R
R
R
H
Targeting Vector
HSV-tk
LacZ
Neo
HSV-tk
A
E
R
R
Pr5F
LacZ
Neo
Targeted Allele
H
A
E
NZTK
R
H
~ 6 kb
Probe

B.

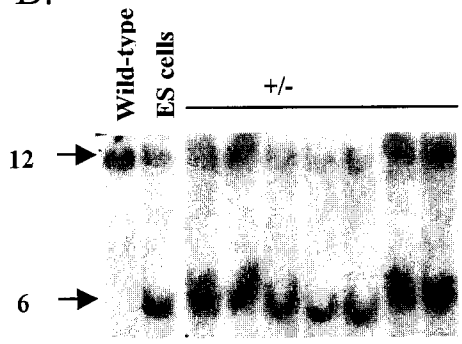
Wild-type
ES cells
+/-
12
6

C.

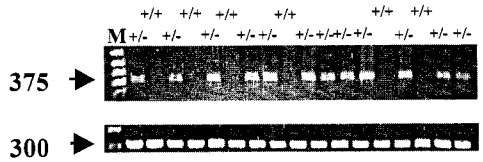
M
375
300

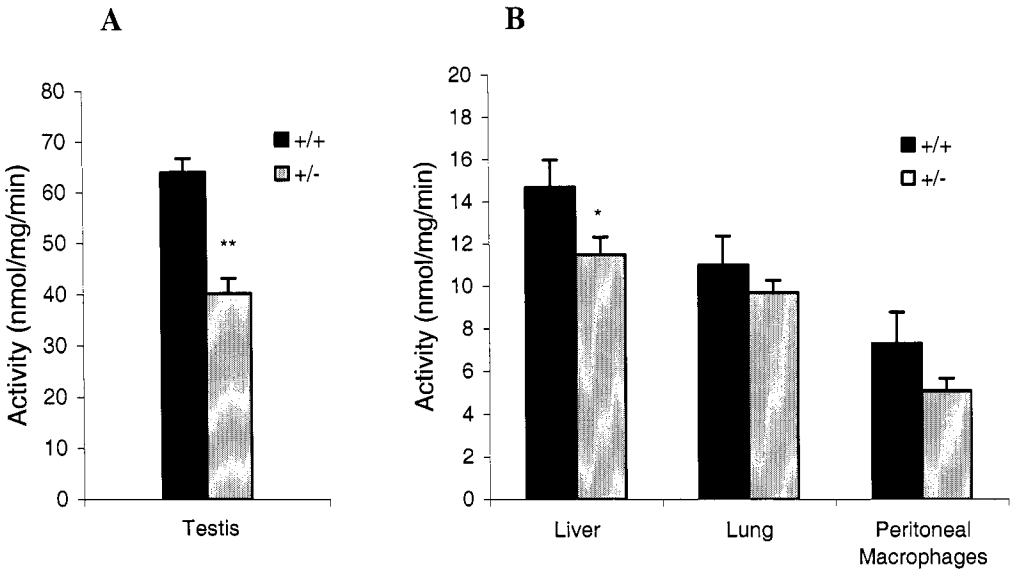

Figure 2.2 – GPx4 activity in selected tissues from *GPx4*$^{+/+}$ and *GPx4*$^{+/-}$ mice. GPx4 activity in selected tissues from *GPx4*$^{+/+}$ and *GPx4*$^{+/-}$ mice (mean + SEM). Whole tissue extracts were isolated from frozen testes, liver, and lung from *GPx4*$^{+/+}$ and *GPx4*$^{+/-}$ mice. Peritoneal macrophages extracts were prepared from fresh cells. Extracts were assayed for GPx4 activity as described in Methods. Sample sizes ranged from 4 (for peritoneal macrophages) to 15 (for testicular tissue). (A). GPx4 activity was approximately 40% lower in testes from *GPx4*$^{+/-}$ mice relative to the *GPx4*$^{+/+}$ mice. (B). GPx4 activity was approximately 20% lower in liver from *GPx4*$^{+/-}$ mice relative to the *GPx4*$^{+/+}$ mice. There were no significant genotype related differences in GPx4 activity in lung tissue or peritoneal macrophages. (*$p<0.05$;**$p<0.001$).

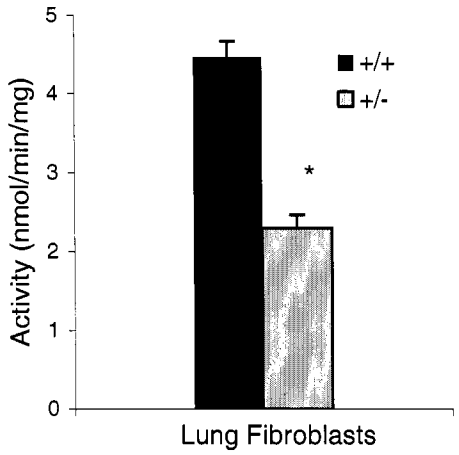

Figure 2.3 – GPx4 activity in cultured lung fibroblast cells from *GPx4*$^{+/+}$ and *GPx4*$^{+/-}$ mice.

GPx4 activity in cultured lung fibroblast cells from *GPx4*$^{+/+}$ and *GPx4*$^{+/-}$ mice (mean + SEM). Fibroblast cells were grown out from freshly isolated lung tissue from *GPx4*$^{+/+}$ and *GPx4*$^{+/-}$ mice, as described in Methods. Cell extracts were assayed for GPx4 activity as described in Methods. GPx4 activity was approximately 50% lower in *GPx4*$^{+/-}$ cells relative to *GPx4*$^{+/+}$ cells. (*$p<0.001$).

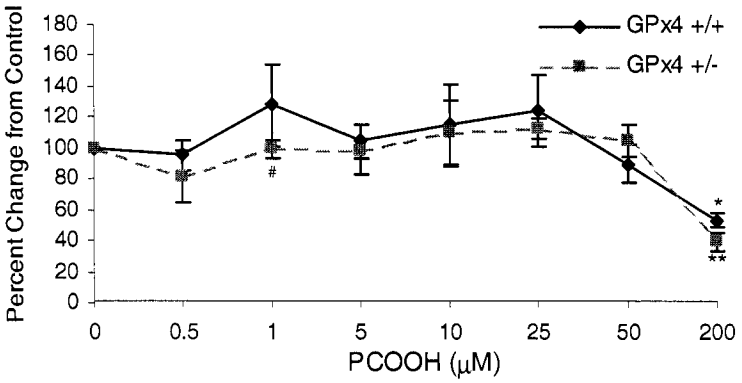

Figure 2.4 – Cytotoxicity in cultured lung fibroblasts from *GPx4*$^{+/+}$ and *GPx4*$^{+/-}$ mice.

Cytotoxicity in early passage lung fibroblasts was assessed using neutral red, as described in Methods. Results are expressed as the percent change from the control and represent the combined data from at least three independent experiments (mean ± SD). Cells from both genotypes were sensitive to PCOOH-induced cytotoxicity only at 200 μM PCOOH (*$p<0.05$; **$p<0.001$). A genotype-associated difference in cytotoxicity was observed only at 1 μM PCOOH (#$p<0.05$), but the difference was small and survival was not significantly different that than the controls for either genotype.

Figure 2.5 – Cytotoxicity in cultured lung fibroblasts from *GPx4*$^{+/+}$ and *GPx4*$^{+/-}$ mice.

Cytotoxicity in early passage lung fibroblasts was assessed using neutral red, as described in Methods. Results are expressed as the percent change from the control and represent the combined data from at least three independent experiments (mean ± SD). (A). *GPx4*$^{+/-}$ LFs were more sensitive to H_2O_2-induced cytotoxicity than *GPx4*$^{+/+}$ LFs. (B). *GPx4*$^{+/-}$ LFs were more sensitive to cadmium-induced cytotoxicity than *GPx4*$^{+/+}$ LFs. (C). *GPx4*$^{+/-}$ LFs were more sensitive to cumene hydroperoxide (CuOOH)-induced cytotoxicity than *GPx4*$^{+/+}$ LFs. Significant differences from same genotype control are indicated (*$p<0.05$; **$p<0.001$). Significant differences from *GPx4*$^{+/+}$ genotype cells at same concentration are indicated ($^{\#}p<0.05$; $^{\#\#}p<0.001$).

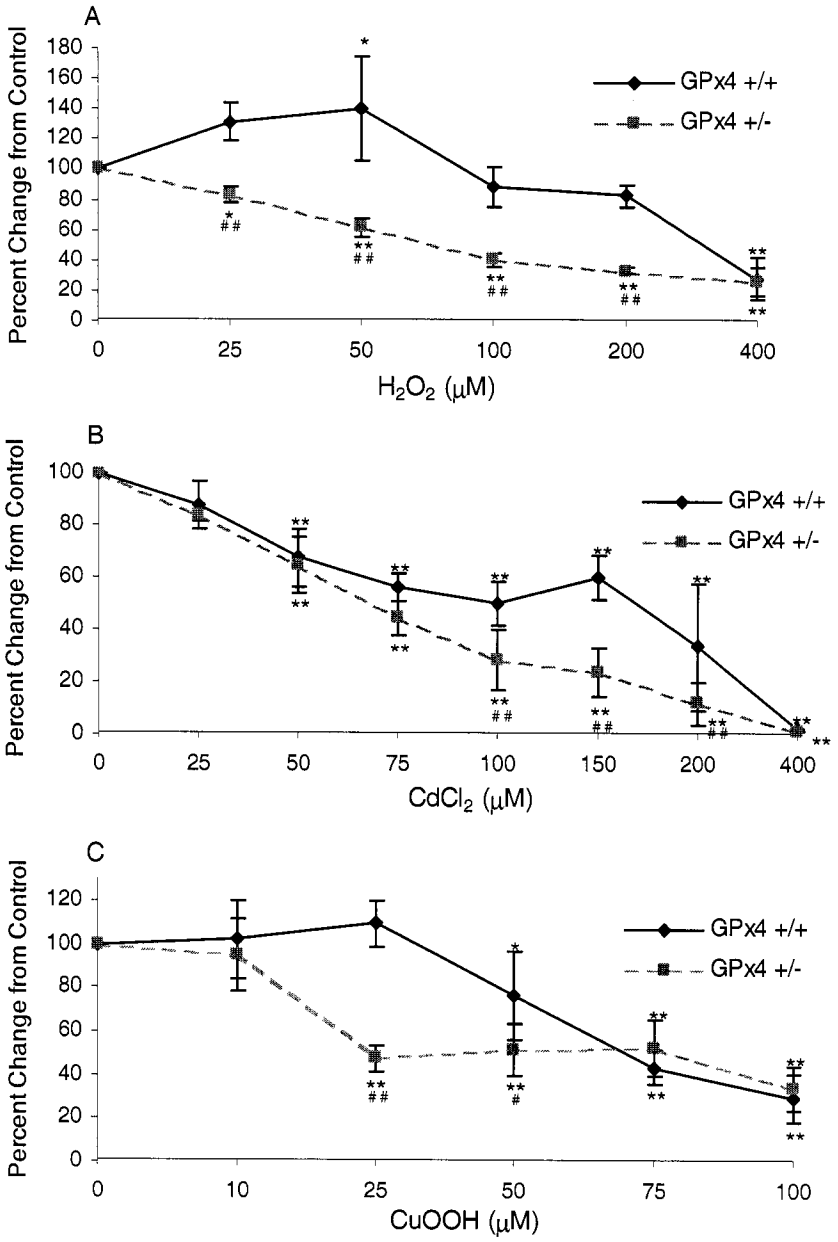
A
Percent Change from Control
180
160
140
120
100
80
60
40
20
0
0
25
50
100
200
400
H2O2 (μM)
GPx4 +/+
GPx4 +/-
B
Percent Change from Control
100
80
60
40
20
0
0
25
50
75
100
150
200
400
CdCl2 (μM)
GPx4 +/+
GPx4 +/-
C
Percent Change from Control
120
100
80
60
40
20
0
0
10
25
50
75
100
CuOOH (μM)
GPx4 +/+
GPx4 +/-

Figure 2.6 – Mitochondrial membrane potential in lung fibroblasts treated with PCOOH.

Cells were incubated for 2 hours with the indicated concentration of PCOOH. For the final 20 minutes of treatment, Mitotrackers red (MTR) and green (MTG) were added to the culture medium. Images were recorded of 6 randomly selected fields from each plate. Red and green fluorescence were quantified in each cell of all images recorded. The ratio of red (from MTR) to green (from MTG) fluorescence indicates mitochondrial membrane potential corrected for mitochondrial number. Results are expressed as distributions of red/green fluorescence for all values recorded. A shift downward in the red/green ratio (i.e., to the left along the x-axis) indicates a lower mitochondrial membrane potential. A $GPx4^{+/-}$ genotype is associated with lower mitochondrial membrane potential relative to wild-type cells in cultured LFs without treatment (Figure 2.6B and A, respectively). PCOOH induced a loss of mitochondrial membrane potential in wild-type LFs (Figure 2.6A, C, and E), as indicated by a downward shift in red to green fluorescence after a 2-hour treatment with PCOOH. $GPx4^{+/-}$ cells, however, were resistant to PCOOH-induced loss of membrane potential (Figure 6B, D, and F); mitochondrial membrane potential was slightly increased in $GPx4^{+/-}$ LFs following 5μM PCOOH treatment (Figure 2.6D). Results are combined from two separate experiments. (* significantly different than same genotype control at $p<0.05$ (*) or $p<0.001$ (**); # significantly different than $GPx4^{+/+}$ genotype cells at same concentration at $p<0.001$).

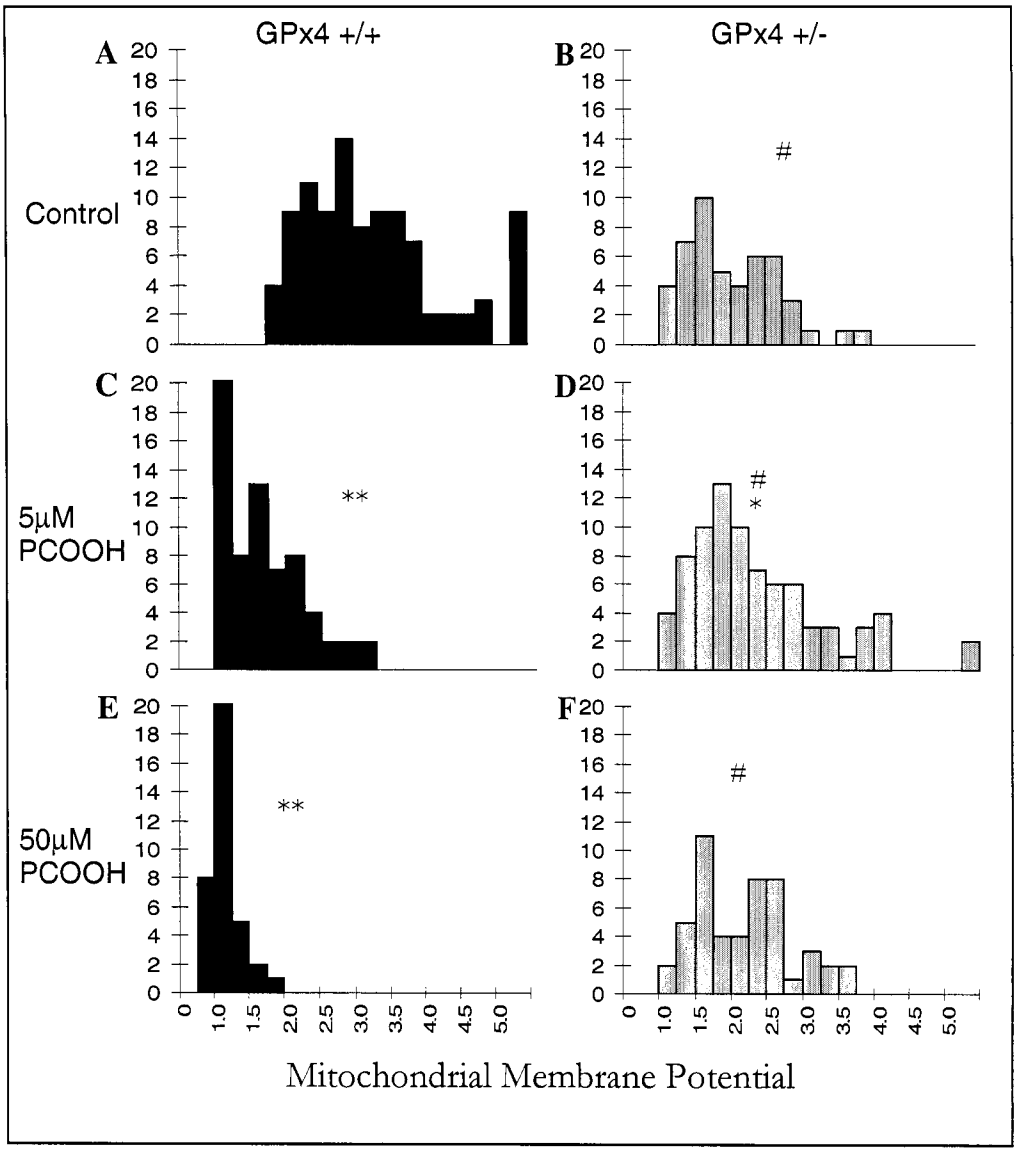
GPx4 +/+
GPx4 +/-
A
B
C
D
E
F
Control
5μM PCOOH
50μM PCOOH
0 2 4 6 8 10 12 14 16 18 20
0 1.0 1.5 2.0 2.5 3.0 3.5 4.0 4.5 5.0
**
#
*
Mitochondrial Membrane Potential

Figure 2.7 – Reduced thiol status in lung fibroblasts treated with PCOOH. Cells were incubated for 2 hours with the indicated concentration of PCOOH. For the final 20 minutes of treatment, MBB was added to the culture medium. Images were recorded of 6 randomly selected fields from each plate. Blue fluorescence was quantified in each cell of all images recorded. Results are expressed as distributions of blue fluorescence for all values recorded. A shift downward in blue fluorescence (i.e., to the left along the x-axis) indicates lower amounts of reduced thiols. Without treatment, *GPx4*$^{+/-}$ LFs have lower levels of reduced thiols than wild-type cells, as indicated by lower MBB blue fluorescence (Figure 2.7B and A, respectively). PCOOH treatment induced a shift towards lower MBB fluorescence in wild-type cells (Figure 2.7A, C, and E), indicating treatment associated thiol oxidation. Less of a shift occurred in *GPx4*$^{+/-}$ cells (B, D, and F), suggesting a lower sensitivity relative to wild-type cells to further PCOOH-induced thiol oxidation. Results are combined from two separate experiments. (* significantly different than same genotype control at $p<0.05$ (*) or $p<0.001$(**); # significantly different than *GPx4*$^{+/+}$ genotype cells at same concentration at $p<0.001$).

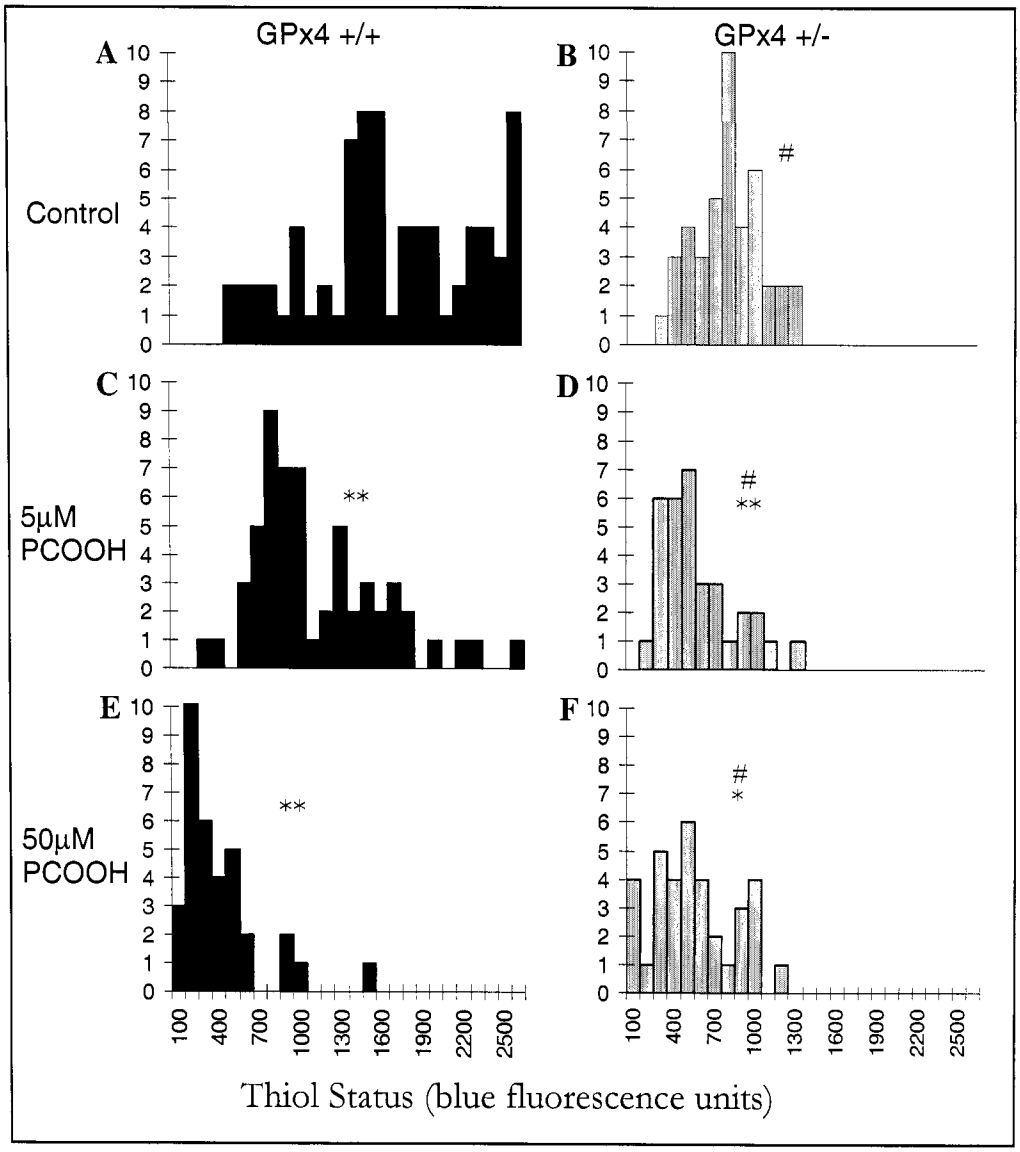
GPx4 +/+
GPx4 +/-
A
B
C
D
E
F
Control
5μM PCOOH
50μM PCOOH
#
**
#
**
#
*
0 1 2 3 4 5 6 7 8 9 10
100 400 700 1000 1300 1600 1900 2200 2500
Thiol Status (blue fluorescence units)

Figure 2.8 – PCOOH treatment induces cardiolipin oxidation in both *GPx4*$^{+/-}$ and *GPx4*$^{+/+}$ cultured lung fibroblasts.
Cells were incubated for 2 hours with the indicated concentration of PCOOH. For the final 20 minutes of treatment, nonyl acridine orange (NAO) was added to the culture medium. Images were recorded of 6 randomly selected fields from each plate. Red fluorescence was quantified in each cell of all images recorded. Results are expressed as distributions of red fluorescence for all values recorded. A shift downward in red fluorescence (i.e., to the left along the x-axis) indicates lower cardiolipin content (i.e., a greater degree of cardiolipin oxidation). *GPx4*$^{+/+}$ LFs had higher cardiolipin content than *GPx4*$^{+/-}$ LFs without treatment (A and B, respectively). PCOOH treatment resulted in cardiolipin oxidation in both wild-type (A, C, and E) and GPx4$^{+/-}$ LFs (B, D, and F), as indicated by a downward shift in the distribution of red fluorescence. Wild-type LFs were more highly impacted than GPx4$^{+/-}$ LFs, shown as a greater downward shift in red fluorescence with PCOOH treatment. After a 2-hour 50μM PCOOH treatment, wild-type cells had a lower cardiolipin content than *GPx4*$^{+/-}$ cells (E and F). Results are combined from two separate experiments. (** significantly different than same genotype control at $p<0.001$; # significantly different than *GPx4*$^{+/+}$ genotype cells at same concentration at $p<0.001$).

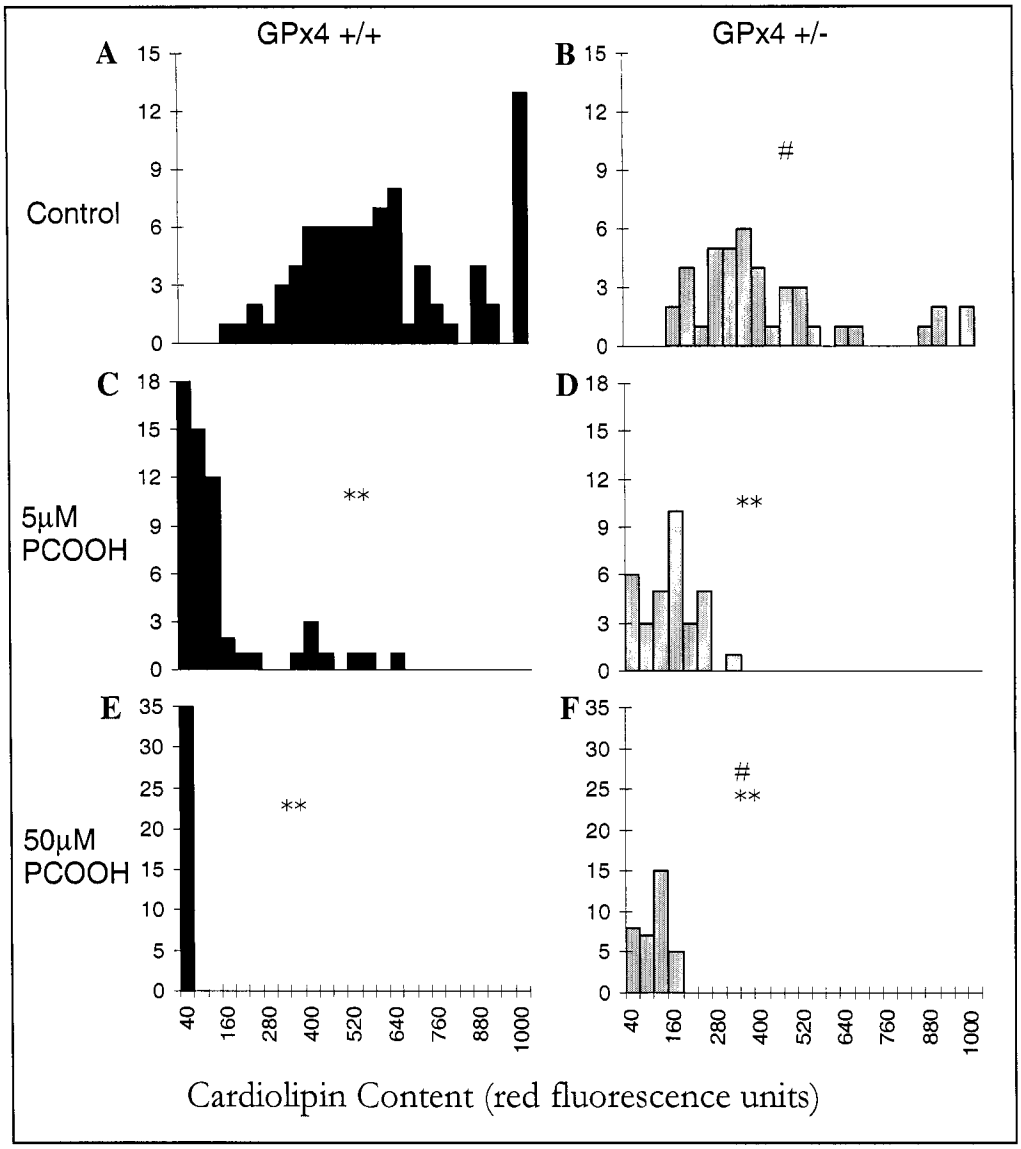
GPx4 +/+
GPx4 +/-
A
B
C
D
E
F
Control
5μM PCOOH
50μM PCOOH
#
**
Cardiolipin Content (red fluorescence units)

Chapter 3 – Differential modulation of stress and ubiquitination signaling pathways by cadmium in cultured mouse lung fibroblasts heterozygous for GPx4

Summary of Chapter 3

Cadmium is a widely dispersed environmental and occupational toxicant and has been associated with mutagenic, carcinogenic, teratogenic and neurotoxic endpoints. Inhalation exposure to cadmium has been associated with airway inflammation, pulmonary edema, emphysema, and cancer. Cadmium causes oxidative stress in cells by formation of reactive oxygen species (ROS), induction of lipid peroxidation, binding to protein thiols, and alteration of intracellular glutathione status. Oxidative stress can lead to structural changes in proteins, ubiquitination of the damaged proteins, and subsequent proteolysis of the ubiquitin-tagged proteins. In mouse neuronal cells and yeast, cadmium has been shown to affect the ubiquitin-proteasome pathway (UPS) through an accumulation of ubiquitinated proteins. Glutathione peroxidase 4 (GPx4) is a member of the family of selenium dependent enzymes that catalyze the reduction of peroxides. GPx4 specifically reduces mitochondrial membrane-bound phospholipid hydroperoxides *in situ* and thus, protects against membrane peroxidative damage. Mouse lung fibroblasts deficient in GPx4 have increased susceptibility to cadmium-induced cytotoxicity. In the present study cultured mouse lung fibroblasts from wild-type (+/+) and GPx4 heterozygous (+/-) mice were exposed to cadmium chloride ($CdCl_2$), and cell extracts were analyzed for stress (p38, JNK), survival (Akt), apoptotic (caspase 3) and proteosomal (ubiquitin-conjugated proteins) pathway activation by Western blot analyses. A differential response was observed between the two genotypes for each of the endpoints measured. Levels of phosphorylated p38 and JNK were increased following $CdCl_2$ treatment in $GPx4^{+/+}$ cells, but less so in $GPx4^{+/-}$ cells. Phosphorylated Akt levels, though decreased slightly, remained high in $GPx4^{+/+}$ cells, but dropped to only 10% or less of control in

GPx4$^{+/-}$ cells. However, *GPx4*$^{+/-}$ cells exhibited an attenuated survival response, as measured by the ratio of survival pathway activation (Akt) to stress pathway activation (p38 and JNK). *GPx4*$^{+/-}$ cells also exhibited a higher level of caspase-3 activation and diminished accumulation of high molecular weight poly-ubiquitinated proteins than *GPx4*$^{+/+}$ cells in response to $CdCl_2$ treatment. These results implicate the involvement of survival and stress signaling pathways and the ubiquitin proteasomal system in cadmium-induced cytotoxicity, and the potential involvement of these pathways in the differential susceptibility to cadmium-induced stress in cells deficient in GPx4. Efforts are currently underway to identify specific targets of cadmium-induced ubiquitination to further elucidate the key players in this susceptibility.

Introduction

Cadmium is a widely dispersed environmental and occupational toxicant and has been associated with mutagenic, carcinogenic, teratogenic and neurotoxic endpoints (Chang 1996) (Filipic *et al.* 2006) (Goering *et al.* 1994). Outside of occupational settings, the most significant sources of human exposure to cadmium are the diet and cigarette smoke (Satarug *et al.* 2003; Satarug and Moore 2004). Inhalation exposure to cadmium has been associated with airway inflammation (Kirschvink *et al.* 2006), pulmonary edema (Beton *et al.* 1966), emphysema (Davison *et al.* 1988; Leduc *et al.* 1993), and cancer (Stayner *et al.* 1992; Takenaka *et al.* 1983; Thun *et al.* 1985). Exposure to cadmium is linked with numerous detrimental molecular events including cytotoxicity (Son *et al.* 2001), increased reactive oxygen species (ROS) (Lopez *et al.* 2006) (Alvarez *et al.* 2004), lipid peroxidation (Lopez *et al.* 2006), DNA damage (Fernández *et al.* 2003), and apoptosis (Watjen and Beyersmann 2004). These responses have been observed in numerous cell types, at various exposure levels. However, their underlying mechanisms have yet to be fully characterized.

Numerous studies have demonstrated the significant role of oxidative stress in cadmium related toxic responses (Lopez *et al.* 2006) (Huang *et al.* 2006) (Elbekai and El-Kadi 2005) (Watjen and Beyersmann 2004) (Alvarez *et al.* 2004). Cadmium exposure has been shown to generate reactive oxygen species through the depletion of glutathione and protein-bound sulfhydroxyl groups leading to lipid peroxidation and apoptosis (Stohs *et al.* 2001). In addition, cadmium-induced apoptosis is attenuated with the addition of antioxidants, further supporting a role for oxidative stress in cadmium toxicity (Poliandri *et al.* 2003). One of the main signaling pathways involved in both the stress response and apoptosis is the mitogen-activated protein kinase pathway (MAPK). Key players in this cascade are the stress-activated kinases p38 MAPK and SAPK/JNK, whose activation modulate cell growth and apoptotic response to stress (Torres and Forman 2003).

MAPK-mediated signaling pathways are involved in cadmium-induced cell cycle arrest (Chao and Yang 2001), cytotoxicity (Rockwell *et al.* 2004) and apoptosis (Kefaloyianni *et al.* 2005; Lag *et al.* 2005) (Kim *et al.* 2005) (Jonak *et al.* 2004). Both phosphorylated p38 and JNK levels were increased in rat lung primary alveolar type 2 cells and Clara cells following 10μM cadmium acetate. Levels increased within 15 minutes to 2 hours and remained elevated for as long as 12 hours (Lag *et al.* 2005). On the other hand, p38 activation is blocked in rat basophile leukemia cells that overexpress GPx4 and are resistant to oxidative stress induced cytotoxicity (Sakamoto *et al.* 2002). The roles of p38 and JNK in cadmium-induced apoptosis have predominately been reported to involve caspase-3 dependent mechanisms (Kefaloyianni *et al.* 2005; Kim and Sharma 2004, 2006; Lee *et al.* 2005; Papadakis *et al.* 2006), although a caspase-3 independent pathway has also been reported for mouse neuronal cells following cadmium exposure (Rockwell *et al.* 2004).

The ubiquitin proteasomal system (UPS) may also play a role in cadmium-induced oxidative stress and cytotoxicity. The UPS regulates cellular proteins such as p53 and p21, key proteins involved in cell cycle regulation, cellular stress responses and apoptosis (Naujokat and Hoffmann 2002). A dysfunctional UPS can lead to the accumulation of damaged proteins and lead to cytotoxicity. Cadmium-mediated oxidative stress has been linked to the accumulation of high molecular weight polyubiquitinated protein conjugates (HMW-Ub) (Figueiredo-Pereira *et al.* 1997). In addition, defects in the UPS have been shown to sensitize cells to cadmium (Tsirigotis *et al.* 2001).

Glutathione peroxidase 4 (GPx4), also known as phospholipid hydroperoxide glutathione peroxidase, is a member of the family of selenium dependent enzymes that catalyze the reduction of peroxides using glutathione or other thiols (e.g., cysteine, thioredoxin) as reducing agents (Imai and Nakagawa 2003; Takebe *et al.*

2002). GPx4 has a high specific affinity for larger, membrane bound substrates such as phospholipid and cholesterol hydroperoxides, can associate with cellular membranes, and directly reduces membrane bound hydroperoxides *in situ*, thus protecting against membrane damage. Studies using mice heterozygous for GPx4 demonstrated that it plays a critical role in antioxidant defense (Garry *et al.* 2006; Yant *et al.* 2003). Embryonic fibroblasts heterozygous for GPx4 ($GPx4^{+/-}$) exhibit an increased sensitivity to oxidative stress induced by t-butyl hydroperoxide (t-BuOOH) (Ran *et al.* 2003) and mice that over-express GPx4 showed protection against t-BuOOH and diquat-induced apoptosis (Ran *et al.* 2004). Lung fibroblasts (LFs) from adult $GPx4^{+/-}$ mice have increased sensitivity to cadmium and hydrogen peroxide-induced cytotoxicity, and exhibit constitutively lower reduced thiol levels and increased cardiolipin oxidation relative to LFs from $GPx4^{+/+}$ mice, as described in Chapter 2 and elsewhere (Garry *et al.* 2006). In the present study, we investigate the role of oxidative stress and the UPS in the differential susceptibility to cadmium-induced toxicity in $GPx4^{+/-}$ LFs. We demonstrate differential cadmium-induced stress and apoptotic signaling responses associated with the $GPx4^{+/-}$ genotype, along with alterations in the ubiquitin proteosomal pathway.

Materials and Methods

Reagents

Dulbecco's modified Eagle's medium (DMEM), fetal bovine serum (FBS) and penicillin-streptomycin liquid (PenStrep) were purchased from Gibco BRL (Grand Island, NY). Cadmium chloride ($CdCl_2$) and neutral red (NR) were purchased from Sigma (St. Louis, MO, USA).

Lung Fibroblast Isolation and Culture

Generation of the transgenic $GPx4^{+/-}$ mice and lung fibroblast cell isolation was previously described in Chapter 2 and elsewhere (Garry *et al.* 2006). Briefly,

freshly dissected lung tissue was macerated with sterile razor blades in 100mm tissue culture plates with 1 ml of medium (DMEM supplemented with 10% FBS (v/v), 100 μg/ml streptomycin, 100 units/ml penicillin, and 2 mM L-glutamine). The resulting slurry was mixed with 10ml of medium and cells and tissue fragments were allowed to adhere to tissue culture plates. The plates were incubated for 7-10 days at 37°C in a humidified atmosphere of 95% air/5% CO_2. Fibroblasts that migrated out of the tissue fragments were trypsinized and diluted into 10 plates for further passage, experimentation, and/or storage at -80°C. All experiments were conducted on cells in passage two through seven.

Neutral Red Cytotoxicity Assays

The neutral red cytoxicity assay was conducted as described previously in Chapter 2 and elsewhere (Garry *et al.* 2006). Briefly, lung fibroblast cells were concentrated to 500,000 cells per milliliter and plated on 30mm tissue culture plates (four islands of 25,000 cells each) and allowed to attach and stabilize for 12 hours. Cells were then treated with $CdCl_2$ for 6 hours, at which point treatment media was replaced with fresh media containing 0.005% NR (w/v) and cells were incubated for an additional three hours. Cells were washed in PBS, and then cell-bound NR was eluted with 200 milliliters of 0.05% acetic acid in 50% ethanol. NR absorbance was recorded at 540nm on a 96-well plate reader.

Cultured Lung Fibroblast Treatment, Harvest, and Protein Determination

Serial dilutions were prepared from a stock solution of $CdCl_2$ and added to culture medium at the indicated concentrations. Cadmium containing medium was added directly to the tissue culture plates to initiate exposures. Cell morphology was recorded at the beginning of the exposures and at the stated time intervals. At the appropriate time points, cultured cells were rinsed twice with ice-cold phosphate buffered saline (PBS). Cell lysis buffer (Cell Signaling Technology Inc, Beverly, MA) was added to each dish and cells were scraped with a rubber policeman.

Harvested cells were subjected to three successive freeze thaw cycles using liquid nitrogen, and cell lysates were centrifuged at 16,000 x g for 15 min at 4°C. Supernatant fractions were transferred to clean tubes and stored at -80°C until assayed after an aliquot was removed for protein determination using a commercially available kit (Protein Assay kit, Bio-Rad Laboratories, Hercules, CA) with bovine serum albumin as a standard.

Cell Morphology and Imaging

All cultures were viewed with a Nikon inverted microscope equipped with phase-contrast optics (Nikon, Tokyo, Japan) to qualitatively assess general appearance and viability. At least three fields of view were photographed for each treatment and time point, and the experiments were replicated at least three times. Images were captured and digitized using a Coolsnap Camera (Roper Scientific Incorporated, Duluth, GA). The digitized image was processed using Photoshop Elements 1.0.1 (Adobe Systems Incorporated, San Jose, CA).

Western Blot Analysis

Western blot analyses were performed according to previously described methods (Yu *et al.*, 2001; Sidhu *et al.*, 2004). Gels were transferred to PVDF membranes (Millipore, Billerica, MA) using a vertical transfer apparatus (Bio-Rad Laboratories, Hercules, CA). Membranes were rinsed briefly in Tris buffered saline, pH 7.6 (TBS), blocked with 5% nonfat dried milk in TBS with 0.1% Tween-20 (TTBS) for 20 min and rinsed again with TTBS. Membranes were then incubated overnight with primary antibody followed by four washes with TTBS. The primary antibodies included phosphor-p38 MAPK and non-phosphorylated p38, phospho-SAPK/JNK, phospho-Akt and non-phosphorylated Akt, cleaved caspase-3 and uncleaved caspase-3, and high molecular weight polyubiquitin (Cell Signaling, Inc, Beverly, MA). β-Actin (Santa Cruz Biotechnology, Inc. Santa Cruz, CA) was also analyzed to corroborate other measures of protein loading. After

hybridization with relevant secondary antibodies conjugated to horseradish peroxidase, the resulting immuno-complex was detected with the ECL detection reagent (Amersham Biosciences Corp, Piscataway, NJ) followed by exposure to X-ray films. The resulting films were scanned using HP Scanjet 5400C scanner equipped with Precisionscan Pro 3.1 software and the TIF image data were analyzed. Band density was analyzed using ImageJ software (Version 1.33, NIH public domain software, http://rsb.info.nih.gov/ij/). To normalize data across blots, blot background was subtracted from the signal for each sample. Data are presented as fold change relative to control.

Statistical analysis

All results are expressed as the mean ± standard error from three independent experiments. Genotype associated differences in cytotoxicity and stress signaling response were analyzed using two-way analysis of variance (ANOVA) followed by the Bonferroni multiple comparison post-test. In addition, differences between wild-type and heterozygous LFs in the dose-response patterns of stress signaling proteins were examined using non-linear regression and an F test. All other data were analyzed using one-way ANOVA followed by either the Bonferroni (for normally distributed data), or a Kruskal-Wallis test followed by Dunn's multiple comparison post-test (for data not normally distributed). For statistical analysis, densitometry data were division-normalized by average signal density for all samples on a given blot. All statistical analyses were performed using Prism software (Version 3.0.3, GraphPad Software Inc., San Diego, CA). A p-value of less than 0.05 was considered statistically significant.

Results

$GPx4^{+/+}$ and $GPx4^{+/-}$ LFs exhibit differential cytotoxicity in response to cadmium exposure

We previously reported that *$GPx4^{+/-}$* LFs, which have approximately 50% the GPx4 activity of wild-type LFs, are more susceptible to cadmium-induced cytotoxicity

than wild-type LFs, as determined by neutral red assay (Garry *et al.* 2006). While both *GPx4*$^{+/+}$ and *GPx4*$^{+/-}$ cells showed similar sensitivity to 6-hour treatment to $CdCl_2$ at concentrations up to 50μM (approximately 65% viability), their respective sensitivities began to diverge thereafter (Figure 3.1). Treatment with 100μM $CdCl_2$ revealed a significant difference in susceptibility between the two genotypes ($p<0.001$), with *GPx4*$^{+/+}$ LFs exhibiting 50% viability ($p<0.001$) and *GPx4*$^{+/-}$ LFs having only 28% viability ($p<0.001$). This difference continued with all succeeding dose levels up to 400μM, at which point LFs of both genotypes exhibited nearly 0% survival.

The qualitative effects on cell morphology and attachment observed by phase-contrast microscopy following $CdCl_2$ treatment were consistent with the quantitave cytotoxicity results of the neutral red assays (Figure 3.2). Differences between wild-type (first row) and heterozygous cells (second row) were not readily apparent for up to 8 hours of 50μM $CdCl_2$ treatment. After 24 hours of treatment, cell attachment was greatly diminished in wild-type cells, but there were still a substantial fraction of cells present. Among the heterozygous cells there were few if any cells still attached after 24 hours of treatment with 50μM $CdCl_2$. With 100μM $CdCl_2$, however, differences in response between the two genotypes were apparent earlier. *GPx4*$^{+/+}$ LFs exhibit apoptotic characteristics, including cell rounding and pyknosis, by 8 hours of treatment. By 24 hours most cells were no longer adhering to the plate, and these cells that remained were pyknotic. *GPx4*$^{+/-}$ LFs begin to show morphological signs of stress as soon as 4 hours of treatment with 100μM $CdCl_2$, with most cells appearing pyknotic by 8 hours and no cells adhering after 24 hours.

A GPx4$^{+/-}$ *genotype is associated with diminished activation of stress signaling MAPK pathways in response to* $CdCl_2$ *treatment*

In order to determine whether differences in MAPK pathway responses are associated with the differential susceptibility of *GPx4*$^{+/-}$ LFs to cadmium-induced

cytotoxicity, we evaluated the phosphorylation status of two stress signaling MAPK pathways, p38 and JNK. P38 is activated through dual phosphorylation at Thr180/Tyr182. This activation is induced by a number of intra- and extracellular stresses, including cadmium (Lag *et al.* 2005; Wenk *et al.* 2004). Phosphorylated p38 MAPK levels increased following a 4-hour treatment with $CdCl_2$ in $GPx4^{+/+}$ and $GPx4^{+/-}$ cells ($p<0.05$) (Figure 3.3A). For $GPx4^{+/+}$ LFs, the increases were approximately 20- and 35-fold compared to controls at 4 hours with 50μM and 100μM $CdCl_2$, respectively. A similar pattern was observed when cells were treated with 50μM for increasing periods of time (Figure 3.3B). Phoshorylated p38 MAPK levels were increased 7, 21, and 24-fold following 2, 4, and 6 hours of treatment, respectively, over same genotype and time period controls in $GPx4^{+/+}$ LFs ($p<0.05$), whereas levels in $GPx4^{+/-}$ LFs were only 5, 10, and 8-fold that found controls ($p<0.05$).

JNK is activated through dual phosphorylation at Thr183/Tyr185. Cadmium has been shown to activate both JNK1 (p45) and JNK2 (p54) isoforms (Chuang *et al.* 2000), and induce the transcription factor *c-jun* (Jin and Ringertz 1990; Zhou *et al.* 1999), a target of JNK activation. Similar to p38, JNK was phosphorylated in both $GPx4^{+/+}$ and $GPx4^{+/-}$ LFs following a 4 hour $CdCl_2$ treatment, and this activation was about 50% in $GPx4^{+/-}$ compared to $GPx4^{+/-}$ cells ($p<0.001$) (Figure 3.4A). However, unlike with p38, JNK induction was greater with 50μM than 100μM $CdCl_2$ ($p<0.01$). Interestingly, both $GPx4^{+/-}$ and $GPx4^{+/-}$ LFs exhibited a 6 to 7-fold increase in JNK phosphorylation following 2 hours of treatment ($p<0.05$), but thereafter the responses diverged (Figure 3.4B). In wild-type LFs, JNK activation increased to a 15-fold induction at 4 hours and remained at that level through at least 6 hours ($p<0.05$). In contrast, $GPx4^{+/-}$ LFs exhibited only a 9-fold induction at 4 hours ($p<0.001$), and then decreased back to a 6-fold induction at 6 hours ($p<0.05$).

Phosphorylated Akt levels remained high $GPx4^{+/+}$ LFs following cadmium exposure, but decreased in $GPx4^{+/-}$ LFs

The Akt signaling pathway is an important anti-apoptotic factor in promoting cell survival in the face of endogenous and exogenous stresses (Franke *et al.* 2003). Akt can be activated by a number of stressors, including cadmium (Konishi *et al.* 1997; Yu *et al.* 2005). This activation is dependent upon phosphorylation at Ser473 or Thr308. In order to evaluate whether the Akt signaling status might play a role in the decreased survival of $GPx4^{+/-}$ LFs in the face of cadmium exposure, we examined Akt phosphorylation status. In wild-type cells, phosphorylated Akt levels were not significantly different than controls after 4 hours treatment with 50μM $CdCl_2$ or 100μM $CdCl_2$ (Figure 3.5A). The time course also does not show a significant difference than controls after 2, 4, and 6 hours treatment with 50μM $CdCl_2$ (Figure 3.5B). In contrast, phosphorylated Akt levels in $GPx4^{+/-}$ cells dropped precipitously to only 15 and 10% of control after 4 hour treatment with 50μM and 100μM $CdCl_2$, respectively ($p<0.001$) (Figure 3.5A). This decrease was observed at the earliest time point (2 hours) and continued through at least 6 hours for the 50μM exposure level ($p<0.001$) (Figure 3.5B).

We also examined the relative stress to survival signaling balance by dividing p-p38 and p-JNK levels by p-Akt levels and evaluating fold changes from controls (Figures 3.6 and 3.7). When viewed in this way, $GPx4^{+/-}$ LFs exhibit an increased stress/survival ratio response for both p38 ($p<0.05$) (Figures 3.6A and 3.7A) and JNK ($p<0.05$) (Figures 3.6B and 3.7B).

Cadmium-induced elevation of cleaved caspase-3 was more pronounced $GPx4^{+/-}$ than $GPx4^{+/+}$ LFs

One mechanism by which Akt may modulate cell survival is through its ability to phosphorylate and thereby inactive caspase-9 (Cantley and Neel 1999; Franke *et al.* 2003). Caspase-9 is an initiator caspase in the mitochondrial regulated apoptotic pathway regulated by cytochrome c release from the mitochondria, and an activator

of the downstream effector caspase-3. Cadmium can induce cytochrome c release, caspase-9 activation, and caspase 3 activation followed by apoptotic cell death (Kondoh *et al.* 2002). GPx4 overexpression suppresses cytochrome c release, caspase-3 cleavage, and apoptosis induced by 2-deoxyglucose in RBL2H3 cells (Imai and Nakagawa 2003; Nomura *et al.* 1999). Therefore, we evaluated whether caspase 3 may play a role in the differential susceptibility of $GPx4^{+/+}$ and $GPx4^{+/-}$ LFs to cadmium-induced cytotoxicity by measuring the levels of the p17 and p19 cleavage products of caspase-3. After 4 hours of treatment, cleaved caspase-3 levels were not significantly increased in $GPx4^{+/+}$ cells with either 50μM or 100μM $CdCl_2$ (Figure 3.8A). Only after 6 hours treatment did the 2.5-fold increased levels reach significance ($p<0.05$) (Figure 3.8B). In contrast, cleaved caspase 3 levels were increased 3-fold in $GPx4^{+/-}$ cells after a 4 hour treatment with 50μM $CdCl_2$ ($p<0.05$), but were reduced back to control levels with 100μM $CdCl_2$ (Figure 3.8A). The 4 hour increase at 50μM was sustained through at least 6 hours ($p<0.05$) (Figure 3.8B).

Cadmium was associated with an accumulation of high molecular weight ubiquitinated proteins in $GPx4^{+/+}$ LFs, but not $GPx4^{+/-}$ LFs

Cadmium exposure is associated with disruption of the ubiquitin proteosome degradation system, which is important for a wide array of cellular functions, including stress response and regulatory protein turnover. The effect differs depending on the dose. Treatment of a mouse neuronal cell line with a sub-cytotoxic dose of cadmium resulted in accumulation of ubiquitinated proteins, whereas cytotoxic doses were not accompanied by such an accumulation (Figueiredo-Pereira et al. 1998). Therefore, we examined extracts from cadmium treated $GPx4^{+/-}$ and $GPx4^{+/-}$ LFs for levels of high molecular weight polyubiquitinated (HMW-Ub) proteins that would be destined for recognition, degradation, and disposal by the 26S proteosome. Wild-type cells showed a 1.5 to 1.7-fold increase in HMW-Ub compared to control cells after 4 hours treatment

with $CdCl_2$ at both 50 and 100μM ($p<0.01$) (Figure 3.9A). A similar increase was observed after 2, 4, and 6 hours treatment with 50μM $CdCl_2$ ($p<0.01$) (Figure 3.9B). No such increase was observed in $GPx4^{+/-}$ cells.

Discussion

Cadmium-induced cytoxicity is associated with oxidative stress and apoptotic cell death in a number of cell types (Bagchi *et al.* 2000; Hansen *et al.* 2006; Jimi *et al.* 2004; Stohs *et al.* 2001). Further, the apoptosis observed following cadmium exposure is mediated, at least in part, by activation of p38 and JNK MAPK stress signaling pathways (Chuang *et al.* 2000; Kim *et al.* 2005; Lag *et al.* 2005). The Akt signaling pathway typically associated with a survival response and cell proliferation. Akt activation can be either induced or attenuated in response to cadmium exposure, depending on dose and duration of exposure (Konishi *et al.* 1997; Murata *et al.* 2003; Yu *et al.* 2005). More specifically, Akt activation can be transiently increased following cadmium exposure followed by dephosphorylation and diminished signaling with prolonged exposure. Indeed, LFs from our mice exhibit significant cadmium-induced cytotoxicity, with increased susceptibility in cells from mice heterozygous for GPx4. The differential susceptibility is evident beginning at $CdCl_2$ concentrations of 50μM and above following a 6-hour treatment (Figure 3.1). The morphological changes observed in these cells following 50μM and 100μM $CdCl_2$ treatment are consistent with this pattern: evidence of apoptosis occurs earlier and appears more prevalent in GPx4 heterozygous cells (Figure 3.2).

Based on the increased cadmium-induced cytotoxicity observed in *GPx4*$^{+/-}$ LFs, and the known relationship between cadmium and MAPK signaling pathways, one might also expect increased activation of the p38 and JNK MAPK stress pathways stress signaling pathways and decreased activation of the Akt survival pathway in *GPx4*$^{+/-}$ LFs relative to *GPx4*$^{+/+}$ LFs. This relationship held true for Akt, but the

opposite pattern occurred for both stress pathways. *GPx4*$^{+/-}$ cells actually had an attenuated response for both p38 and JNK. While the mechanism behind this differential signaling response is not at present known, the increased cytoxicity in heterozygous cells despite reduced stress signaling could be explained by the relative stress-to-survival signaling occurring. Although *GPx4*$^{+/-}$ LFs exhibited somewhat diminished p38 and JNK phosphorylation, Akt phosphorylation was diminished to a greater extent in *GPx4*$^{+/-}$ cells. When viewed as a ratio of stress to survival signaling (Figures 3.6 and 3.7), however, the result is consistent with the relative sensitivity of these two cell strains as reflected by the cytotoxicity assay and morphological changes. *GPx4*$^{+/-}$ LFs exhibit an increased stress/survival ratio response for both p38 ($p<0.05$) (Figures 3.6A and 3.7A) and JNK ($p<0.05$) (Figures 3.6B and 3.7B).

GPx4 overexpression protects against apoptosis induced by a number of chemical agents that cause oxidative stress. One mechanism by which GPx4 affords this protection may involve its ability to suppress specific apoptotic signals, cytochrome c release from the mitochondria and caspase-3 cleavage, by protecting against oxidation of cardiolipin in the mitochondrial membrane (Imai and Nakagawa 2003; Nomura *et al.* 1999). Akt also plays a role in maintaining cytochrome c in the mitochondria and in diminishing the response to cytochrome c when it is released (Franke *et al.* 2003; Kennedy *et al.* 1999). Akt phosphorylates and inactivates caspase-9 (Cantley and Neel 1999; Cardone *et al.* 1998), which is itself activated by cytochrome c release and is an upstream regulator of caspase-3 cleavage. Akt is redox sensitive and its function is regulated by cellular levels of glutathione and glutaredoxin (Murata *et al.* 2003). Glutaredoxin overexpression protects Akt from H_2O_2-induced oxidation and subsequent dephosphorylation, and apoptosis. This protection is diminished, however, by cadmium (Murata *et al.* 2003). It is therefore plausible that GPx4 affords protection from oxidation of Akt in the mitochondria, as it does for mitochondrial cardiolipin, providing an additional mechanism by

which cytochrome c release is avoided. Our finding that reduced levels of GPx4 are associated with an attenuated Akt response is consistent with this hypothesis.

Another aspect of the apparent role of Akt in the increased susceptibility of GPx4 deficient cells to oxidative stress that warrants additional investigation is the demonstrated role of Akt in development. In two transgenic mouse systems whereby a constitutively active or a kinase deficient Akt was specifically expressed in the heart, Akt was shown to regulate organ growth and ultimate size (Shioi *et al.* 2002). Akt is a downstream target in the phosphoinositide 3-kinase (PI3K) pathway, which has been shown to regulate cell and organ growth in Drosophila (Weinkove and Leevers 2000). Could an Akt~GPx4 interaction be involved in the embryonic lethality in the *GPx4* null genotype? Clearly, the redox sensitivity and modulation of Akt, and the role of this sensitivity in regulating cytochrome c release from the mitochondria(Kennedy *et al.* 1999; Kennedy *et al.* 1997), provide an intriguing overlap with GPx4 in terms of cellular location and function. Further research is necessary to examine the possible role of the Akt signaling pathway, and its redox sensitivity, in the mechanisms of embryolethality of the *GPx4* null genotype.

Our finding that a $GPx4^{+/-}$ genotype is also associated with diminished function of the UPS may also point to an important interaction between GPx4 and Akt. Akt is a negative regulator of the protein kinase glycogen synthase kinase 3 (GSK3), which is itself a constitutively active negative regulator of cyclin D and c-myc, two proteins that positively regulate the UPS and are important in cell proliferation (Cantley 2002). Thus, activation of Akt will deactivate GSK3. Without GSK3, cyclin D and c-myc will be activated and will upregulate the UPS, resulting in increased ubiquitination of and turnover of damaged proteins. Our results are consistent with this pathway. However, while cells of both genotypes had increased levels of HMW-Ub following 4 hours of treatment with 50μM and

100μM $CdCl_2$, the response was attenuated in *GPx4*$^{+/-}$ LFs (Figure 3.9A). Similarly, HMW-Ub levels were consistently lower in *GPx4*$^{+/-}$ cells relative to *GPx4*$^{+/+}$ cells with 2, 4, and 6 hours treatment with 50μM $CdCl_2$ (Figure 3.9B). It is unknown whether the attenuated UPS response is part of the mechanism that mediates differential cytotoxicity in GPx4 deficient cells, or simply a by product of increased levels of oxidative stress leading to inhibition of enzymes necessary for UPS function. Similar to our findings, Figueiredo-Pereira and colleagues reported that subcytotoxic doses of cadmium (25μM and below) were associated with increased levels of ubiquitinated proteins in HT4 cells, while cytotoxic doses (50μM and above) led to an attenuated UPS response (Figueiredo-Pereira *et al.* 1998). Thus, diminished function of the UPS system accompanies increased levels of oxidative stress induced cytotoxicity. Whether this diminished function is a necessary step in the pathway that ultimately leads to cell death in the cadmium-induced cytotoxicity must be further studied. It is possible that cadmium exerts and effect on the UPS by impacting function of enzymes in the UPS. Gene expression studies from our laboratory of cadmium-treated mouse embronic fibroblast cells using microarray analysis indicate that cadmium disrupted levels of ubiquitin ligases such as the multi-function ligase/hydrolase UCH-L1 (unpublished data). Finally, elucidation of the specific targets of ubiquitination in this pathway is necessary to understand the underlying mechanism, and the role of GPx4.

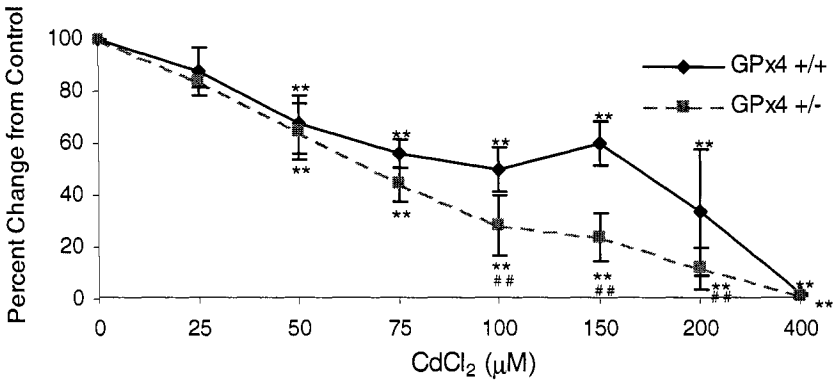

Figure 3.1 – $CdCl_2$-induced cytotoxicity in cultured lung fibroblasts. $CdCl_2$-induced cytotoxicity in cultured LFs from *GPx4*$^{+/+}$ and *GPx4*$^{+/-}$ mice (from Garry et. al. 2006). Cytotoxicity was assessed using neutral red, as described in Methods, in early passage lung fibroblasts. Results are expressed as the percent change from the control and represent the combined data from at least three independent experiments (mean ± SD). Treatment with 50uM $CdCl_2$ was associated with a 30-35% decrease in viability for both *GPx4*$^{+/+}$ and *GPx4*$^{+/-}$ LFs. *GPx4*$^{+/-}$ LFs were more sensitive to cadmium induced cytotoxicity than *GPx4*$^{+/+}$ LFs. Susceptibility to cadmium-induced cytotoxicity begins to diverge at $CdCl_2$ concentrations greater than 50uM, with significant genotype associated differerences beginning at 100uM. Significant differences from same genotype control are indicated (*p<0.05; **p<0.001). Significant differences from *GPx4*$^{+/+}$ genotype cells at same concentration are indicated (#p<0.05; ##p<0.001).

Figure 3.2 – Morphological changes in *GPx4*$^{+/+}$ and *GPx4*$^{+/-}$ lung fibroblasts. Typical phase-contrast photography showing morphological changes in *GPx4*$^{+/+}$ and *GPx4*$^{+/-}$ LFs treated with 50μM and 100μM $CdCl_2$. LFs were seeded at a density of 2×10^6 cells per 100mm tissue culture plate and allowed to grow until 70 to 80% confluence before initiation of treatment with $CdCl_2$. The first and second rows of panels show *GPx4*$^{+/+}$ and *GPx4*$^{+/-}$ LFs, respectively, treated with 50μM $CdCl_2$ for the indicated time periods. The third and fourth rows show *GPx4*$^{+/+}$ and *GPx4*$^{+/-}$ LFs, respectively, treated with 100μM $CdCl_2$. At least three fields of view were photographed for each treatment and time point, and the experiments were replicated at least three times.

50uM $CdCl_2$

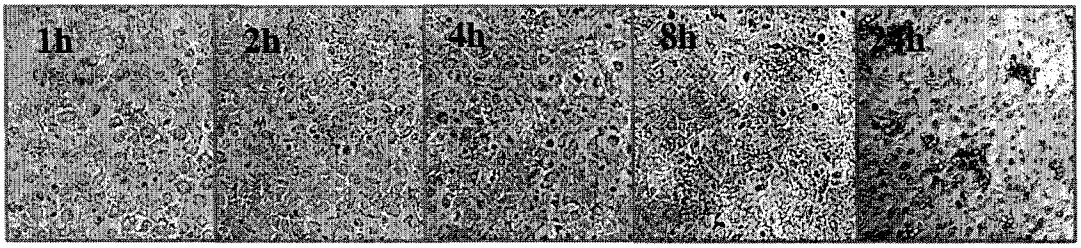

GPx4+/+

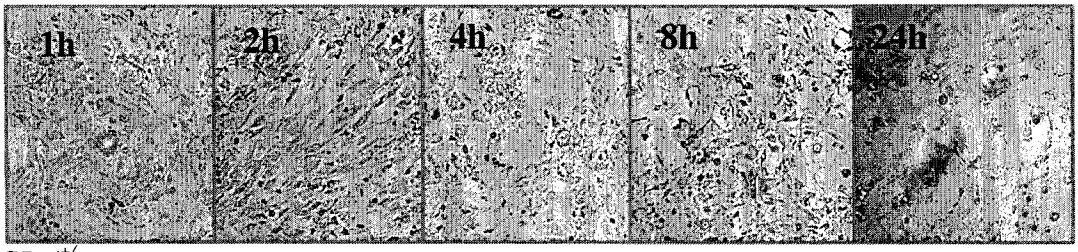

GPx4$^{+/-}$

100uM $CdCl_2$

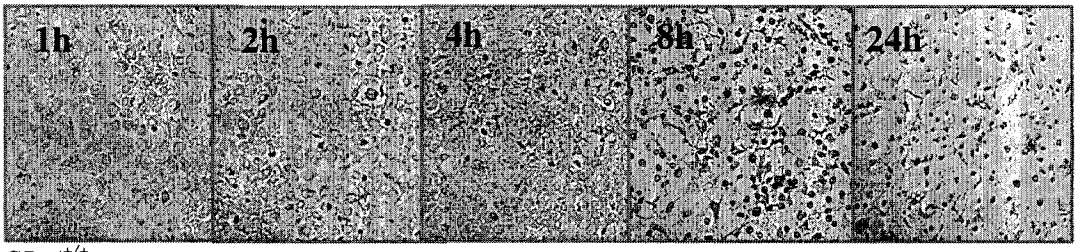

GPx4$^{+/+}$

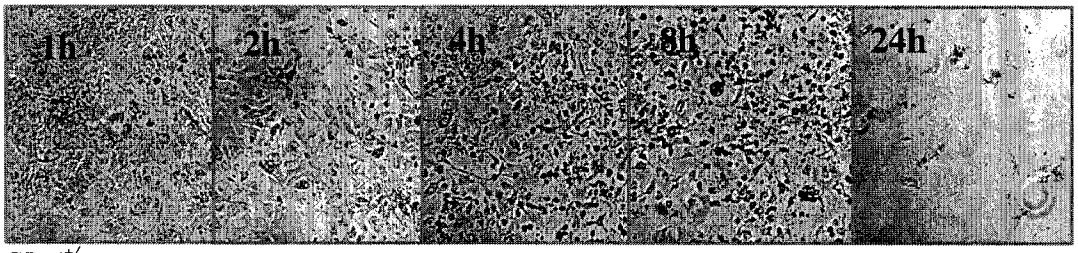

GPx4$^{+/-}$

Figure 3.3 – Effect of $CdCl_2$ treatment on p38 activation in *GPx4*$^{+/+}$ and *GPx4*$^{+/-}$ lung fibroblasts.

Effect of $CdCl_2$ treatment on p38 activation in *GPx4*$^{+/+}$ and *GPx4*$^{+/-}$ LFs at the indicated concentrations and time points. The levels of phosphorylated p-38 (p-p38), indicating activation, and total p-38, as an indicator of total protein loading, were measured by Western blot analysis as described in Methods. Bar graph results are presented as a mean $\pm$ SE (n=3) of the fold change from control. Representative blots are shown and are consistent with the results between replicates. (A). p38 activation after 4 hours treatment with the indicated concentrations of $CdCl_2$. (B). p38 activation at the indicated time points after treatment with 50μM $CdCl_2$. Bars not sharing a letter notation differ significantly at $p<0.05$ based on the results of an ANOVA followed by a Bonferroni multiple comparison test. Bars without a letter "a" differ significantly from same genotype control ($p<0.05$). Dose-response curves differ significantly between genotypes as modeled using non-linear regression ($p<0.05$).

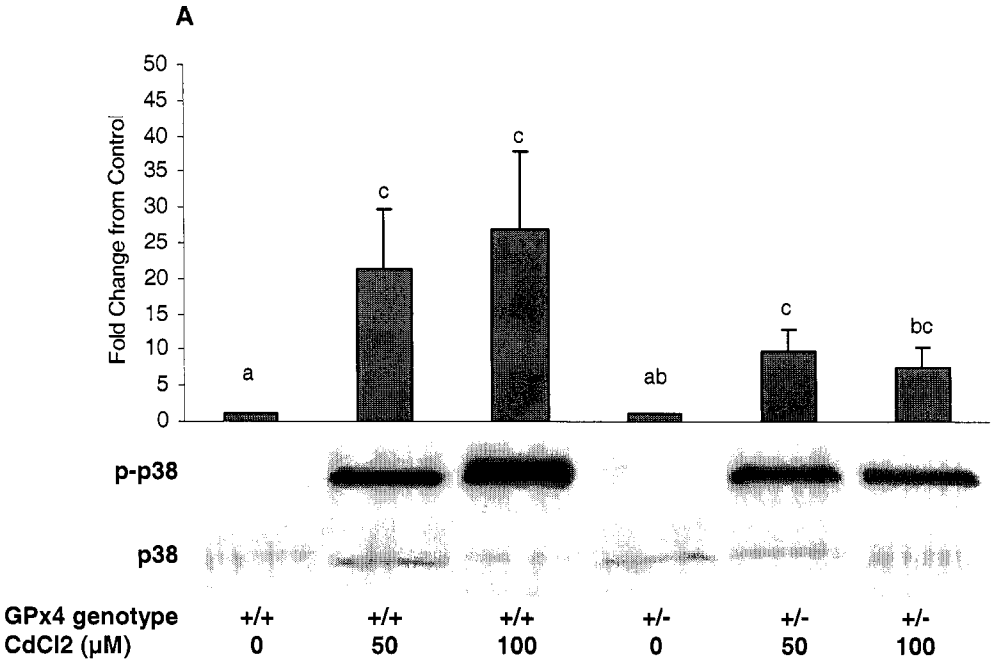
A
Fold Change from Control
50
45
40
35
30
25
20
15
10
5
0
a
c
c
ab
c
bc
p-p38
p38
GPx4 genotype +/+ +/+ +/+ +/- +/- +/-
CdCl2 (μM) 0 50 100 0 50 100

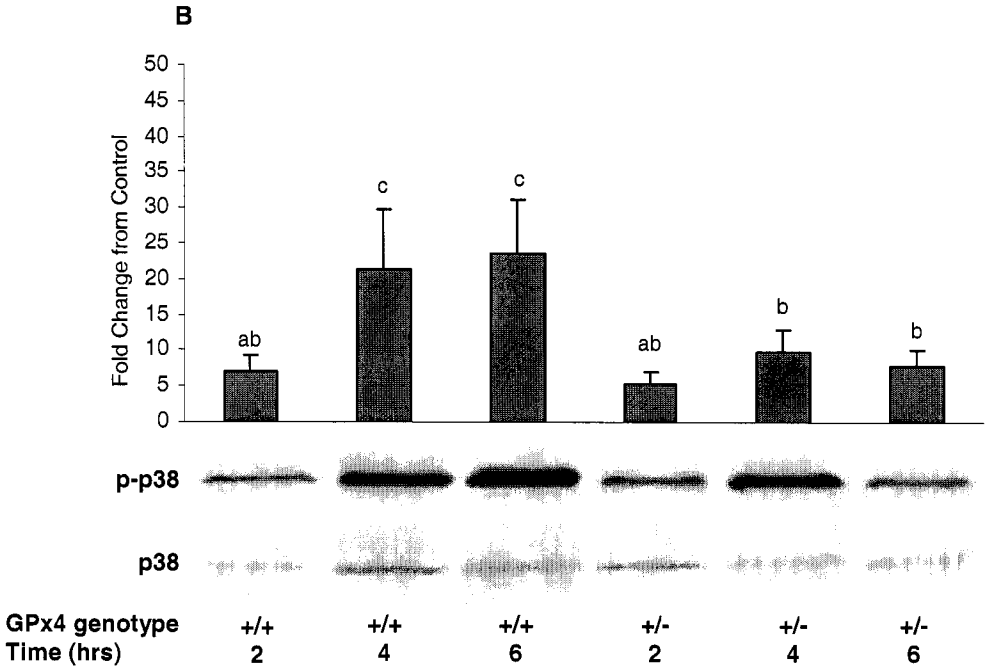
B
Fold Change from Control
50
45
40
35
30
25
20
15
10
5
0
ab
c
c
ab
b
b
p-p38
p38
GPx4 genotype +/+ +/+ +/+ +/- +/- +/-
Time (hrs) 2 4 6 2 4 6

Figure 3.4 – Effect of $CdCl_2$ treatment on JNK activation in *GPx4*$^{+/+}$ and *GPx4*$^{+/-}$ lung fibroblasts.

Effect of $CdCl_2$ treatment on JNK activation in *GPx4*$^{+/+}$ and *GPx4*$^{+/-}$ LFs after treatment with 50uM and 100uM $CdCl_2$ at the indicated concentrations and time points. The levels of phosphorylated JNK (p-JNK), indicating activation, were measured by Western blot analysis as described in Methods. Both p-JNK1 (p46) and p-JNK2 (p54) were detected. Bar graph results are presented as a mean ± SE (n=3) of the fold change from control for p54; relative responses were identical when p46 was analyzed. Representative blots are shown and are consistent with the results between replicates. (A). JNK activation after 4 hours treatment with the indicated concentrations of $CdCl_2$. (B). JNK activation at the indicated time points after treatment with 50μM $CdCl_2$. Bars not sharing a letter notation differ significantly at $p<0.05$ based on the results of an ANOVA followed by a Bonferroni multiple comparison test. Bars without a letter "a" differ significantly from same genotype control ($p<0.05$). Dose-response curves differ significantly between genotypes as modeled using non-linear regression ($p<0.05$).

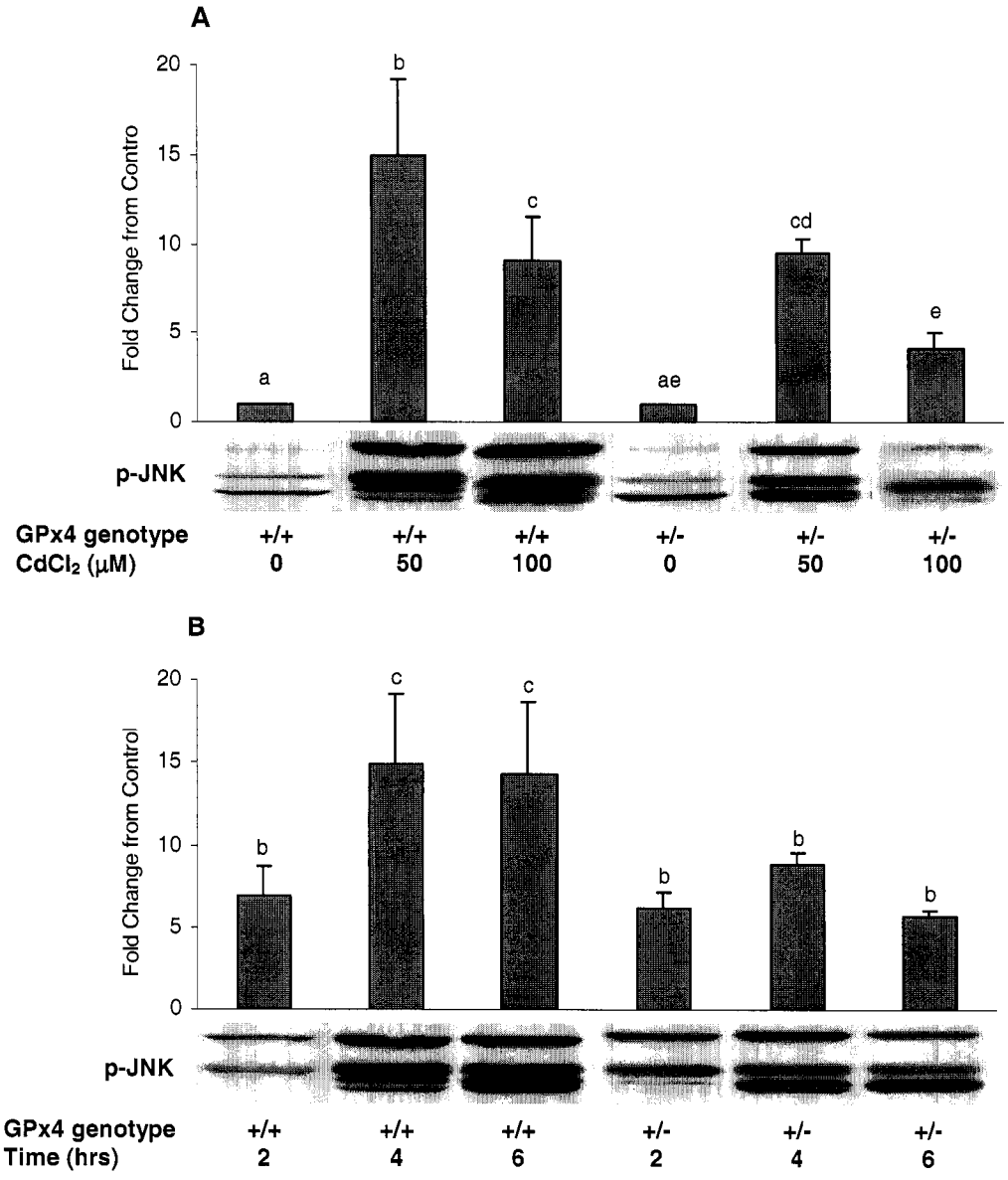
A
Fold Change from Contro
20
15
10
5
0
a
b
c
ae
cd
e
p-JNK
GPx4 genotype
CdCl2 (μM)
+/+ +/+ +/+ +/- +/- +/-
0 50 100 0 50 100
B
Fold Change from Control
20
15
10
5
0
b
c
c
b
b
b
p-JNK
GPx4 genotype
Time (hrs)
+/+ +/+ +/+ +/- +/- +/-
2 4 6 2 4 6

Figure 3.5 – Effect of $CdCl_2$ treatment on Akt phosphorylation in *GPx4*$^{+/+}$ and *GPx4*$^{+/-}$ lung fibroblasts.

Effect of $CdCl_2$ treatment on Akt phosphorylation in *GPx4*$^{+/+}$ and *GPx4*$^{+/-}$ LFs at the indicated concentrations and time points. The levels of phosphorylated Akt (p-Akt), indicating activation, and total Akt, as an indicator of total protein loading, were measured by Western blot analysis as described in Methods. Bar graph results are presented as a mean $\pm$ SE (n=3) of the fold change from control. Representative blots are shown and are consistent with the results between replicates. (A). Akt activation after 4 hours treatment with the indicated concentrations of $CdCl_2$. (B). Akt activation at the indicated time points after treatment with 50μM $CdCl_2$. Bars not sharing a letter notation differ significantly at $p<0.05$ based on the results of an ANOVA followed by a Bonferroni multiple comparison test. Bars without a letter "a" differ significantly from same genotype control ($p<0.01$). Dose-response curves differ significantly between genotypes as modeled using non-linear regression ($p<0.001$).

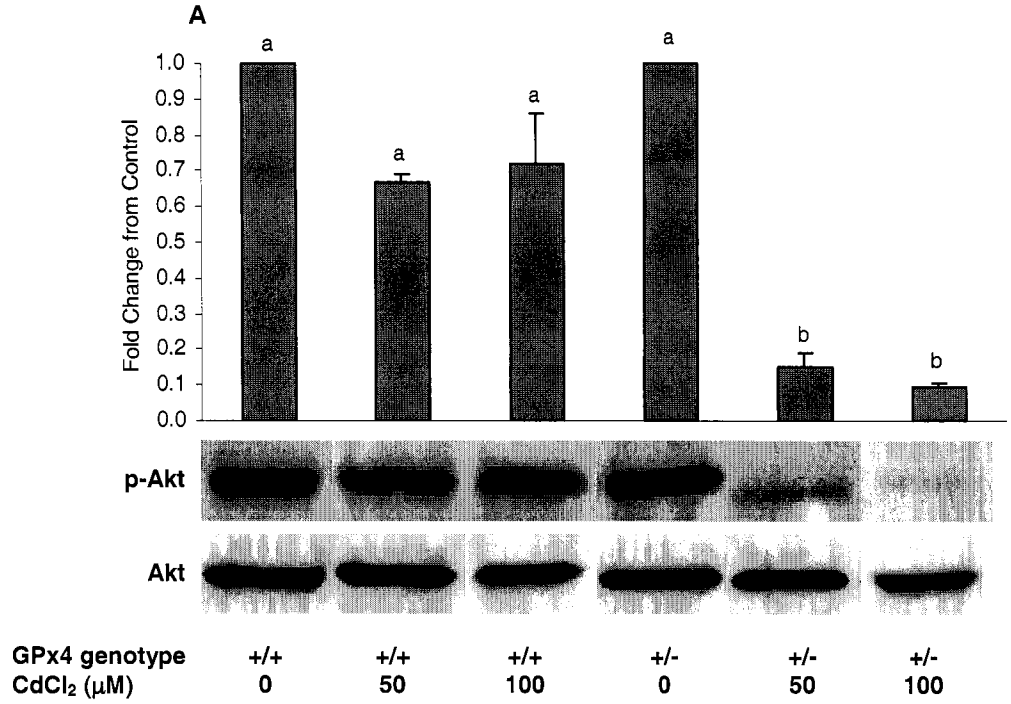
A
Fold Change from Control
1.0
0.9
0.8
0.7
0.6
0.5
0.4
0.3
0.2
0.1
0.0
a
a
a
a
b
b
p-Akt
Akt
GPx4 genotype +/+ +/+ +/+ +/- +/- +/-
CdCl2 (μM) 0 50 100 0 50 100

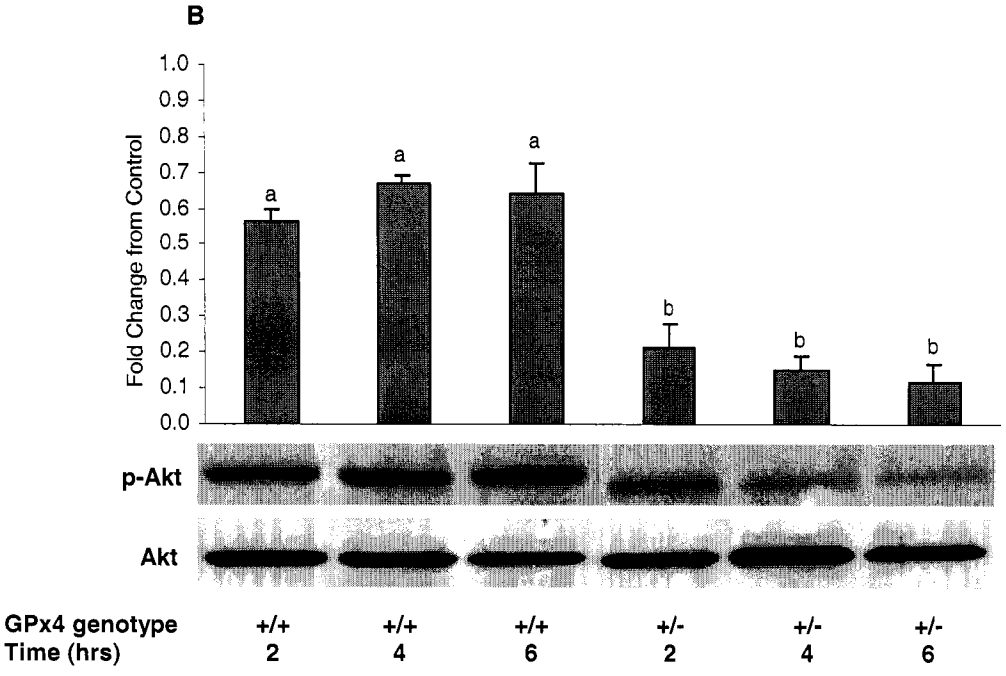
B
Fold Change from Control
1.0
0.9
0.8
0.7
0.6
0.5
0.4
0.3
0.2
0.1
0.0
a
a
a
b
b
b
p-Akt
Akt
GPx4 genotype +/+ +/+ +/+ +/- +/- +/-
Time (hrs) 2 4 6 2 4 6

Figure 3.6 – Effect of 50uM and 100uM $CdCl_2$ treatment on the ratios of p38 and JNK activation to Akt activation

Effect of $CdCl_2$ treatment on the ratios of p38 and JNK activation to Akt activation in GPx4 +/+ and +/- LFs after treatment with 50uM and 100uM $CdCl_2$ for 4 hours. The levels of phosphorylated p38 (p-p38) and JNK (p-JNK) were normalized to the level of phosphorylated Akt (p-Akt) as an indicator of the relative amount of stress to survival signaling. Bar graph results are presented as a mean $\pm$ SE (n=3) of the ratio of fold change from control for stress signal (p-p38 or p-JNK) divided by the survival signal (p-Akt). (A). Ratio of fold change p38 activation to Akt activation with the indicated concentrations of $CdCl_2$. (B). Ratio of fold change JNK activation to Akt activation with the indicated concentrations of $CdCl_2$. Bars not sharing a letter notation differ significantly at $p<0.05$ based on the results of an ANOVA followed by a Bonferroni multiple comparison test. Bars without a letter "a" differ significantly from same genotype control ($p<0.05$). Dose-response curves differ significantly between genotypes as modeled using non-linear regression ($p<0.05$).

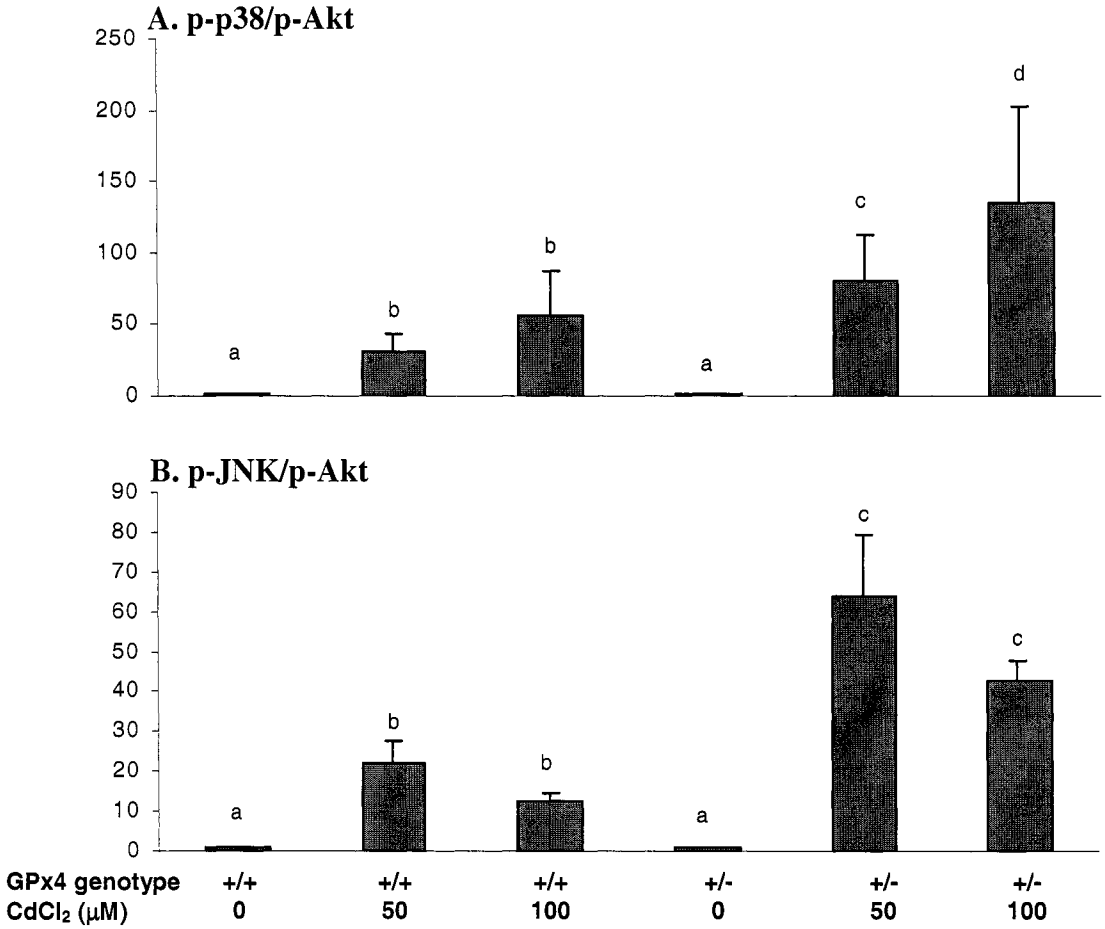
A. p-p38/p-Akt
250
200
150
100
50
0
a
b
b
a
c
d
B. p-JNK/p-Akt
90
80
70
60
50
40
30
20
10
0
a
b
b
a
c
c
GPx4 genotype +/+ +/+ +/+ +/- +/- +/-
CdCl2 (μM) 0 50 100 0 50 100

Figure 3.7 – Effect of four-hour $CdCl_2$ treatment on the ratios of p38 and JNK activation to Akt activation

Effect of $CdCl_2$ treatment on the ratios of p38 and JNK activation to Akt activation in GPx4 +/+ and +/- LFs after treatment with 50uM $CdCl_2$ at the indicated time points. The levels of phosphorylated p38 (p-p38) and JNK (p-JNK) were normalized to the level of phosphorylated Akt (p-Akt) as an indicator of the relative amount of stress to survival signaling. Bar graph results are presented as a mean $\pm$ SE (n=3) of the ratio of fold change from control for stress signal (p-p38 or p-JNK) divided by the survival signal (p-Akt). (A). Ratio of fold change p38 activation to Akt activation at the indicated time points. (B). Ratio of fold change JNK activation to Akt activation at the indicated time points. Bars not sharing a letter notation differ significantly at $p<0.05$ based on the results of an ANOVA followed by a Bonferroni multiple comparison test. Bars without a letter "a" differ significantly from same genotype control ($p<0.05$). Dose-response curves differ significantly between genotypes as modeled using non-linear regression ($p<0.05$).

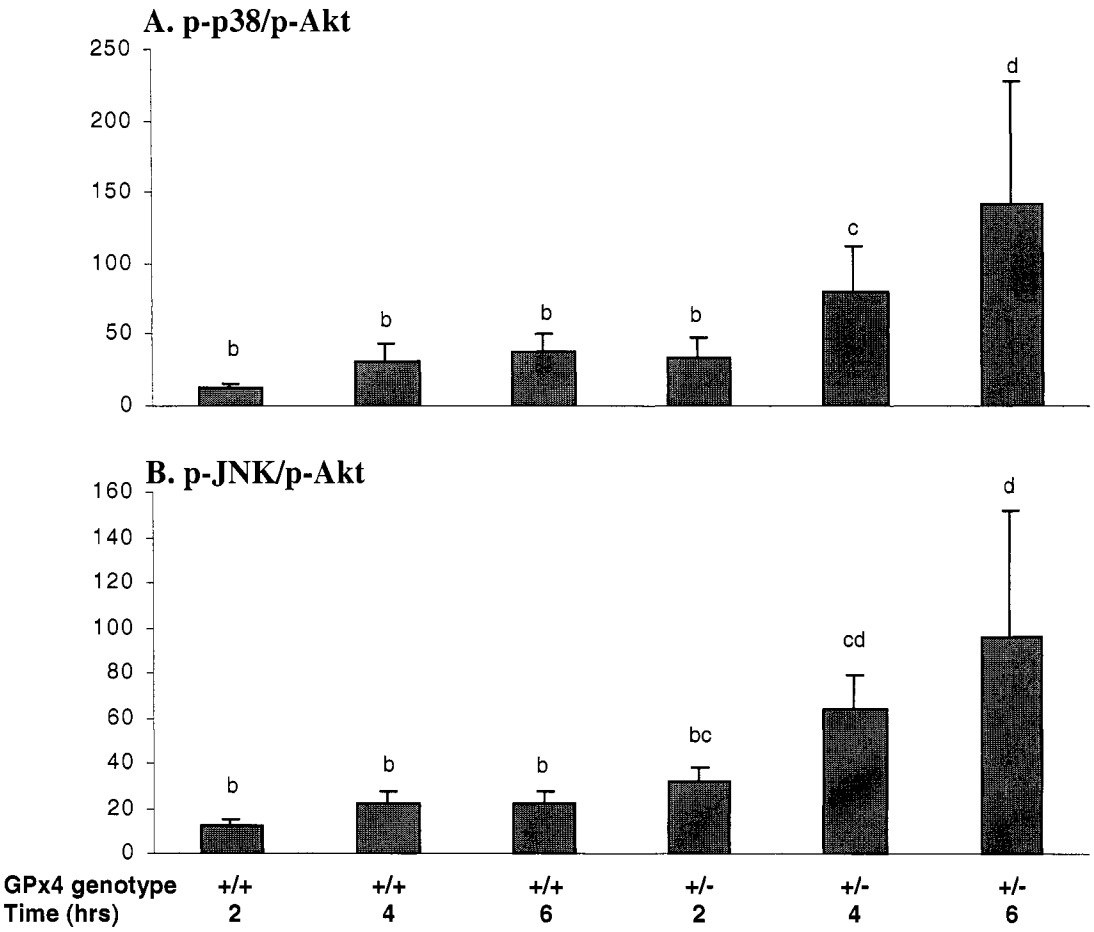
A. p-p38/p-Akt
250
200
150
100
50
0
b
b
b
b
c
d
B. p-JNK/p-Akt
160
140
120
100
80
60
40
20
0
b
b
b
bc
cd
d
GPx4 genotype +/+ +/+ +/+ +/- +/- +/-
Time (hrs) 2 4 6 2 4 6

Figure 3.8 – Effect of $CdCl_2$ treatment on caspase-3 cleavage in *GPx4*$^{+/+}$ and *GPx4*$^{+/-}$ lung fibroblasts.

Effect of $CdCl_2$ treatment on caspase-3 cleavage in *GPx4*$^{+/+}$ and *GPx4*$^{+/-}$ LFs at the indicated concentrations and time points. The levels of cleaved caspase-3, indicating activation, and uncleaved Caspase-3, as an indicator of total protein loading, were measured by Western blot analysis as described in Methods. Both the p17 and p19 subunits of cleaved caspase-3 are detected with the cleaved caspase-3 antibody. Bar graph results are presented as a mean $\pm$ SE (n=3) of the fold change from control. Representative blots are shown and are consistent with the results between replicates. (A). Caspase-3 activation after 4 hours treatment with the indicated concentrations of $CdCl_2$. (B). Caspase-3 activation at the indicated time points after treatment with 50μM $CdCl_2$. Bars not sharing a letter notation differ significantly at $p<0.05$ based on the results of an ANOVA followed by a Bonferroni multiple comparison test. Bars without a letter "a" differ significantly from same genotype control ($p<0.05$). Dose-response curves differ significantly between genotypes as modeled using non-linear regression ($p<0.01$).

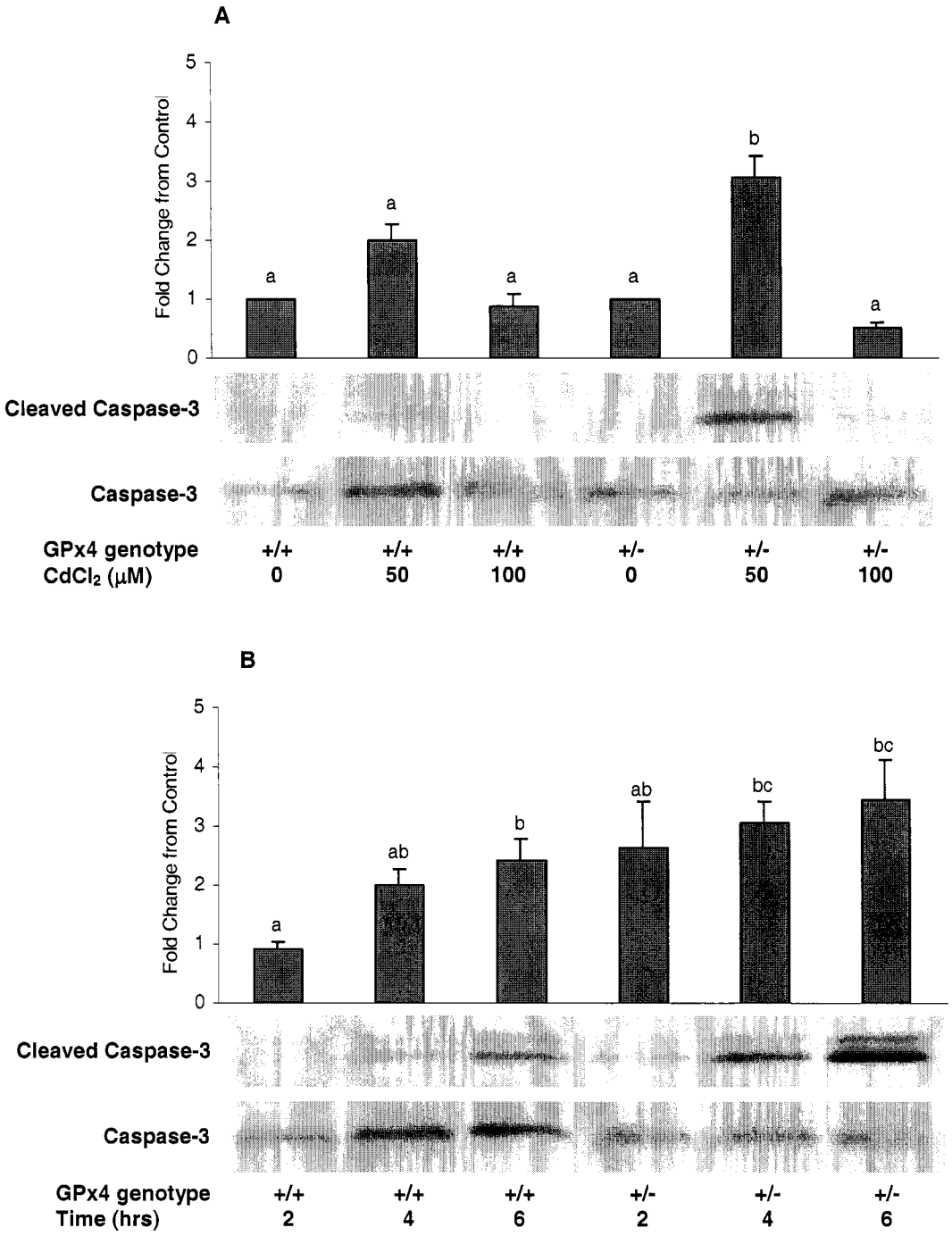
A
Fold Change from Control
5
4
3
2
1
0
a
a
a
a
b
a
Cleaved Caspase-3
Caspase-3
GPx4 genotype +/+ +/+ +/+ +/- +/- +/-
CdCl2 (μM) 0 50 100 0 50 100
B
Fold Change from Control
5
4
3
2
1
0
a
ab
b
ab
bc
bc
Cleaved Caspase-3
Caspase-3
GPx4 genotype +/+ +/+ +/+ +/- +/- +/-
Time (hrs) 2 4 6 2 4 6

Figure 3.9 – Effect of $CdCl_2$ treatment on post-translational modification with high molecular weight polyubiquitin.
Effect of $CdCl_2$ treatment on post-translational modification with high molecular weight polyubiquitin (HMW-Ub) at the indicated concentrations and time points. The levels of HMW-Ub were measured by Western blot analysis as described in Methods. Bar graph results are presented as a mean $\pm$ SE (n=3) of the fold change from control. Representative blots are shown and are consistent with the results between replicates. (A). HMW-Ub levels after 4 hours treatment with the indicated concentrations of $CdCl_2$. (B). HMW-Ub levels at the indicated time points after treatment with 50μM $CdCl_2$. Bars not sharing a letter notation differ significantly at $p<0.05$ based on the results of an ANOVA followed by a Bonferroni multiple comparison test. Bars without a letter "a" differ significantly from same genotype control ($p<0.05$). Dose-response curves differ significantly between genotypes as modeled using non-linear regression ($p<0.001$).

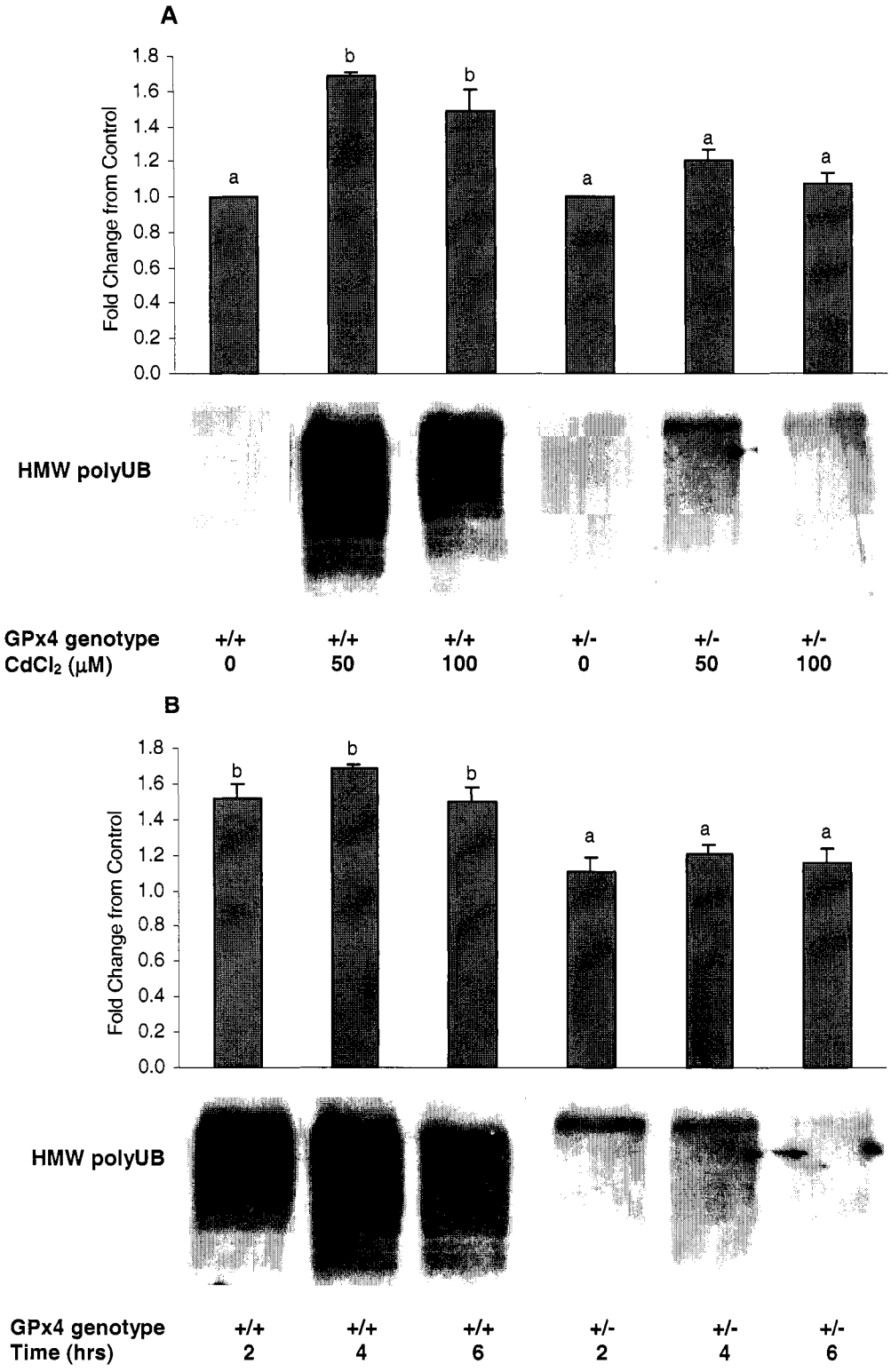
A
Fold Change from Control
1.8
1.6
1.4
1.2
1.0
0.8
0.6
0.4
0.2
0.0
a
b
b
a
a
a
HMW polyUB
GPx4 genotype +/+ +/+ +/+ +/- +/- +/-
CdCl2 (μM) 0 50 100 0 50 100
B
Fold Change from Control
1.8
1.6
1.4
1.2
1.0
0.8
0.6
0.4
0.2
0.0
b
b
b
a
a
a
HMW polyUB
GPx4 genotype +/+ +/+ +/+ +/- +/- +/-
Time (hrs) 2 4 6 2 4 6

Chapter 4 – Discussion and Conclusions

Summary of Findings

The focus of the research described in this dissertation was to 1) characterize the GPx4 activity levels of *GPx4*$^{-/-}$ mice and cells from those mice, 2) develop a cell culture model that provides a physiologically relevant basis for evaluating the roles of GPx4 and the mechanisms of its actions, and 3) investigate the relative susceptibility to toxicant-induced oxidative stress using this model.

It was demonstrated that a *GPx4*$^{-/-}$ genotype is embryonic lethal, but that *GPx4*$^{+/-}$ mice survive and appear phenotypically normal. GPx4 activity is significantly lower in testis and liver tissue from *GPx4*$^{+/-}$ mice than *GPx4*$^{+/+}$ mice. Cultured LFs isolated from adult *GPx4*$^{+/-}$ mice had approximately 50% of the GPx4 activity of LFs from *GPx4*$^{+/+}$ mice, and were significantly more susceptible to H_2O_2, cadmium, and cumene hydroperoxide-induced cytotoxicity. In addition, *GPx4*$^{+/-}$ LFs have lower mitochondrial membrane potential, greater cardiolipin oxidation, and lower amounts of reduced thiols relative to *GPx4*$^{+/+}$ LFs, but are more resistant than *GPx4*$^{+/+}$ LFs to further decrements in these endpoints following PCOOH treatment.

After treatment with $CdCl_2$, *GPx4*$^{+/-}$ LFs had a decreased survival response compared to *GPx4*$^{+/+}$ LFs. Specifically, a *GPx4*$^{+/-}$ genotype was associated with increased morphological evidence of stress, decreased Akt activation, and increased caspase 3 activation. *GPx4*$^{+/-}$ cells did exhibit decreased p38 and JNK activation, but the overall survival response, as measured by the ratio of survival pathway activation (Akt) to stress pathway activation (p38 and JNK), was attenuated in the GPx4 heterozygous cells. *GPx4*$^{+/-}$ cells also exhibited diminished accumulation of high molecular weight poly-ubiquitinated proteins than *GPx4*$^{+/+}$ cells in response to $CdCl_2$ treatment.

Based on the research described in this dissertation, the *GPx4*$^{+/-}$ mouse appears to provide a useful model for studying susceptibility to chemically induced oxidative stress, particularly where lipid peroxidation is a primary mediator of cellular injury. Furthermore, the lung fibroblast cells used in this research provide a useful model for understanding the mechanisms by which GPx4 protects against oxidative injury and mediates cellular functions in the face of chemical insult.

Although the research described in this dissertation focused on differential response to cadmium, an important environmental and public health concern, the results of the cytotoxicity experiments described in Chapter 2, not surprisingly, suggest agent specificity in the patterns of response to different oxidants. Additional studies aimed at furthering our understanding of the role that GPx4 plays in modulating response to other agents of public health concern would be useful. In particular, *GPx4*$^{+/-}$ LFs may provide a useful model for understanding susceptibility to lung toxicants of environmental concern. For example, ozone exposure results in reactive oxygen species generation and airway epithelial injury (Pryor *et al.* 2006; Voter *et al.* 2001), and there is some evidence of a correlation between ozone exposure and respiratory tract neoplasms (Pereira *et al.* 2005). Furthermore, both children and the elderly are more susceptible to ozone-induced lung injury than young and middle-aged adults (Servais *et al.* 2005). Ozone induces GPx1, as well as other major antioxidant enzymes such as SOD and catalase (Servais *et al.* 2005), but the effect of ozone on GPx4 is unknown.

Future Research Efforts Using the GPx4$^{+/-}$ *Lung Fibroblast Model*

One intriguing finding in this research was that, although *GPx4*$^{+/-}$ lung fibroblasts had lower mitochondrial membrane potential, lower amounts of reduced thiols, and more cardiolipin oxidation than *GPx4*$^{+/+}$ lung fibroblasts, they were more resistance to further decrements in these endpoints following a 2-hour PCOOH treatment. This resistance could not be explained by the presence of differential

levels of either extracellular GPx4 activity or extracellular glutathione. This is a surprising finding considering that PCOOH is a specific substrate of GPx4. One potential explanation for this resistance is that other enzymes with peroxidase activity towards PCOOH have been upregulated. For example, peroxiredoxin 6 has activity towards phospholipid hydroperoxides and is found in all major mammalian organs, but is particularly highly expressed in the lung (Manevich and Fisher 2005). Purified human GSTs of alpha, mu, and theta class exhibit glutathione peroxidase activity towards phospholipids hydroperoxides, albeit with much lower specific activity than GPx4 (Hurst *et al.* 1998). It is possible that other antioxidant enzymes, even with low or no specific activity towards phospholipids hydroperoxides, may compensate for increased production of reactive oxygen species when GPx4 levels are reduced. Thus, an important area of future research must focus on the relative expression of other enzymes that could compensate for diminished GPx4 activity. Although there are obvious challenges in identifying candidate enzymes among many possibilities, perhaps the most appropriate first step is DNA microarray analysis to evaluate global gene expression patterns both with and without chemical insult.

Considering the differential stress and survival signaling responses in *GPx4*$^{+/-}$ and wild-type cells, further research in this area is warranted. Of particular interest are the redox sensitive aspects of these pathways. Akt is redox sensitive and its function is regulated by cellular levels of glutathione and glutaredoxin, which protects Akt from H_2O_2-induced oxidation and apoptosis (Murata *et al.* 2003). This protection is diminished, however, by cadmium (Murata *et al.* 2003). Akt plays a role in maintaining cytochrome c in the mitochondria and in diminishing the response to cytochrome c when it is released (Franke *et al.* 2003; Kennedy *et al.* 1999). Akt also plays a role in embryonic development, regulating organ growth and ultimate size (Shioi *et al.* 2002). The redox sensitivity and modulation of Akt, and the role of this sensitivity in regulating cytochrome c release from the

mitochondria(Kennedy *et al.* 1999; Kennedy *et al.* 1997), provide an intriguing overlap with GPx4 in terms of cellular location and function. Further research to examine the possible role of the Akt signaling pathway, and its redox sensitivity, in the mechanisms of embryolethality of the *GPx4* null genotype is also warranted.

MAPK signaling pathways are also redox sensitive. Apoptosis signal-regulating kinase 1 (ASK1) is a redox sensitive MAPKKK that activates both the p38 and JNK signaling cascades (Takeda *et al.* 2003). ASK1 can be activated either directly by ROS or through a receptor-mediated mechanism involving the tumor necrosis factor (TNF) receptor. Although p38 and JNK activation are not ASK1 dependent, sustained activation of these pathways by H_2O_2 and TNF is reduced in mouse embryonic fibroblasts with an $ASK^{-/-}$ genotype (Takeda *et al.* 2003). Thus, ASK1 is a likely target of further research to characterize the mechanisms of GPx4 function.

Finally, the finding that diminished function of the UPS system accompanies increased levels of cadmium-induced cytotoxicity is consistent with the findings of others (Figueiredo-Pereira *et al.* 1998). Whether this diminished function is a necessary step in the pathway that ultimately leads to cell death in the cadmium-induced cytotoxicity must be further studied. It is possible that cadmium exerts and effect on the UPS by impacting function of enzymes in the UPS. Gene expression studies from our laboratory of cadmium-treated mouse embronic fibroblast cells using microarray analysis indicate that cadmium disrupted levels of ubiquitin ligases such as the multi-function ligase/hydrolase UCH-L1 (unpublished data). In addition, elucidation of the specific targets of ubiquitination in this pathway is necessary to understand the underlying mechanism, and the role of GPx4.

Relevance of GPx4 to Public Health and Susceptibility to Disease

Considering the embryonic lethality of the $GPx4^{-/-}$ genotype, the heterozygous null model that gives reduced expression of GPx4 is likely to more closely mimic the

genetic and phenotypic variation present in human populations, and provide the means to understand the potential role of GPx4 in human disease and the underlying mechanisms of action.

In fact, reduced expression of GPx4 has been associated with male infertility in two separate human populations. Imai and colleagues analyzed sperm from 73 infertile patients and 31 fertile controls (Imai *et al.* 2001). Although 66 of the infertile males expressed GPx4 at levels similar to the fertile controls, 7 individuals had between an 80 and 90% reduction in GPx4 expression. Further, motility in sperm from GPx4-deficient infertile males was significantly reduced compared to both fertile males and GPx4-sufficient infertile males. Foresta and colleagues measured rescued GPx4 activity in sperm from 75 infertile men and 37 fertile controls (Foresta *et al.* 2002). GPx4 activity was 50% lower in the infertile group relative to the controls, and nearly 70% lower in sperm from patients diagnosed with asthenozooospermia compared to the fertile controls. The reduced activity was also associated with decrements in morphology and motility. Despite these findings, it is unknown whether reduced GPx4 levels are a cause or a result of the sperm dysfunction. GPx4 is a necessary structural component of sperm, comprising as much as 50% of the capsule material (Ursini *et al.* 1999). Degradation of GPx4 could be a non-specific by-product of the damage to sperm integrity associated with the unknown primary cause of the infertility. Nevertheless, a putative role for GPx4 deficiency in sperm dysfunction is plausible and should be further evaluated.

Twenty-three polymorphisms were identified in the *GPx4* coding and flanking regions of genomic DNA from 43 infertile men and 21 control males, including single nucleotide polymorphisms (SNPs), insertions, and deletions (Maiorino *et al.* 2003). None were associated with infertility in the study population as a whole. However, any association between a polymorphism and a specific condition was likely undetectable in this heterogeneous population that included eight separate

diagnoses and 20 individuals identified with idiopathic infertility. Nevertheless, one sequence variation, Ala93-Thr, identified in a patient with cryptorchidsm is homologous to a porcine *gpx4* mutation associated with decreased GPx4 activity.

GPx4 may play a role in protection from other pathological states as well. GPx4 overexpression in cancer cell lines appears to confer protection against markers of disease progression. For example, overexpression of GPx4 in pancreatic cancer cell lines was associated with 95% lower tumor growth in mice injected with the cells (Liu *et al.* 2006). Overexpression of GPx4 in a human dermal fibroblast cell line completely inhibited UVA-induced expression of interstitial collagenase matrix metalloproteinase (MMP-1), the most important metalloproteinase in degradation of the dermal extracellular matrix in photoaging and may be important in dermal epithelial carcinoma formation (Wenk *et al.* 2004). Furthermore, these cells produce lower levels of malondialdehyde, a by-product of lipid peroxidation, upon treatment with UVA (Dissemond *et al.* 2003).

References

Alvarez, S. M., Gomez, N. N., Scardapane, L., Zirulnik, F., Martinez, D., and Gimenez, M. S. (2004). Morphological changes and oxidative stress in rat prostate exposed to a non-carcinogenic dose of cadmium. Toxicol Lett 153, 365-76.

Antunes, F., Salvador, A., and Pinto, R. E. (1995). PHGPx and phospholipase A2/GPx: comparative importance on the reduction of hydroperoxides in rat liver mitochondria. Free Radic Biol Med 19, 669-77.

Arai, M., Imai, H., Koumura, T., Yoshida, M., Emoto, K., Umeda, M., Chiba, N., and Nakagawa, Y. (1999). Mitochondrial phospholipid hydroperoxide glutathione peroxidase plays a major role in preventing oxidative injury to cells. J. Biol. Chem. 274, 4924-4933.

Arai, M., Imai, H., Sumi, D., Imanaka, T., Takano, T., Chiba, N., and Nakagawa, Y. (1996). Import into mitochondria of phospholipid hydroperoxide glutathione peroxidase requires a leader sequence. Biochem. Biophys. Res. Commun. 227, 433–439.

ATSDR (1999). Toxicological profile for cadmium. Agency for Toxic Substances and Disease Registry, U.S. Public Health Services, Atlanta, GA.

Avery, A. M., Willetts, S. A., and Avery, S. V. (2004). Genetic dissection of the phospholipid hydroperoxidase activity of yeast gpx3 reveals its functional importance. J Biol Chem 279, 46652-8.

Avissar, N., Finkelstein, J. N., Horowitz, S., Willey, J. C., Coy, E., Frampton, M. W., Watkins, R. H., Khullar, P., Xu, Y. L., and Cohen, H. J. (1996). Extracellular glutathione peroxidase in human lung epithelial lining fluid and in lung cells. Am J Physiol 270, L173-82.

Avissar, N., Ornt, D. B., Yagil, Y., Horowitz, S., Watkins, R. H., Kerl, E. A., Takahashi, K., Palmer, I. S., and Cohen, H. J. (1994). Human kidney proximal tubules are the main source of plasma glutathione peroxidase. Am J Physiol 266, C367-75.

Bagchi, D., Joshi, S. S., Bagchi, M., Balmoori, J., Benner, E. J., Kuszynski, C. A., and Stohs, S. J. (2000). Cadmium- and chromium-induced oxidative stress, DNA damage, and apoptotic cell death in cultured human chronic myelogenous leukemic K562 cells, promyelocytic leukemic HL-60 cells, and normal human peripheral blood mononuclear cells. J Biochem Mol Toxicol 14, 33-41.

Beton, D. C., Andrews, G. S., Davies, H. J., Howells, L., and Smith, G. F. (1966). Acute cadmium fume poisoning. Five cases with one death from renal necrosis. Br J Ind Med 23, 292-301.

Borchert, A., Savaskan, N. E., and Kuhn, H. (2003). Regulation of expression of the phospholipid hydroperoxide/sperm nucleus glutathione peroxidase gene. Tissue-specific expression pattern and identification of functional cis- and trans-regulatory elements. J Biol Chem 278, 2571-80.

Borchert, A., Schnurr, K., Thiele, B. J., and Kuhn, H. (1999). Cloning of the mouse phospholipid hydroperoxide glutathione peroxidase gene. FEBS Lett. 446, 223-7.

Brigelius-Flohe, R., Aumann, K. D., Blocker, H., Gross, G., Kiess, M., Kloppel, K. D., Maiorino, M., Roveri, A., Schuckelt, R., Usani, F., and et al. (1994). Phospholipid-hydroperoxide glutathione peroxidase. Genomic DNA, cDNA, and deduced amino acid sequence. J Biol Chem 269, 7342-8.

Brigelius-Flohe, R., Aumann, K. D., Blocker, H., Gross, G., Kiess, M., Kloppel, K. D., Maiorino, M., Roveri, A., Schuckelt, R., Usani, F., Wingender, E., and Flohe, L. (1994). Phospholipid-hydroperoxide glutathione peroxidase. Genomic DNA, cDNA, and deduced amino acid sequence. J. Biol. Chem. 269, 7342-8.

Cantley, L. C. (2002). The phosphoinositide 3-kinase pathway. Science 296, 1655-7.

Cantley, L. C., and Neel, B. G. (1999). New insights into tumor suppression: PTEN suppresses tumor formation by restraining the phosphoinositide 3-kinase/AKT pathway. Proc Natl Acad Sci U S A 96, 4240-5.

Cardone, M. H., Roy, N., Stennicke, H. R., Salvesen, G. S., Franke, T. F., Stanbridge, E., Frisch, S., and Reed, J. C. (1998). Regulation of cell death protease caspase-9 by phosphorylation. Science 282, 1318-21.

Chang, L. (1996). Toxicology of Metals. CRC Press, Boca Raton, Fl.

Chao, J.-I., and Yang, J.-L. (2001). Opposite roles of ERK and p38 mitogen-activated protein kinases in cadmium-induced genotoxicity and mitotic arrest. Chem Res Toxicol 14, 1193-1202.

Chu, F. F., and Esworthy, R. S. (1995). The expression of an intestinal form of glutathione peroxidase (GSHPx-GI) in rat intestinal epithelium. Arch Biochem Biophys 323, 288-94.

Chuang, S. M., Wang, I. C., and Yang, J. L. (2000). Roles of JNK, p38 and ERK mitogen-activated protein kinases in the growth inhibition and apoptosis induced by cadmium. Carcinogenesis 21, 1423-32.

Ciechanover, A., and Brundin, P. (2003). The ubiquitin proteasome system in neurodegenerative diseases: sometimes the chicken, sometimes the egg. Neuron 40, 427-46.

Ciechanover, A., and Schwartz, A. L. (2002). Ubiquitin-mediated degradation of cellular proteins in health and disease. Hepatology 35, 3-6.

Dalton, T. P., Dieter, M. Z., Yang, Y., Shertzer, H. G., and Nebert, D. W. (2000). Knockout of the mouse glutamate cysteine ligase catalytic subunit (GCLc) gene: embryonic lethal when homozygous, and proposed model for moderate glutathione deficiency when heterozygous. Biochem. Biophys. Res. Commun. 279, 324-9.

Davison, A. G., Fayers, P. M., Taylor, A. J., Venables, K. M., Darbyshire, J., Pickering, C. A., Chettle, D. R., Franklin, D., Guthrie, C. J., Scott, M. C., and et al. (1988). Cadmium fume inhalation and emphysema. Lancet 1, 663-7.

de Almeida, E. A., Miyamoto, S., Bainy, A. C., de Medeiros, M. H., and Di Mascio, P. (2004). Protective effect of phospholipid hydroperoxide glutathione peroxidase (PHGPx) against lipid peroxidation in mussels Perna perna exposed to different metals. Mar Pollut Bull 49, 386-92.

Dissemond, J., Schneider, L. A., Brenneisen, P., Briviba, K., Wenk, J., Wlaschek, M., and Scharffetter-Kochanek, K. (2003). Protective and determining factors for the overall lipid peroxidation in ultraviolet A1-irradiated fibroblasts: in vitro and in vivo investigations. Br J Dermatol 149, 341-9.

Dreher, I., Schmutzler, C., Jakob, F., and Kohrle, J. (1997). Expression of selenoproteins in various rat and human tissues and cell lines. J Trace Elem Med Biol 11, 83-91.

Elbekai, R. H., and El-Kadi, A. O. (2005). The role of oxidative stress in the modulation of aryl hydrocarbon receptor-regulated genes by As3+, Cd2+, and Cr6+. Free Radic Biol Med 39, 1499-511.

Ercal, N., Gurer-Orhan, H., and Aykin-Burns, N. (2001). Toxic metals and oxidative stress part I: mechanisms involved in metal-induced oxidative damage. Curr Top Med Chem 1, 529-39.

Esworthy, R. S., Doan, K., Doroshow, J. H., and Chu, F. F. (1994). Cloning and sequencing of the cDNA encoding a human testis phospholipid hydroperoxide glutathione peroxidase. Gene 144, 317-8.

Faustman-Watts, E. M., Namkung, M. J., and Juchau, M. R. (1986). Modulation of the embryotoxicity in vitro of reactive metabolites of 2-acetylaminofluorene by reduced glutathione and ascorbate and via sulfation. Toxicol. Appl. Pharmacol. 86, 400-10.

Fernández, E., Gustafson, A., Andersson, M., Hellman, B., and Dencker, L. (2003). Cadmium-induced changes in apoptotic gene expression levels and DNA damage in mouse embryos are blocked by zinc. Toxicol Sci 76, 162-170.

Figueiredo-Pereira, M. E., Yakushin, S., and Cohen, G. (1997). Accumulation of ubiquitinated proteins in mouse neuronal cells induced by oxidative stress. Mol Biol Rep 24, 35-8.

Figueiredo-Pereira, M. E., Yakushin, S., and Cohen, G. (1998). Disruption of the intracellular sulfhydryl homeostasis by cadmium-induced oxidative stress leads to protein thiolation and ubiquitination in neuronal cells. J Biol Chem 273, 12703-9.

Filipic, M., Fatur, T., and Vudrag, M. (2006). Molecular mechanisms of cadmium induced mutagenicity. Hum Exp Toxicol 25, 67-77.

Flohe, L., Foresta, C., Garolla, A., Maiorino, M., Roveri, A., and Ursini, F. (2002). Metamorphosis of the selenoprotein PHGPx during spermatogenesis. Ann. NY Acad. Sci. 973, 287-288.

Foresta, C., Flohe, L., Garolla, A., Roveri, A., Ursini, F., and Maiorino, M. (2002). Male fertility is linked to the selenoprotein phospholipid hydroperoxide glutathione peroxidase. Biol Reprod 67, 967-71.

Franke, T. F., Hornik, C. P., Segev, L., Shostak, G. A., and Sugimoto, C. (2003). PI3K/Akt and apoptosis: size matters. Oncogene 22, 8983-98.

Garry, M. R., Kavanagh, T. J., Faustman, E. M., Sidhu, J. S., Liao, R., Ware, C., Vliet, P. A., and Deeb, S. S. (2006). Sensitivity of Mouse Lung Fibroblasts Heterozygous for GPx4 to Oxidative Stress. Submitted to Free Radic Biol Med.

Goering, P., Waalkes, M., and Klaassen, C. (1994). Cadmium toxicity. In Handbook of Experimental Pharmacolcogy; Toxicology of Metals, Biochemical effects (R. Goyer and M. Cherian, eds.), pp. 189-214. Springer-Verlag, New Yok.

Hales, B. F., and Brown, H. (1991). The effect of in vivo glutathione depletion with buthionine sulfoximine on rat embryo development. Teratology 44, 251-257.

Halestrap, A. P., Woodfield, K. Y., and C.P., C. (1997). Oxidative stress, thiol reagents, and membrane potential modulate the mitochondrial permeability transition by affecting nucleotide binding to the adenine nucleotide translocase. J. Biol. Chem. 272, 3346-54.

Hansen, J. M., Zhang, H., and Jones, D. P. (2006). Differential oxidation of thioredoxin-1, thioredoxin-2, and glutathione by metal ions. Free Radic Biol Med 40, 138-45.

Harris, C., Namkung, M. J., and Juchau, M. R. (1987). Regulation of intracellular glutathione in rat embryos and visceral yolk sacs and its effect on 2-nitrosofluorene-induced malformations in the whole embryo culture system. Toxicol. Appl. Pharmacol. 88, 141-52.

Hoffman, B., Stockl, A., Schlame, M., Beyer, K., and Klingenberg, M. (1994). The reconstituted ADP/ATP carrier activity has an absolute requirement for cardiolipin as shown in cysteine mutants. J. Biol. Chem. 269, 1940-1944.

Holland, D., Ben-Hayyim, G., Faltin, Z., Camoin, L., Strosberg, A. D., and Eshdat, Y. (1993). Molecular characterization of salt-stress-associated protein in citrus: protein and cDNA sequence homology to mammalian glutathione peroxidases. Plant Mol. Biol. 21, 923-7.

Huang, H.-S., Chang, W. C., and Chen, C. J. (2002). Involvement of reactive oxygen species I arsenite-induced downregulation of phospholipid hydroperoxide glutathione peroxidase in human epidermoid carcinoma A431 cells. Free Rad. Biol. Med. 33, 864-873.

Huang, Y. H., Shih, C. M., Huang, C. J., Lin, C. M., Chou, C. M., Tsai, M. L., Liu, T. P., Chiu, J. F., and Chen, C. T. (2006). Effects of cadmium on structure and enzymatic activity of Cu,Zn-SOD and oxidative status in neural cells. J Cell Biochem.

Hurst, R., Bao, Y., Jemth, P., Mannervik, B., and Williamson, G. (1998). Phospholipid hydroperoxide glutathione peroxidase activity of human glutathione transferases. Biochem J 332 (Pt 1), 97-100.

Imai, H., Hirao, F., Sakamoto, T., Sekine, K., Mizukura, Y., Saito, M., Kitamoto, T., Hayasaka, M., Hanaoka, K., and Nakagawa, Y. (2003). Early embryonic lethality caused by targeted disruption of the mouse PHGPx gene. Biochem. Biophys. Res. Commun. 30, 278-286.

Imai, H., and Nakagawa, Y. (2003). Biological significance of phospholipid hydroperoxide glutathione peroxidase (PHGPx, GPx4) in mammalian cells. Free Radic. Biol. Med. 34, 145-169.

Imai, H., and Nakagawa, Y. (2003). Biological significance of phospholipid hydroperoxide glutathione peroxidase (PHGPx, GPx4) in mammalian cells. Free Radic Biol Med 34, 145-69.

Imai, H., Narashima, K., Arai, M., Sakamoto, H., Chiba, N., and Nakagawa, Y. (1998). Suppression of leukotriene formation in RBL-2H3 cells that overexpressed phospholipid hydroperoxide glutathione peroxidase. J. Biol. Chem. 273, 1990-1997.

Imai, H., Sumi, D., Hanamoto, A., Arai, M., Sugiyama, A., and Nakagawa, Y. (1995). Molecular cloning and functional expression of a cDNA from rat phospholipid hydroperoxide glutathione peroxidase: 3'-untranslated region of the gene is necessary for functional expression. J. Biochem. (Tokyo) 118, 1061-1067.

Imai, H., Suzuki, K., Ishizaka, K., Ichinose, S., Oshima, H., Okayasu, I., Emoto, K., Umeda, M., and Nakagawa, Y. (2001). Failure of expression of phospholipid hydroperoxide glutathione peroxidase in the spermatozoa of human infertile males. Biol. Reprod. 64, 674-683.

Imai, H., Suzuki, K., Ishizaka, K., Ichinose, S., Oshima, H., Okayasu, I., Emoto, K., Umeda, M., and Nakagawa, Y. (2001). Failure of the expression of phospholipid hydroperoxide glutathione peroxidase in the spermatozoa of human infertile males. Biol Reprod 64, 674-83.

Jimi, S., Uchiyama, M., Takaki, A., Suzumiya, J., and Hara, S. (2004). Mechanisms of cell death induced by cadmium and arsenic. Ann N Y Acad Sci 1011, 325-31.

Jin, P., and Ringertz, N. R. (1990). Cadmium induces transcription of proto-oncogenes c-jun and c-myc in rat L6 myoblasts. J Biol Chem 265, 14061-4.

Jonak, C., Nakagami, H., and Hirt, H. (2004). Heavy metal stress. Activation of distinct mitogen-activated protein kinase pathways by copper and cadmium. Plant Physiol 136, 3276-83.

Kaneko, T., Baba, N., and Matsuo, M. (1994). Phospholipid hydroperoxides are significantly less toxic to cultured endothelial cells than fatty acid hydroperoxides. Life Sci. 55, 1443-9.

Kaneko, T., Baba, N., and Matsuo, M. (2000). Protective effect of phenolic antioxidants on the cytotoxicity induced by phosphatidylcholine hydroperoxide. Biosci. Biotechnol. Biochem. 64, 1274-7.

Kefaloyianni, E., Gourgou, E., Ferle, V., Kotsakis, E., Gaitanaki, C., and Beis, I. (2005). Acute thermal stress and various heavy metals induce tissue-specific pro- or anti-apoptotic events via the p38-MAPK signal transduction pathway in Mytilus galloprovincialis (Lam.). J Exp Biol 208, 4427-36.

Kennedy, S. G., Kandel, E. S., Cross, T. K., and Hay, N. (1999). Akt/Protein kinase B inhibits cell death by preventing the release of cytochrome c from mitochondria. Mol Cell Biol 19, 5800-10.

Kennedy, S. G., Wagner, A. J., Conzen, S. D., Jordan, J., Bellacosa, A., Tsichlis, P. N., and Hay, N. (1997). The PI 3-kinase/Akt signaling pathway delivers an anti-apoptotic signal. Genes Dev 11, 701-13.

Kim, J., and Sharma, R. P. (2004). Calcium-mediated activation of c-Jun NH2-terminal kinase (JNK) and apoptosis in response to cadmium in murine macrophages. Toxicol Sci 81, 518-27.

Kim, J., and Sharma, R. P. (2006). Cadmium-induced Apoptosis in Murine Macrophages is Antagonized by Antioxidants and Caspase Inhibitors. J Toxicol Environ Health A 69, 1181-201.

Kim, S. D., Moon, C. K., Eun, S. Y., Ryu, P. D., and Jo, S. A. (2005). Identification of ASK1, MKK4, JNK, c-Jun, and caspase-3 as a signaling cascade involved in cadmium-induced neuronal cell apoptosis. Biochem Biophys Res Commun 328, 326-34.

Kirkland, R. A., Adibhatla, R. M., Hatcher, J. F., and Franklin, J. L. (2002). Loss of cardiolipin and mitochondria during programmed neuronal death: evidence of a role for lipid peroxidation and autophagy. Neuroscience 115, 587-602.

Kirschvink, N., Martin, N., Fievez, L., Smith, N., Marlin, D., and Gustin, P. (2006). Airway inflammation in cadmium-exposed rats is associated with pulmonary oxidative stress and emphysema. Free Radic Res 40, 241-50.

Knopp, E. A., Arndt, T. L., Eng, K. L., Caldwell, M., LeBoeuf, R. C., Deeb, S. S., and O'Brien, K. D. (1999). Murine phospholipid hydroperoxide glutathione peroxidase: cDNA sequence, tissue expression, and mapping. Mamm. Genome 10, 601-605.

Kokoszka, J. E., Waymire, K. G., Levy, S. E., Sligh, J. E., Cai, J., Jones, D. P., MacGregor, G. R., and Wallace, D. C. (2004). The ADP/ATP translocator is not essential for the mitochondrial permeability transition pore. Nature 427, 461-5.

Komatsu, H., Okayasu, I., Mitomi, H., Imai, H., Nakagawa, Y., and Obata, F. (2001). Immunohistochemical detection of human gastrointestinal glutathione peroxidase in normal tissues and cultured cells with novel mouse monoclonal antibodies. J Histochem Cytochem 49, 759-66.

Kondoh, M., Araragi, S., Sato, K., Higashimoto, M., Takiguchi, M., and Sato, M. (2002). Cadmium induces apoptosis partly via caspase-9 activation in HL-60 cells. Toxicology 170, 111-7.

Kong, B. W., Kim, H., and Foster, D. N. (2003). Cloning and expression analysis of chicken phospholipid-hydroperoxide glutathione peroxidase. Anim. Biotechnol. 14, 19-29.

Konishi, H., Matsuzaki, H., Tanaka, M., Takemura, Y., Kuroda, S., Ono, Y., and Kikkawa, U. (1997). Activation of protein kinase B (Akt/RAC-protein kinase) by cellular stress and its association with heat shock protein Hsp27. FEBS Lett 410, 493-8.

Lag, M., Refsnes, M., Lilleaas, E. M., Holme, J. A., Becher, R., and Schwarze, P. E. (2005). Role of mitogen activated protein kinases and protein kinase C in cadmium-induced apoptosis of primary epithelial lung cells. Toxicology 211, 253-64.

Leduc, D., de Francquen, P., Jacobovitz, D., Vandeweyer, R., Lauwerys, R., and De Vuyst, P. (1993). Association of cadmium exposure with rapidly progressive emphysema in a smoker. Thorax 48, 570-1.

Lee, J. S., Zhang, M. H., Yun, E. K., Geum, D., Kim, K., Kim, T. H., Lim, Y. S., and Seo, J. S. (2005). Heat shock protein 27 interacts with vimentin and prevents insolubilization of vimentin subunits induced by cadmium. Exp Mol Med 37, 427-35.

Lei, X. G., Evenson, J. K., Thompson, K. M., and Sunde, R. A. (1995). Glutathione peroxidase and phospholipid hydroperoxide glutathione peroxidase are differentially regulated in rats by dietary selenium. J Nutr 125, 1438-46.

Leyens, G., Knoops, B., and Donnay, I. (2004). Expression of peroxiredoxins in bovine oocytes and embryos produced in vitro. Mol Reprod Dev 69, 243-51.

Lim, M. S., and Elenitoba-Johnson, K. S. (2004). Ubiquitin ligases in malignant lymphoma. Leuk Lymphoma 45, 1329-39.

Liu, J., Du, J., Zhang, Y., Sun, W., Smith, B. J., Oberley, L. W., and Cullen, J. J. (2006). Suppression of the malignant phenotype in pancreatic cancer by overexpression of phospholipid hydroperoxide glutathione peroxidase. Hum Gene Ther 17, 105-16.

Lopez, E., Arce, C., Oset-Gasque, M. J., Canadas, S., and Gonzalez, M. P. (2006). Cadmium induces reactive oxygen species generation and lipid peroxidation in cortical neurons in culture. Free Radic Biol Med 40, 940-51.

Maiorino, M., Bosello, V., Ursini, F., Foresta, C., Garolla, A., Scapin, M., Sztajer, H., and Flohe, L. (2003). Genetic variations of gpx-4 and male infertility in humans. Biol Reprod 68, 1134-41.

Maiorino, M., Thomas, J. P., Girotti, A. W., and Ursini, F. (1991). Reactivity of phospholipid hydroperoxide glutathione peroxidase with membrane and lipoprotein lipid hydroperoxides. Free Radic Res Commun 12-13 Pt 1, 131-5.

Maiorino, M., Wissing, J. B., Brigelius-Flohe, R., Calabrese, F., Roveri, A., Steinert, P., Ursini, F., and Flohe, L. (1998). Testosterone mediates expression of the selenoprotein PHGPx by induction of spermatogenesis and not by direct transcriptional gene activation. FASEB J. 12, 1359-1370.

Manevich, Y., and Fisher, A. B. (2005). Peroxiredoxin 6, a 1-Cys peroxiredoxin, functions in antioxidant defense and lung phospholipid metabolism. Free Radic Biol Med 38, 1422-32.

Metivier, D., Dallaporta, B., Zamzami, N., Larochette, N., Susin, S. A., Marzo, I., and Kroemer, G. (1998). Cytofluorometric detection of mitochondrial alterations in early CD95/Fas/APO-1-triggered apoptosis of Jurkat T lymphoma cells. Comparison of seven mitochondrion-specific fluorochromes. Immunol. Lett. 61, 157-163.

Mirkes, P. E., Wilson, K. L., and Cornel, L. M. (2000). Teratogen-induced activation of ERK, JNK, and p38 MAP kinases in early postimplantation murine embryos. Teratology 62, 14-25.

Misra, U. K., Gawdi, G., and Pizzo, S. V. (2003). Induction of mitogenic signalling in the 1LN prostate cell line on exposure to submicromolar concentrations of cadmium+. Cell Signal 15, 1059-70.

Murata, H., Ihara, Y., Nakamura, H., Yodoi, J., Sumikawa, K., and Kondo, T. (2003). Glutaredoxin exerts an antiapoptotic effect by regulating the redox state of Akt. J Biol Chem 278, 50226-33.

Nam, S., Nakamuta, N., Kurohmaru, M., and Hayashi, Y. (1997). Cloning and sequencing of the mouse cDNA encoding a phospholipid hydroperoxide glutathione peroxidase. Gene 198, 245-9.

Nam, S. Y., Fujisawa, M., Kim, J. S., Kurohmaru, M., and Hayashi, Y. (1998). Expression pattern of phospholipid hydroperoxide glutathione peroxidase messenger ribonucleic acid in mouse testis. Biol. Reprod. 58, 1272-1276.

Naujokat, C., and Hoffmann, S. (2002). Role and function of the 26S proteasome in proliferation and apoptosis. Lab Invest 82, 965-80.

Nomura, K., Imai, H., Koumura, T., Arai, M., and Nakagawa, Y. (1999). Mitochondrial phospholipid hydroperoxide glutathione peroxidase suppresses apoptosis mediated by a mitochondrial death pathway. J. Biol. Chem. 274, 29294–29302.

Nomura, K., Imai, H., Koumura, T., Kobayashi, T., and Nakagawa, Y. (2000). Mitochondrial phospholipid hydroperoxide glutathione peroxidase inhibits the release of cytochrome c from mitochondria by suppressing the peroxidation of cardiolipin in hypoglycaemia-induced apoptosis. Biochem. J. 351, 183-193.

Nomura, K., Imai, H., Koumura, T., Kobayashi, T., and Nakagawa, Y. (2000). Mitochondrial phospholipid hydroperoxide glutathione peroxidase inhibits the release of cytochrome c from mitochondria by suppressing the peroxidation of cardiolipin in hypoglycaemia-induced apoptosis. Biochem J 351, 183-93.

NTP (2005). Report on carcinogens, eleventh edition. Carcinogen profiles 2005. National Toxicology Program. Rep Carcinog 11, i-vi, 1-263, 1-44 passim.

Ozolins, T. R., Siksay, D. L., and Wells, P. G. (1996). Modulation of embryonic glutathione peroxidase activity and phenytoin teratogenicity by dietary deprivation of selenium in CD-1 mice. J. Pharmacol. Exp. Ther. 277, 945-53.

Papadakis, E. S., Finegan, K. G., Wang, X., Robinson, A. C., Guo, C., Kayahara, M., and Tournier, C. (2006). The regulation of Bax by c-Jun N-terminal protein kinase (JNK) is a prerequisite to the mitochondrial-induced apoptotic pathway. FEBS Lett 580, 1320-6.

Pereira, F. A., de Assuncao, J. V., Saldiva, P. H., Pereira, L. A., Mirra, A. P., and Braga, A. L. (2005). Influence of air pollution on the incidence of respiratory tract neoplasm. J Air Waste Manag Assoc 55, 83-7.

Pfeifer, H., Conrad, M., Roethlein, D., Kyriakopoulos, A., Brielmeier, M., Bornkamm, G. W., and Behne, D. (2001). Identification of a specific sperm nuclei selenoenzyme necessary for protamine thiol cross-linking during sperm maturation. Faseb J 15, 1236-8.

Poliandri, A., Cabilla, J., Velardez, M., Bodo, C., and Duvilanski, B. (2003). Cadmium induces apoptosis in anterior pituitary cells that can be reversed by treatment with antioxidants. Toxicol App Pharmacol 190, 17-24.

Pryor, W. A., Houk, K. N., Foote, C. S., Fukuto, J. M., Ignarro, L. J., Squadrito, G. L., and Davies, K. J. (2006). Free Radical Biology and Medicine: It's a Gas, Man! Am J Physiol Regul Integr Comp Physiol.

Pushpa-Rekha, T. R., Burdsall, A. L., Oleksa, L. M., Chisolm, G. M., and Driscoll, D. M. (1995). Rat phospholipid-hydroperoxide glutathione peroxidase. cDNA cloning and identification of multiple transcription and translation start sites. J. Biol. Chem. 270, 26993-9.

Raijmakers, M. T., Steegers, E. A., and Peters, W. H. (2001). Glutathione S-transferases and thiol concentrations in embryonic and early fetal tissues. Hum Reprod 16, 2445-50.

Ran, Q., Liang, H., Gu, M., Qi, W., Walter, C. A., Roberts, L. J., 2nd, Herman, B., Richardson, A., and Van Remmen, H. (2004). Transgenic mice overexpressing glutathione peroxidase 4 are protected against oxidative stress-induced apoptosis. J Biol Chem 279, 55137-46.

Ran, Q., Van Remmen, H., Gu, M., Qi, W., Roberts, L. J., 2nd, Prolla, T., and Richardson, A. (2003). Embryonic fibroblasts from Gpx4+/- mice: a novel model for studying the role of membrane peroxidation in biological processes. Free Radic Biol Med 35, 1101-9.

Ran, Q., Van Remmen, H., Gu, M., Qi, W., Roberts, L. J., Prolla, T. A., and Richardson, A. (2003). Embryonic fibroblasts from GPx4+/- mice: a novel model for studying the role of membrane peroxidation in biological processes. Free Radic. Biol. Med. 35, 1101-9.

Rockwell, P., Martinez, J., Papa, L., and Gomes, E. (2004). Redox regulates COX-2 upregulation and cell death in the neuronal response to cadmium. Cell Signal 16, 343-53.

Roveri, A., Maiorino, M., Nisii, C., and Ursini, F. (1994). Purification and characterization of phospholipid hydroperoxide glutathione peroxidase from rat testis mitochondrial membranes. Biochim. Biophys. Acta 1208, 211-221.

Saillenfait, A. M., Payan, J. P., Langonne, I., Beydon, D., Grandclaude, M. C., Sabate, J. P., and de Ceaurriz, J. (1993). Modulation of acrylonitrile-induced embryotoxicity in vitro by glutathione depletion. Arch. Toxicol. 67, 164-172.

Sakamoto, H., Imai, H., and Nakagawa, Y. (2000). Involvement of phospholipid hydroperoxide glutathione peroxidase in the modulation of prostaglandin D2 synthesis. J. Biol. Chem. 275, 40028-40035.

Sakamoto, H., Tosaki, T., and Nakagawa, Y. (2002). Overexpression of phospholipid hydroperoxide glutathione peroxidase modulates acetyl-CoA, 1-O-alkyl-2-lyso-sn-glycero-3-phosphocholine acetyltransferase activity. J Biol Chem 277, 50431-8.

Satarug, S., Baker, J., Urbenjapol, S., Haswell-Elkins, M., Reilly, P., Williams, D. J., and Moore, M. R. (2003). A global perspective on cadmium pollution and toxicity in non-occupationally exposed population. Toxicol Let 137, 65-83.

Satarug, S., and Moore, M. R. (2004). Adverse health effects of chronic exposure to low-level cadmium in foodstuffs and cigarette smoke. Environ Health Perspect 112, 1099-103.

Schlame, M., Rua, D., and Greenberg, M. L. (2000). The biosynthesis and functional role of cardiolipin. Prog. Lipid Res. 39, 257–288.

Scimeca, M. S., Lisk, D. J., Prolla, T., and Lei, X. G. (2005). Effects of gpx4 haploid insufficiency on GPx4 activity, selenium concentration, and paraquat-induced protein oxidation in murine tissues. Exp Biol Med (Maywood) 230, 709-14.

Servais, S., Boussouar, A., Molnar, A., Douki, T., Pequignot, J. M., and Favier, R. (2005). Age-related sensitivity to lung oxidative stress during ozone exposure. Free Radic Res 39, 305-16.

Shan, S. W., Tang, M. K., Cai, D. Q., Chui, Y. L., Chow, P. H., Grotewold, L., and Lee, K. K. (2005). Comparative proteomic analysis identifies protein disulfide isomerase and peroxiredoxin 1 as new players involved in embryonic interdigital cell death. Dev Dyn 233, 266-81.

Shioi, T., McMullen, J. R., Kang, P. M., Douglas, P. S., Obata, T., Franke, T. F., Cantley, L. C., and Izumo, S. (2002). Akt/protein kinase B promotes organ growth in transgenic mice. Mol Cell Biol 22, 2799-809.

Simpkins, C. O. (2000). Metallothionein in human disease. Cell Mol Biol (Noisy-le-grand) 46, 465-88.

Slott, V. L., and Hales, B. F. (1987). Protection of rat embryos in culture against the embryotoxicity of acrolein using exogenous glutathione. Biochem. Pharmacol. 36, 2187-94.

Son, M. H., Kang, K. W., Lee, C. H., and Kim, S. G. (2001). Potentiation of cadmium-induced cytotoxicity by sulfur amino acid deprivation through activation of extracellular signal-regulated kinasel 1/2 (ERK1/2) in conjunction with p38 kinase or c-jun N-terminal kinase (JNK) complete inhibition of the potentiated toxicity by U0126 an ERK1/2 and p38 kinase inhibitor. Biochem Pharmacol 62, 1379-1390.

Stayner, L., Smith, R., Thun, M., Schnorr, T., and Lemen, R. (1992). A dose-response analysis and quantitative assessment of lung cancer risk and occupational cadmium exposure. Ann Epidemiol 2, 177-94.

Stohs, S. J., Bagchi, D., Hassoun, E., and Bagchi, M. (2001). Oxidative mechanisms in the toxicity of chromium and cadmium ions. J Environ Pathol Toxicol Oncol 20, 77-88.

Sugimoto, M., Furui, S., and Suzuki, Y. (1997). Molecular cloning and characterization of a cDNA encoding putative phospholipid hydroperoxide glutathione peroxidase from spinach. Biosci. Biotechnol. Biochem. 61, 1379-81.

Sun, Q., Kojima, H., Komura, S., Ohishi, N., and Yagi, K. (1997). Effect of selenium on human phospholipid hydroperoxide glutathione peroxidase expression and host cell susceptibility to lipid hydroperoxide-mediated injury. Biochem. Mol. Biol. Int. 42, 957-63.

Sunde, R. A., Dyer, J. A., Moran, T. V., Evenson, J. K., and Sugimoto, M. (1993). Phospholipid hydroperoxide glutathione peroxidase: full-length pig blastocyst cDNA sequence and regulation by selenium status. Biochem. Biophys. Res. Commun. 193, 905-11.

Szuster-Ciesielska, A., Stachura, A., Slotwinska, M., Kaminska, T., Sniezko, R., Paduch, R., Abramczyk, D., Filar, J., and Kandefer-Szerszen, M. (2000). The inhibitory effect of zinc on cadmium-induced cell apoptosis and reactive oxygen species (ROS) production in cell cultures. Toxicology 145, 159-71.

Takebe, G., Yarimizu, J., Saito, Y., Hayashi, T., Nakamura, H., Yodoi, J., Nagasawa, S., and Takahashi, K. (2002). A comparative study on the hydroperoxide and thiol specificity of the glutathione peroxidase family and selenoprotein P. J Biol Chem 277, 41254-8.

Takebe, G., Yarimizu, J., Saito, Y., Hayashi, T., Nakamura, H., Yodoi, J., Nagasawa, S., and Takahashi, K. (2002). A comparative study on the hydroperoxide and thiol specificity of the glutathione peroxidase family and seleoprotein P. J. Biol. Chem. 277, 41254-41258.

Takeda, K., Matsuzawa, A., Nishitoh, H., and Ichijo, H. (2003). Roles of MAPKKK ASK1 in stress-induced cell death. Cell Struct Funct 28, 23-9.

Takenaka, S., Oldiges, H., Konig, H., Hochrainer, D., and Oberdorster, G. (1983). Carcinogenicity of cadmium chloride aerosols in W rats. J Natl Cancer Inst 70, 367-73.

Thomas, J. P., Maiorino, M., Ursini, F., and Girotti, A. W. (1990). Protective action of phospholipid hydroperoxide glutathione peroxidase against membrane-damaging lipid peroxidation. In situ reduction of phospholipid and cholesterol hydroperoxides. J Biol Chem 265, 454-61.

Thun, M. J., Schnorr, T. M., Smith, A. B., Halperin, W. E., and Lemen, R. A. (1985). Mortality among a cohort of U.S. cadmium production workers--an update. J Natl Cancer Inst 74, 325-33.

Torres, M., and Forman, H. J. (2003). Redox signaling and the MAP kinase pathways. Biofactors 17, 287-96.

Tournier, C., Hess, P., Yang, D. D., Xu, J., Turner, T. K., Nimnual, A., Bar-Sagi, D., Jones, S. N., Flavell, R. A., and Davis, R. J. (2000). Requirement of JNK for stress-induced activation of the cytochrome c- mediated death pathway. Science 288, 870-4.

Tsirigotis, M., Zhang, M., Chiu, R., Wouters, B., and Gray, D. (2001). Sensitivity of mammalian cells expressing mutant ubiquitin to protein-damaging agents. J Biol Chem 276, 46073-46078.

Ursini, F., Heim, S., Kiess, M., Maiorino, M., Roveri, A., Wissing, J., and Flohe, L. (1999). Dual function of the selenoprotein PHGPx during sperm maturation. Science 285, 1393-6.

Ursini, F., Heim, S., Kiess, M., Maiorino, M., Roveri, A., Wissing, J., and Flohe, L. (1999). Dual function of the selenoprotein PHGPx during sperm maturation. Science 285, 1393-1395.

Ursini, F., Maiorino, M., and Gregolin, C. (1985). The selenoenzyme phospholipid hydroperoxide glutathione peroxidase. Biochim Biophys Acta 839, 62-70.

Vernet, P., Rock, E., Mazur, A., Rayssiguier, Y., Dufaure, J. P., and Drevet, J. R. (1999). Selenium-independent epididymis-restricted glutathione peroxidase 5 protein (GPX5) can back up failing Se-dependent GPXs in mice subjected to selenium deficiency. Mol Reprod Dev 54, 362-70.

Vieira, H. L., Haouzi, D., El Hamel, C., Jacotot, E., Belzacq, A. S., Brenner, C., and Kroemer, G. (2000). Permeabilization of the mitochondrial inner membrane during apoptosis: impact of the adenine nucleotide translocator. Cell Death Differ. 7, 1146–1154.

Villette, S., Kyle, J. A. M., Brown, K. M., Pickard, K., Milne, J. S., Nicol, F., Arthur, J. R., and Hesketh, J. E. (2002). A novel single nucleotide

polymorphism in the 3' untranslated region of human glutathione peroxidase 4 influences lipoxygenase metabolism. Blood Cell. Mol. Dis. 29, 174-178.

Vismara, C., Vailati, G., and Bacchetta, R. (2001). Reduction in paraquat embryotoxicity by ascorbic acid in Xenopus laevis. Aquatic Toxicol. 51, 293-303.

Voter, K. Z., Whitin, J. C., Torres, A., Morrow, P. E., Cox, C., Tsai, Y., Utell, M. J., and Frampton, M. W. (2001). Ozone exposure and the production of reactive oxygen species by bronchoalveolar cells in humans. Inhal Toxicol 13, 465-83.

Waisberg, M., Joseph, P., Hale, B., and Beyersmann, D. (2003). Molecular and cellular mechanisms of cadmium carcinogenesis. Toxicology 192, 95-117.

Watjen, W., and Beyersmann, D. (2004). Cadmium-induced apoptosis in C6 glioma cells: influence of oxidative stress. Biometals 17, 65-78.

Weinkove, D., and Leevers, S. J. (2000). The genetic control of organ growth: insights from Drosophila. Curr Opin Genet Dev 10, 75-80.

Wells, P. G., Kim, P. M., Laposa, R. R., Nicol, C. J., Parman, T., and Winn, L. M. (1997). Oxidative damage in chemical teratogenesis. Mut. Res. 396, 65-78.

Wenk, J., Schuller, J., Hinrichs, C., Syrovets, T., Azoitei, N., Podda, M., Wlaschek, M., Brenneisen, P., Schneider, L. A., Sabiwalsky, A., Peters, T., Sulyok, S., Dissemond, J., Schauen, M., Krieg, T., Wirth, T., Simmet, T., and Scharffetter-Kochanek, K. (2004). Overexpression of phospholipid-hydroperoxide glutathione peroxidase in human dermal fibroblasts abrogates UVA irradiation-induced expression of interstitial collagenase/matrix metalloproteinase-1 by suppression of phosphatidylcholine hydroperoxide-mediated NFkappaB activation and interleukin-6 release. J Biol Chem 279, 45634-42.

Willems, A. R., Schwab, M., and Tyers, M. (2004). A hitchhiker's guide to the cullin ubiquitin ligases: SCF and its kin. Biochim Biophys Acta 1695, 133-70.

Yagi, K., Komura, S., Kojima, H., Sun, Q., Nagata, N., Ohishi, N., and Nishikimi, M. (1996). Expression of human phospholipid hydroperoxide glutathione peroxidase gene for protection of host cells from lipid hydroperoxide-mediated injury. Biochem. Biophys. Res. Commun. 219, 486-91.

Yagi, K., Shidoji, Y., Komura, S., Kojima, H., and Ohishi, N. (1998). Dissipation of mitochondrial membrane potential by exogenous phospholipid monohydroperoxide and protection against this effect by transfection of cells with phospholipid hydroperoxide glutathione peroxidase gene. Biochem. Biophys. Res. Commun. 245, 528-533.

Yang, Y., Cheng, J. Z., Singhal, S. S., Saini, M., Pandya, U., Awasthi, S., and Awasthi, Y. C. (2001). Role of glutathione S-transferases in protection against lipid peroxidation. Overexpression of hGSTA2-2 in K562 cells protects against

hydrogen peroxide-induced apoptosis and inhibits JNK and caspase 3 activation. J Biol Chem 276, 19220-30.

Yant, L. J., Ran, Q., Rao, L., Van Remmen, H., Shibatani, T., Belter, J. G., Motta, L., Richardson, A., and Prolla, T. A. (2003). The selenoprotein GPX4 is essential for mouse development and protects from radiation and oxidative damage insults. Free Radic Biol Med 34, 496-502.

Yant, L. J., Ran, Q., Rao, L., Van Remmen, H., Shibatani, T., Belter, J. G., Motta, L., Richardson, A., and Prolla, T. A. (2003). The selenoprotein GPx4 is essential for mouse development and protects from radiation and oxidative damage insults. Free Radic. Biol. Med. 34, 496-502.

Yoshino, T., Kishi, H., Nagata, T., Tsukada, K., Saito, S., and Muraguchi, A. (2001). Differential involvement of p38 MAP kinase pathway and Bax translocation in the mitochondria-mediated cell death in TCR- and dexamethasone-stimulated thymocytes. Eur J Immunol 31, 2702-8.

Yu, X., Sidhu, J. S., Hong, S., and Faustman, E. M. (2005). Essential role of extracellular matrix (ECM) overlay in establishing the functional integrity of primary neonatal rat Sertoli cell/gonocyte co-cultures: an improved in vitro model for assessment of male reproductive toxicity. Toxicol Sci 84, 378-93.

Zhou, T., Zhou, G., Song, W., Eguchi, N., Lu, W., Lundin, E., Jin, T., and Nordberg, G. (1999). Cadmium-induced apoptosis and changes in expression of p53, c-jun and MT-I genes in testes and ventral prostate of rats. Toxicology 142, 1-13.

VITA

Michael Garry was born in Inglewood, California across the street from the Fabulous Forum. He grew up in southern California, first in Los Angeles and then in a small high desert town called Yucca Valley. He has also lived for periods of time in Davis, California, Washington DC, Cameroon, West Africa, and Seattle, Washington. At the University of California, Davis he earned a Bachelor of Sciences degree in Zoology with a minor in Philosophy. He earned a Master of Sciences degree in Nutritional Biochemistry from the University of Washington. In 2006, after much suffering, he earned a Doctor of Philosophy degree in Toxicology in the Department of Environmental and Occupational Health Sciences from the University of Washington.

Publications

Garry, M.R., Kavanagh, T.J., Faustman, E.M., Sidhu, J.S., Liao, R., Ware, C., Vliet, P.A., and Deeb, S.S. 2006. Sensitivity of Mouse Lung Fibroblasts Heterozygous for GPx4 to Oxidative Stress. Submitted to Free Radic Biol Med.

Garry, M.R., Deeb, S.S, Kavanagh, T.J., Sidhu, J.S., Yu, X., Vredevoogd, M.A., Kim, E., and Faustman, E.M. 2006. Differential modulation of stress and ubiquitination signaling pathways by cadmium in cultured mouse lung fibroblasts heterozygous for GPx4. In preparation.

Petito Boyce, C and M.R. Garry. 2003. Developing risk-based target concentrations for carcinogenic polycyclic aromatic hydrocarbon compounds assuming human consumption of aquatic biota. J Tox. Env. Health, Part B. 6:497-520.

Yost, L.J., S. Shock, M. Garry, Y.N. Garson, A.K. Sugino, and W.J. Shields. 2003. Health risk evaluation of PCBs from joint compound measured on surfaces and in air. Organohalogen Compounds 63: 413416.

Petito Boyce, C. and M.R. Garry. 2002. Review of information resources supporting human exposure assessment models. Hum. Ecol. Risk Assess. 8(6):1445-1487.

Chew, C.M., R.M. Lorenzana, and M.R. Garry. 1997. U.S. EPA Region 10 screening model for indirect exposure to air emissions: risk-based air concentrations. In: Environmental Toxicology and Risk Assessment: Modeling

and Risk Assessment. 6th Volume. ASTM STP 1317. F.J. Dwyer, T.R. Doane, and M.L. Hinman (eds.). American Society for Testing and Materials.

National Health Care Reorganization Task Force. 1992. Methodologie pour la mise au point de grilles de supervision des centres de sante. Ministry of Health, Republic of Cameroon.

Presentations

Garry, M.R., S.S. Shock, L.J. Yost, J. Kulas, and W.J. Shields. 2006. Human health risk assessment of metals exposure through subsistence foods consumption and subsistence harvest activities near a mining transport road in northwest Alaska. Poster presented at the Society of Toxicology's 45th Annual Meeting San Diego, CA.

Shock, S.S., Y.W. Lowney, L.D. Peterson, B.A. Bessinger, and M.R. Garry. 2006. Assessment of solubility and bioaccessibility of barite in mine-impacted soils. Poster presented at the Society of Toxicology's 45th Annual Meeting San Diego, CA.

Garry, M.R., S.S. Shock, L.J. Yost, J. Kulas, and W.J. Shields. 2005. Assessment of metals concentrations in salmonberries and sourdock collected near a mining transport road in northwest Alaska. Poster presented at the Society of Toxicology's 44th Annual Meeting New Orleans, LA.

Garry, M.R., L.J. Yost, S.S. Shock, and W.J. Shields. 2004. Assessment of metals exposure associated with subsistence use of caribou collected near a mining transport road in northwest Alaska. Poster presented at the Society of Toxicology's 43rd Annual Meeting Baltimore, MD.

Garry, M.R., J.S. Sidhu, T.J. Kavanagh, and E.M. Faustman. 2003. Differential modulation of stress and ubiquitination signaling pathways by cadmium, H2O2, and serum withdrawal in cultured mouse fibroblasts. Oral presentation at the Society of Toxicology's 44th Annual Meeting, Salt Lake City, UT. Abstract 311.

Yost, L.J., S. Shock, M. Garry, Y.N. Garson, A.K. Sugino. 2003. Health risk evaluation of PCBs measured in wipe samples from joint compound. Poster presented at the Society of Toxicology's 44th Annual Meeting, Salt Lake City, UT.

Garry, M.R. 2003. Red Dog mine DMTS Risk Assessment Workplan. Oral presentation at the Alaska Forum for the Environment, Anchorage, AK, February 2003.

Garry, M.R., T.J. Kavanagh, and E.M. Faustman, J.S. Sidhu, and S.S. Deeb. 2002. Differential susceptibility to oxidative stress in mouse lung fibroblasts heterozygous for GPx4. Poster presented at the 9th Annual Meeting of The Society for Free Radical Biology and Medicine, San Antonio, TX.

Garry, M.R. and J.S. Tsuji. 2002. Evaluating lead exposure at mining sites with heterogeneous soil types and lead bioavailability. Poster presented at the Society of Toxicology's 42nd Annual Meeting, Nashville, TN. The Toxicologist, 66(1-S), 500.

Yost, L.J., R.A. Schoof, and M.R. Garry. 2002. Estimation of dietary intake of inorganic arsenic in children. Fifth International Arsenic Meeting, Society of Environmental Geochemistry and Health, San Diego, CA.

Garry, M.R., Y.W. Lowney, and J.S. Tsuji. 2001. A critical analysis of assumptions used when evaluating intake of metals from homegrown vegetables. Poster presented at the Society of Toxicology's 41st Annual Meeting, San Francisco, CA. The Toxicologist, 60(1), Abstract 2007.

Tsuji, J.S. and M.R. Garry. 2001. Metals exposure from homegrown produce at mining and smelting sites. Poster presented at the Society of Toxicology's 41st Annual Meeting, San Francisco, CA. The Toxicologist, 60(1), Abstract 95.

Garry, M.R., T.J. Kavanagh, and E.M. Faustman. 2000. Phosphatidylcholine hydroperoxide decreases mitochondrial membrane potential and oxidizes cardiolipin. Poster presented at the Society of Toxicology's 40th Annual Meeting, Philadelphia, PA. Toxicological Sciences, 54(1), Abstract 767:163.

Petito Boyce, C. and M.R. Garry. 2000. Development of carcinogenic PAH trigger levels for human consumption of aquatic biota based on modifications to the default bioconcentration factor and the use of toxicity equivalency factors. Presented at the Society for Risk Analysis annual meeting, December 4, 2000.

Garry, M.R., M. Vredevoogd, and E.M. Faustman. 1999. Gene expression as a potential biomarker of inorganic mercury exposure in terrestrial ecosystem. Poster presented at the Society of Toxicology's 39th Annual Meeting, New Orleans, LA.

Garry, M.R., S.C. Kirchner, J.L. Schroeder, and E.M. Faustman. 1997. Amplification and detection of RNA from mature human sperm. Poster presented at Pacific Northwest Association of Toxicology, Regional Chapter of the Society of Toxicology.